TRANSCRIPTIONAL RESPONSES OF SOYBEAN (*GLYCINE MAX*) AND THALE CRESS (*ARABIDOPSIS THALIANA*) PLANTS EXPOSED TO DIFFERENT CLASSES OF ENVIRONMENTAL CONTAMINANTS

A Dissertation
Submitted to
the Temple University Graduate Board

In Partial Fulfillment
of the Requirements for the Degree
DOCTOR OF PHILOSOPHY

---

by
Rashid Kaveh
Diploma Date (December 2014)

Examining Committee Members:

Dr. Benoit Van Aken, Thesis Advisory Committee Chair, Civil and Environmental Engineering, Temple University
Dr. Sasha Eisenman, Department of Landscape Architecture, Temple University
Dr. Daniel R. Strongin, Department of Chemistry, Temple University
Dr. Rominder Suri, Department Chair, Civil and Environmental Engineering, Temple University
Dr. Rouzbeh Tehrani, Civil and Environmental Engineering, Temple University

ABSTRACT

Plants are exposed to various environmental contaminants through irrigation with reclamation water and land application of municipal biosolids. Plants have been shown to take up contaminants from soil and groundwater, and to some extent, metabolize them in their tissues. These mechanisms have potential important implications for the environment and human health. First, as plants constitute the basis of the terrestrial food chain, accumulation of toxic chemicals or their metabolites inside plant tissues may lead to contamination of animals and humans. Second, the recognition of the capability of plants to take up and metabolize contaminants has led to the development of a plant-based remediation technology, referred to as phytoremediation. Phytoremediation is defined as the use of higher plants for the removal of environmental contaminants from soil and groundwater. Although phytoremediation is conceptually attractive as a green, environmental-friendly technology, the metabolism of xenobiotic compounds by plants is often slow and incomplete, possibly resulting in the accumulation of toxic pollutants and/or their metabolites inside plant tissues. Without further detoxification, phytoremediation may result in pollution transfer, potentially threatening the food chain, and eventually humans. Gaining further knowledge about the fate of environmental contaminants inside plant tissues is therefore of paramount importance for conducting environmental risk assessment and enhancing the efficiency of phytoremediation applications. It's an attractive concept today to cultivate plants on contaminated lands, in order to combine the benefits of phytoremediation with plant-based biofuel production. Unlike conventional plant bioenergy production, plant biomass grown on marginal contaminated soil will not compete with land for food production. However, the effect of contaminants on the plant biomass and bioenergy feedstock yield have received little

attention. Molecular biology techniques, such as high-throughput gene expression analysis, constitute powerful tools to understand the molecular bases of the plant metabolism and response to environmental contaminants. The objective of this thesis is to understand the physiological and transcriptional responses of two model plants, thale cress (*Arabidopsis thaliana*) and soybean (*Glycine max*), exposed to various classes of contaminants, including silver nanoparticles (AgNPs), pharmaceuticals (zanamivir – ZAN and oseltamivir phosphate - OSP), explosives (2,4,6-trinitrotoluene - TNT), and polychlorinated biphenyls (PCBs). Detection of the contaminants inside plants tissues was performed using advance analytical methods, including inductively-coupled plasma – mass spectrometry (ICP-MS), gas-chromatography – mass spectrometry (GC-MS), and liquid-chromatography (LC-MS). The effects of contaminants on plants were assessed by recording various plant metrics, including biomass, root and shoot length, and soybean production. The transcriptional response of plants to exposure to selected contaminants (AgNPs, OSP, and ZAN) was investigated using whole-genome expression microarrays and reverse-transcription real-time (quantitative) PCR (RT-qPCR).

In the first experimental phase of this research, the effects of AgNPs and soluble silver (Ag^+) on *A. thaliana* plants were investigated. AgNPs are widely used nanomaterials, which have raised environmental concerns because of their toxicity to most living organisms, including plants. Exposure of hydroponic *A. thaliana* plants for 14 days to 20-nm AgNPs resulted in a slight increase of the biomass at low concentrations (1.0 and 2.5 mg / L) and a significant decrease of the biomass at higher concentrations (5.0 to 100 mg / L). Exposure to Ag^+ for 14 days resulted in a significant reduction of the biomass after 14 days at concentration at and above 5.0 mg / L. Genome-wide expression

microarrays revealed that exposure of *A. thaliana* to AgNPs and Ag^+ at the concentration of 5 mg / L for 14 days resulted in differential expression of many genes involved in the plant response to stress and to biotic and abiotic stimuli. Although distinct gene expression patterns developed upon exposure to AgNPs and Ag^+, a significant overlap of differentially expressed genes was observed between the two treatments, suggesting that AgNP-induced stress originated partly from silver toxicity and partly from nanoparticle-specific effects.

In the second experimental phase of this research, the effects of the antiviral drugs, OSP and ZAN, on *A. thaliana* were investigated using an approach similar as the one described above. OSP and ZAN are pharmaceutical drugs that currently constitute the last line of defense against influenza infection. These drugs have been widely detected in wastewater effluents, especially during the influenza season, and they have the potential to contaminate agricultural plants through irrigation and land application of biosolids. Exposure of *A. thaliana* to OSP showed a significant decrease in the plants biomass at the concentrations of 20 and 100 mg / L, although no significant effect on the biomass was recorded upon exposure to ZAN (up to 100 mg / L), suggesting low acute toxicity of these compounds to plants. On the other hand, *Arabidopsis* exposure to OSP and ZAN at 20 mg / L resulted in significant transcriptional changes, including up- and down-regulation of many genes involved in the plant response to oxidative stresses and response to stimuli. Comparison with an *Arabidopsis* gene expression database (Genevestigator), revealed that many genes significantly up- and down-regulated by exposure to OSP and/or ZAN were similarly affected by exposure to biotic and abiotic

stresses, toxic chemicals, and hormonal stimuli, suggesting that OSP and ZAN have negative chronic effects on plant health.

The third experimental phase of this thesis focuses on the effects of two important persistent pollutants, TNT and PCBs, on the growth of soybean plants, with the objective of assessing the potential of using energy crops for the combined benefit of land remediation and biofuel (biodiesel) production. Explosives, such as TNT, are common toxic contaminants frequently observed at explosive manufacturing sites and military training ranges. PCBs are ubiquitous and toxic contaminants that are found in virtually every compartment of the environment. Short-term growth inhibition tests conducted with TNT and selected PCBs (e.g., 2,4'-dichlorobiphenyl - 2,4'-DCB) showed that these compounds exerted no or mild observable effects on plant growth even when applied at very high concentrations (i.e., 100 to 250 mg / kg soil, respectively). Analysis of TNT and 2,4'-DCB in exposed plant tissues showed average concentrations of 30 - 40 ng/g of TNT and 9,000 to 17,000 ng/g of 2,4'-DCB, which is consistent with biotransformation of TNT inside plant tissues. On the other hand, long-term exposure experiments show that exposure to TNT significantly affected soybean growth and production of bean in TNT-exposed plants (25 – 50 mg / kg soil). Exposure to TNT resulted in a significant decrease of the biomass of harvested beans after 120 days, which may have important consequences on the yield of biodiesel obtained from plants grown on contaminated land. Soybean were then exposed to 2,4'-DCB and its major transformation products, 4-OH-2,4'-DCB). Although high concentrations of the parent PCB (100 and 200 mg / kg) resulted in significant decrease of the biomass, high concentrations of the OH-metabolite resulted in increase of the plant biomass. Future research work will include the

determination of the molecular bases of the effects – both positive and negative – of TNT, PCBs, and OH-PCBs on soybean plants and beans.

To my parents,

Nahid and Esfandiar Kaveh,

for their love, support and encouragement all the days of my life.

I hope this achievement will complete the dreams you had for me and the sacrifices you made so that I could have a great education.

And to my beloved twin sister, Golshid,

for her support and for being there for me during the good times and the bad.

You complete me.

"Genius is one percent inspiration, ninety-nine percent perspiration."

Thomas A. Edison

ACKNOWLEDGEMENTS

First and foremost, I would like to express gratitude to my adviser, Dr. Benoit Van Aken, for his constant support and guidance throughout my doctorate research.

I also would like to acknowledge my advisory committee members, Dr. Rominder Suri, Dr. Sasha Eisenman, Dr. Rouzbeh Tehrani and Dr. Daniel R. Strongin, for their valuable input.

Thank you to my research group and close friends Dr. Rouzbeh Tehrani and Sibia Ranjbar for their contribution to my research.

Special thanks to my dear friend Dr. Sara Karjoo for her support and encouragement in the difficult moments during my pursuit of my doctorate degree.

I would like to recognize my colleagues and friends Dr. Kate Fenlon and Dr. Katja Rokhina for their inspiration and scientific insights.

The research presented in this document has been supported by a grant from U.S. Department of Agriculture (USDA), the National Institute of Food and Agriculture (NIFA) (2012-67009-19982) and a grant from the Water and Environmental Technology (WET) Center, Temple University.

I also would like to acknowledge the International Phytotechnology Society for granting me a travel scholarship to attend the 10th International Phytotechnologies Conference (October 2013, Syracuse, NY) and Temple University Graduate School for awarding me the Summer Fellowship grant in 2014.

TABLE OF CONTENT

ABSTRACT ..... **II**

ACKNOWLEDGEMENTS ..... **VII**

LIST OF FIGURES ..... **XIII**

LIST OF TABLES ..... **XVIII**

LIST OF ACRONYMS ..... **XIX**

CHAPTER 1 INTRODUCTION **1**

1.1 Problem Statement 1

1.2 Objectives 3

1.3 Selection of Plants Used in this Study 4

1.4 Selection of Contaminants Used in this Study 5

1.5 Study Overview 5

1.6 Publications, Presentations, and Awards 8

CHAPTER 2 LITERATURE REVIEW **10**

2.1 Introduction 10

2.2 Environmental Contaminants Selected for this Study 10

2.2.1 Ecotoxicology and Fate of AgNPs in the Environment 10

2.2.2 Ecotoxicology and Fate of Antiviral Drugs in the Environment 14

2.2.3 Ecotoxicology and Fate of TNT in the Environment 20

2.2.4 Ecotoxicology and Fate of PCBs in the Environment 22

2.3 Plant Species Used in this Study 25

2.4 Phytoremediation 27

2.4.1 The Bioremediation Concept 28

2.4.2 Bioremediation by Higher Plants (Phytoremediation) 29

2.4.3 Advantages and Limitations of Phytoremediation 29

2.4.4 Phytoremediation Processes 30

2.4.5 Metabolism of Xenobiotic Compounds by Plants 33

2.4.6 Phytoremediation and Effect of AgNPs and Ag^+ on Plants 34
2.4.7 Phytoremediation and Effect of TNT on plants 36
2.4.8 The effect of PCBs on Plants 37
2.5 Genetic Methods for Studying the Plant Response to Environmental Contaminants 39
2.6 Prior Gene Expression Analysis in Plants Exposed to Environmental Contaminants 40
2.7 Biodiesel Production from Plant Feedstock 42
CHAPTER 3 EXPOSURE OF *ARABIDOPSIS THALIANA* TO SILVER NANOPARTICLES 46
3.1 Introduction 46
3.2 Objective 47
3.3 Materials and Methods 47
3.3.1 Chemicals 47
3.3.2 Nanoparticle Characterization 47
3.3.3 Plant species and culture conditions 48
3.3.4 Growth inhibition experiment 48
3.3.5 Analysis of AgNP and Ag^+ in plants tissues 49
3.3.6 Gene expression analysis using microarray method 50
3.3.7 Reverse-transcription real-time PCR 51
3.3.8 Data validation and statistical analysis 53
3.4 Results and Discussion 53
3.4.1 Nanoparticle characterization 53
3.4.2 Effect of AgNPs and Ag^+ on *A. thaliana* growth 55
3.4.3 Analysis of Ag content in plant tissues 56
3.4.4 Gene expression microarrays 57
3.4.5 Functional categories of differentially expressed genes 60
CHAPTER 4 EXPOSURE OF ARABIDOPSIS THALIANA TO ANTIVIRAL DRUGS 67
4.1 Introduction 67
4.2 Objective 68
4.3 Materials and Methods 68

4.3.1 Chemicals 68
4.3.2 Plant species and culture conditions 68
4.3.3 Growth inhibition experiment 69
4.3.4 Gene expression analysis using microarray method 69
4.3.5 Reverse-transcription real-time PCR 70
4.4 Results and Discussion 72
4.4.1 Effect of OSP and ZAN on *A. thaliana* growth 72
4.4.2 Gene expression analysis using microarrays 74
4.4.3 Functional categories of differentially expressed genes 76
CHAPTER 5 EXPOSURE OF SOY PLANTS TO PCBS AND TNT 86
5.1 Introduction 86
5.2 Objectives 87
5.3 Materials and Methods 87
5.3.1 Chemicals 87
5.3.2 Plant species and culture conditions 87
5.3.3 Growth inhibition experiments 88
5.3.4 Analysis of TNT and PCBs 89
5.3.5 Data validation and statistical analysis 90
5.4 Results and Discussion 91
5.4.1 Soybean exposure to TNT 91
5.4.1 Analysis of TNT in plant tissues 94
5.4.2 Soybean exposure to PCBs and OH-PCBs 104
5.4.3 Analysis of PCBs inside plant tissues 109
5.5 Discussion 110
CHAPTER 6 CONCLUSION 113
6.1 Effect of Silver Nanoparticles on *Arabidopsis thaliana* 113
6.2 Effect of Antiviral Drugs on *Arabidopsis thaliana* 114
6.3 Effect of TNT and PCBs on Soybean 115

6.4 Review of Gene Expression Studies Conducted with *A. thaliana* Exposed to AgNPs, ZAN and OSP, TNT, and PCBs....116

6.5 Further Perspectives....120

6.6 Practical Considerations for Phytoremediation....121

6.7 Future Research....122

REFERENCES....125

APPENDIX A REGULATED GENES IN EXPOSURE TO AGNP AND AG^{+}....143

APPENDIX B REGULATED GENES IN EXPOSURE TO ZANAMIVIR AND OSELTAMIVIR....153

LIST OF FIGURES

Figure 2.1. Chemical structure of zanamivir (ZAN - left) and oseltamivir phosphate 17

Figure 2.2. Hydrolysis of oseltamivir (OS) to its active metabolite, oseltamivir carboxilate (OC) [42].....17

Figure 2.3. Chemical structure of 2,4,6-trinitortoluene (TNT).....20

Figure 2.4. General structure of PCBs.....23

Figure 2.5. *Arabidopsis thaliana* plants, final growth phase [96, 97]. 26

Figure 2.6. Soybean (*Glycine max*) growth phases (left); soybean farm (right) [101, 102]. 27

Figure 2.7. Phytoremediation involves several processes: Pollutants in soil and groundwater can be taken up inside plant tissues (phytoextraction) or adsorbed to the roots (rhizofiltration); pollutants inside plant tissues can be transformed by plant enzymes (phytotransformation) or can volatilize into the atmosphere (phytovolatilization); pollutants in soil can be degraded by microbes in the root zone (rhizosphere bioremediation) or incorporated to soil material (phytostabilization) (adapted from Van Aken, 2008) [121]. 31

Figure 2.8. The three phases of the green liver model: Hypothetical pathway representing the metabolism of carbamazepine in plant tissues: phase I: Activation of carbamazepine by hydroxylation and hydrolysis to 2-hydroxyiminostilbene; phase II: Conjugation with a glucose to form a O-glucuronide; phase III: Sequestration of the conjugate into the cell wall or in the vacuole (adapted from Van Aken 2008 and Celiz et al. 2009) [121, 34]. 34

Figure 3.1. A TEM image of 20-nm AgNPs used in this study.....49

Figure 3.2. Absorption spectra (300 – 800 nm) of 20 nm silver nanoparticle (AgNP) suspensions prepared in 0.5 strength Murashige and Skoog (MS) medium with polyvinylpyrrolidone (molecular weight 40000 Dalton, PVP40). **Red spectrum**: fresh suspension. **Blue spectrum**: suspension after agitation at 55 °C, 150 rpm for 24 h. 54

Figure 3.3. Size distribution of 20 nm silver nanoparticle (AgNP) suspensions prepared in 0.5 strength Murashige and Skoog (MS) medium with polyvinylpyrrolidone (molecular weight 40000 Dalton, PVP40). **Panel A**: fresh suspension. **Panel B**: suspension after agitation at 55 °C, 150 rpm for 24 h. 55

Figure 3.4. Relative fresh biomass of *A. thaliana* exposed to AgNP and Ag^{+} 56

Figure 3.5. Ag content measured in tissues of *A. thaliana* exposed to AgNP and Ag^+. Panel A: Leaves. Panel B: Roots. Error bars represent standard deviations of 3 biological replicates. 57

Figure 3.6. Venn diagrams showing the number of genes significantly up-regulated (**Panel A**) and down-regulated (**panel B**) by exposure to AgNPs and Ag^+ individually, and by both compounds simultaneously. 58

Figure 3.7. Log_2 microarray relative expression levels versus log_2 RT-qPCR relative expression levels for exposure to panel A: AgNPs and panel B: silver ions (Ag^+). Error bars represent the standard deviations between three biological replicates. 60

Figure 3.8. Major gene ontology (GO) process categories of genes up (fold change > 2.0) and down-regulated (fold change < 0.5). Panel A: Genes differentially expressed by exposure to AgNPs. Panel B: Genes differentially expressed by exposure to Ag+. 62

Figure 3.9. Major gene ontology (GO) functional categories of genes up (fold change > 2.0) and down-regulated (fold change < 0.5) Panel A: Genes differentially expressed by exposure to AgNPs. Panel B: Genes differentially expressed by exposure to Ag^+. 63

Figure 4.1. *A. thaliana* plants exposed to OSP and ZAN after three weeks. Panel a) Non-exposed controls, Panel b) OSP 20 mg / L, and Panel c) ZAN 20 mg / L. 72

Figure 4.2. *A. thaliana* plants fresh weight biomass after exposure to OSP and ZAN for three weeks. Error bars represent standard deviations. Asterisks (*) show Statistically significant differences. 73

Figure 4.3. Venn diagrams showing the number of genes significantly up-regulated (**Panel A**) and down-regulated (**panel B**) by exposure to the antiviral drugs, oseltamivir phosphate (OSP) and zanamivir (ZAN) individually, and by both compounds simultaneously. 75

Figure 4.4. Log2 microarray relative expression levels versus log2 RT-qPCR relative expression levels for exposure to panel A: oseltamivir phosphate (OSP) and panel B: zanamivir (ZAN). Error bars represent the standard deviations between three biological replicates. 76

Figure 4.5. Major gene ontology (GO) process categories of up- and down-regulated genes. Distribution of genes into GO categories was performed using BLAST2GO® (GO level 2). Panel A: Genes differentially expressed by exposure to ZAN, Panel B: Genes differentially expressed by exposure to OSP. 78

Figure 4.6. Major gene ontology (GO) functional categories of genes up (fold change > 2.0) and down-regulated (fold change < 0.5) Panel A: Genes differentially expressed by exposure to ZAN. Panel B: Genes differentially expressed by exposure OSP. 79

Figure 4.7. Genes up-regulated by exposure to OSP and/or ZAN in *A. thaliana* and the number of times they were reported similarly overexpressed by various stresses in other microarray experiment (Genevestigator). 83

Figure 4.8. Genes down-regulated by exposure to OSP and/or ZAN in *A. thaliana* and the number of times they were reported similarly repressed by various stresses in other microarray experiments (Genevestigator). 84

Figure 5.1. Soybean plantlets exposed for 10 days to TNT at concentration from 0.0 to 10 mg / kg soil (fresh weight). 91

Figure 5.2. Soybean plantlets exposed for 10 days to TNT at concentration from 0.0 to 100 mg / kg soil (fresh weight). 92

Figure 5.3. Organ weight of soybean plantlets exposed for two weeks to TNT at concentration ranging from 0.0 to 100 mg / kg soil (fresh weight). Panel A: Root weight. Panel B: Aerial part weight. 93

Figure 5.4. Exposure of soybean plants to TNT at concentration ranging from 0.0 to 250 mg / kg soil. Weight and length of plants are presented. Data sets labeled with similar letters are significantly different. 94

Figure 5.5. TNT detected in soybean tissues after 28 days of exposure in soil containing supplemented with 25, 50, and 100 mg TNT/kg soil. 95

Figure 5.6. Residual concentration of TNT in soil. Left: soil vegetated with soybean plants and supplemented with 25, 50, and 100 mg TNT/kg soil after 28 days of exposure. Right: soil supplemented with 50 mg TNT/kg soil vegetated and non-vegetated (NV) with soybean plants (V) after 15 days of exposure. 96

Figure 5.7. Long term soybean exposure to TNT during the first month of growth. Germination started exposed to TNT concentrations of 0, 25, and 50 mg / kg (left to right). Plants showed a lag in the plants' growth rate after A) 10 days, B) 12 days, and C) 24 days. 98

Figure 5.8. Bamboo poles to hold the bean stalk upright for the long term experiment. Picture is taken after 72 days from planting the seeds. 99

Figure 5.9. A) Beginning seed period for soybean plants happen at this stage. Lower leaves fall and yellowing starts. At this time pods start filling with seeds. B) Beginning seed C) Full seed. 100

Figure 5.10. Effects of TNT applied at concentration of 0.0, 25, and 50 mg / L on various metrics of soybean plants. Plants metrics were recorded after 120 days of exposure. 101

Figure 5.11. Effects of TNT applied at concentration of 0.0, 25, and 50 mg / L on the size and biomass of soybean plants. Plants metrics were recorded after 120 days of exposure. Asterisks (*) indicate statistically significant differences ($p < 0.05$) by comparison to control plants. 101

Figure 5.12. Effects of TNT applied at concentration of 0.0, 25, and 50 mg / L on the number and weight of bean produced. Plants metrics were recorded after 120 days of exposure. Asterisks (*) indicate statistically significant differences ($p < 0.05$) by comparison to control plants. 103

Figure 5.13. Effect of 2,4'-DCB on soybean plants. The picture shows that exposure to 12.5 and 25 mg / L caused a visible lag phase in soybean growth. From left to right, applied treatments are 0.0 (control), 6.25, 12.5, and 25 /kg-soil. 104

Figure 5.14. Soybean exposed to 2,4'-DCB at concentrations of 0.0, 10, 25, and 50 mg / kg soil after 17 days of growth. 105

Figure 5.15. Effect of 2,4'-DCB on the root and shoot biomass in soybean plants exposed to concentrations of 0.0, 10, 25, and 50 mg / kg. The asterisks (*) shows the statistical significance of the changes in the treatments versus control (at 95% confidence level). 105

In a first experiment, soybean plants were exposed to increasing concentrations of 2,4'-DCB and 4-OH-2',4-DCB: 0.0, 10, and 25 mg / kg soil. Plant shoot/leaf biomass showed a significant decrease upon exposure to 25 mg / L in to both the parent PCB (2,4'-DCB) and the OH-metabolite (4-OH-2',4-DCB) (Figure 5.16 and Figure 5.17). 106

Figure 5.18. Weight of soybeans' roots and aerial parts after 11 days of exposure to 0.0, 10, and 25 mg / kg 2,4'-DCB. Asterisks (*) indicate statistically significant differences ($p < 0.05$) by comparison to control plants. 107

Figure 5.19. Weight of soybeans' roots and aerial parts after 11 days of exposure to 0.0, 10, and 25 mg / kg 4-OH-2,4'-DCB. Asterisks (*) indicate statistically significant differences ($p < 0.05$) by comparison to control plants. 107

Figure 5.20. Biomass of soybean plants exposed to 2,5-DCB (6.4, 16, 40, 100, and 250 mg / kg soil) and 4-OH-DCB (0.0, 1.3, 3.2, 8, 20, and 50 mg / kg soil) after two weeks of growth. Data showed no statistical significance across the different treatments. 108

Figure 5.21. The amount of 2,4'-DCB in roots (right) and shoots (left) for different exposure concentrations. 109

LIST OF TABLES

Table 2.1. OSP acute and chronic toxicity in surface water 19

Table 3.1. List of primers used for the reverse-transcription real-time PCR (RT-qPCR) amplification of selected genes 52

Table 4.1. List of primers used for the reverse-transcription real-time PCR (RT-qPCR) amplification of selected genes 71

Table 5.1. TNT mass balances in soil and soybean plants. Total TNT amounts used for each treatment are shown. Corresponding percentages are shown in parentheses. Bioaccumulation factors are defined as the ratios of TNT concentration in plant tissues over its concentration in soil. 96

Table 5.2. PCB compounds and Hydroxylated PCBs tested on soybean or *A. thaliana*. 106

Table 5.3. 2,4'-DCB mass balances in soil and soybean plants. Total 2,4'-DCB amounts used for each treatment are shown. Corresponding percentages are shown in parentheses. Bioaccumulation factors are defined as the ratio of 2,4'-DCB concentration in plant tissues over its concentration in soil. 110

Table A-1. Genes significantly upregulated (fold change > 2.0) in A. thaliana plants exposed for 10 days to silver nanoparticles (AgNPs) or silver ions (Ag^+) 144

Table A-2. Gene significantly downregulated (fold change < 0.5) in A. thaliana plants exposed for 10 days to silver nanoparticles (AgNPs) or silver ions (Ag^+) 151

Table B-1. Genes significantly up-regulated (fold change ≥ 2.0) in A. thaliana plants exposed to oseltamivir phosphate and zanamivir for 21 days 154

Table B-2. Genes significantly down-regulated (fold change ≤ 0.5) in A. thaliana plants exposed to oseltamivir phosphate and zanamivir for 21 days 155

LIST OF ACRONYMS

Ag	Silver
AgNPs	Silver nanoparticles
ANOVA	Analysis of variance
ARGOS	Auxin-regulated gene involved in organ size
BRB-Array Tools	Biometric research branch-array tools
DAVID	Database for Annotation, Visualization and Integrated Discovery
DI	Deionized
EPA	Environmental Protection Agency
ESI	Electrospray ionization
FAO	Food and Agricultural Organization
GC-ECD	Gas chromatography-electron capture detector
GO	Gene ontology
HPLC-MS	high-performance liquid chromatography–mass spectrometry
ICP-MS	Inductively coupled plasma mass spectrometry
K_{oc}	Organic carbon-water partitioning coefficient
K_{ow}	Octanol-water partitioning coefficient
LC-MS	Liquid chromatography–mass spectrometry
MI	Mitotic index
MS0	Murashige and Skoog medium with zero amount of sugar
NCBI	National Center for Biotechnology Information
OC	Oseltamivir carboxylate
OSP	Oseltamivir phosphate
PCBs	Polychlorinated biphenyls
PCR	polymerase chain reaction
POP	Persistent organic pollutants
PVP	Polyvinylpyrrolidone
RT-qPCR	Real-time quantitative polymerase chain reaction
SAR	Systemic acquired resistance
SIM	Single ion mode
SNUR	Significant new use rule
STP	Sewage treatment plant
STP	Sewage treatment plants
TAIR	The Arabidopsis information resource
TEM	Transmission electron microscopy
TNT	2,4,6-trinitortoluene
TSCA	Toxic substances control act
ZAN	Zanamivir

CHAPTER 1 INTRODUCTION

1.1 Problem Statement

The presence of toxic contaminants in the environment increases the likelihood of animal and human exposure. As a consequence, various remediation methods have been developed to help clean up contaminated environments. Using plants for the remediation of soil and water -- a process referred to as phytoremediation -- is a promising and attractive technology because of its low cost and maintenance and its environmental-friendly character. Plants have been shown to have the ability to take up, accumulate, and, to some extent, detoxify environmental contaminants. However, the metabolism of most environmental contaminants in plants is poorly characterized. Moreover, the static accumulation of toxic contaminants inside plant tissues, or their conversion into more toxic metabolites, may result in pollution transfer. Indeed, in the absence of efficient biotransformation, the parent contaminants and/or their potential toxic metabolites will sooner or later return to the soil or otherwise contaminate the food chain. Understanding further the catabolic pathways of toxic contaminants in plants as well as the plant response to contaminant exposure is likely to allow to improve the efficiency and safety of phytoremediation processes.

Besides bioremediation purposes, plants are the basis of the terrestrial food chain and their contamination by toxic pollutants may threaten wildlife and human health. In particular, agricultural plants are known to accumulate various contaminants present in reclamation water used for irrigation and in municipal sludge applied on land as organic fertilizers. With this respect, understanding the metabolism of contaminants in plants is

expected to help environmental risk assessment investigations and regulatory standards for treated water and biosolids intended to be used at farms.

Because most cell activities are regulated at the transcriptional level, gene expression analysis is a powerful tool to study the effects and metabolic response of plants to environmental contaminants. Transcriptional analyses help understand deeper the molecular bases of plant catabolic pathways and identify new genes that are involved in the plant response to toxicants in the environment. Recently, the changes in gene expression in plants that are exposed to various environmental contaminants (e.g., TNT, PCBs, heavy metals) have been studied using the microarray technology, which has provided a better understanding of the molecular mechanisms of phytotoxicity and plant responses. Identification of genes involved in the metabolism of environmental contaminants may also support the generation of transgenic plants that are designed for specific phytoremediation applications.

Biodiesel production from vegetable oil is a promising option for reducing fossil fuel dependency and mitigating atmospheric pollutions. However, most bioenergy plants currently cultivated in the U.S. are sugar-producing crops for bioethanol production and oilseed crops for biodiesel production. These bioenergy feedstock plants are generally considered being associated with a net positive carbon dioxide emission and a low net energy balance (NEB). In addition, these plants are also conventional agricultural species that compete for land in food production. Large areas in the U.S. are heavily contaminated by industrial and agricultural wastes and are considered improper for residential or agricultural uses, hence the idea of cultivating energy plants on polluted lands for the combined benefit of phytoremediation and bioenergy production sounds

beneficial. In this research, the tolerance of an important energy crop, soybean, to various organic pollutants (TNT and PCBs) was investigated to determine the potential positive effect of plants on land remediation and the impact of the contaminants on the plant growth and bean production yield.

1.2 Objectives

The objective of this research is to gain further understanding of the metabolism and response of two important model plant species, thale cress (*Arabidopsis thaliana*) and soybean (*Glycine max*), exposed to different classes of environmental contaminants at the physiological and transcriptional levels. This objective was pursued through the completion of the following specific technical objectives (that correspond to three distinct chapters of the present thesis):

1. To investigate the physiological and transcriptional response of A. thaliana exposed to silver nanoparticles (AgNPs) and silver ions (Ag^{+}).

   AgNPs are widely used nanoparticles that are introduced in many medical and personal products because of their antimicrobial properties. Release of AgNPs in the environment poses a health hazard because of their toxicity for different species as reported in several studies. Because of their likely occurrence in wastewater and municipal biosolids, AgNPs have the potential to contaminate plants and the food chain.

2. To investigate the physiological and transcriptional response of *A. thaliana* exposed to the antiviral drugs, zanamivir (ZAN) and oseltamivir phosphate (OSP).

Neuraminidase inhibitor antiviral drugs, such as ZAN and OSP, are rather new environment contaminants and for which limited ecotoxicological investigations have been conducted. They are important drugs used for treatment of influenza and they have been shown to be released to wastewater during flu seasons, leading to the fear of massive discharge in the case of an influenza pandemic.

3. To investigate the plant growth, physiological response, and the bean production yield of soybean plants (*G. max*) exposed to the explosive, 2,4,6-trinitrotoluene (TNT), and to selected polychlorinated biphenyls (PCBs) and their hydroxylated metabolites (OH-PCBs).

   TNT and PCBs have long been detected in different environments and their toxicity has been demonstrated in many living organisms including humans. Although they have been shown to be efficiently removed by phytoremediation, their recognized phytotoxic effect could potentially affect the biomass yield of energy plants.

Besides fundamental knowledge about the molecular mechanisms of the plant response and metabolism of toxic contaminants, results from this research are expected to contribute to enhance phytoremediation technologies, support environmental risk assessment, and design strategies combining land bioremediation with biofuel production.

1.3 Selection of Plants Used in this Study

Two different plants were used in this research, thale cress (*Arabidopsis thaliana*) and soybean (*Glycine max*). *A. thaliana* is a model plant for laboratory studies. It is

physically small and easy to cultivate. In addition, the genome of *A. thaliana* has been fully sequenced and various genetic tools are commercially available, including expression microarrays (Affymetrix). Soybean is a popular plant cultivated for its beans used in food industry and for bioenergy (biodiesel) production. In addition, the soybean genome has been fully sequenced and expression microarrays are also commercially available (Affymetrix).

1.4 Selection of Contaminants Used in this Study

The environmental pollutants being studied in this research are representatives of both conventional and emerging contaminants. TNT and PCBs are two important pollutants that have been present in the environment for decades. The antiviral drugs, OSP and ZAN, are important pharmaceuticals that could be released at high levels in the environment in the case of an influenza pandemic. Because of its antimicrobial properties, AgNPs have been widely used in a multitude of products and they are likely to be released in the environment. AgNPs pose a serious environmental concern because of their documented toxic effects on all living organisms, including plants and mammals [1].

1.5 Study Overview

Beside the present introductory section (Chapter 1), this thesis include a comprehensive literature review focusing on the toxicity and environmental fate of the selected contaminants, selected plant species, phytoremediation technology, biofuel production, and gene expression technology. The experimental research reported in this thesis was organized into three major phases, each of which is the objective of a separate chapter: (a) the effects of AgNPs and Ag^{+} on *A. thaliana* (Chapter 3), (b) the effects of

OSP and ZAN on *A. thaliana* (Chapter 4), and (c) the effects of TNT and PCBs on soybean plants (Chapter 5).

(a) Effects of AgNPs on *A. thaliana*: The first experimental section of this thesis (Chapter 3) focuses on the physiological and transcriptional responses of *A. thaliana* to AgNPs and silver ions (Ag^+). The results obtained from this research showed that exposure of hydroponic *A. thaliana* plantlets to AgNPs and Ag^+ resulted in significant growth inhibition at concentrations equal and above 5 mg / L (even though exposure to low concentrations, 1.0 and 2.5 mg / L, enhanced plant growth). A dose-dependent concentration of silver (Ag) was measured in the tissues of plants exposed to both AgNPs and Ag^+, with the highest levels being detected in root tissues exposed to high levels of Ag^+. Whole-genome expression microarray experiments showed that exposure to 5 mg / L of AgNPs and Ag^+ resulted in up- and down-regulation of many genes encoding proteins involved in the plant response to abiotic and biotic stresses: e.g., vacuolar superoxide dismutase, cytochrome P-450-dependent oxidase, and auxin-regulated gene involved in organ size (ARGOS). A significant overlap was observed between genes differentially expressed in response to AgNPs and Ag^+, suggesting that AgNP-induced stresses originate partly from Ag toxicity and partly from nanosize-specific effects.

(b) Effects of OSP and ZAN on *A. thaliana*: The second experimental section of this thesis (Chapter 4) focuses on the effects of the antiviral drugs, OSP and ZAN, on *A. thaliana* plants. OSP and ZAN are major medications currently used for the treatment of influenza. These drugs have been detected in municipal wastewater effluent and water catchments. They are likely to contaminate agricultural plants through irrigation with reclamation water and land application of sludge. Exposure of *A. thaliana* to OSP showed

a significant decrease of the plant biomass at high concentrations (20 and 100 mg / L), although no significant effect on the biomass was recorded upon exposure to ZAN (up to 100 mg / L), suggesting a low acute toxicity. On the other hand, as observed with AgNPs and Ag^{+}, exposure to OSP and ZAN at 20 mg / L resulted in statistically significant up- and down-regulation of many genes involved in the plant response to oxidative stresses, including superoxide dismutase, cytochrome P-450-dependent oxidases, and peroxidases. These results suggest that whole genome expression analysis may be useful for detection of the chronic toxicity of emerging contaminants on plants, even though short-term exposure does not result in observable physiological effects.

(c) Effects of TNT and PCBs on Soybean Plants: The third experimental section (Chapter 5) of this research investigates the effects of two major soil contaminants, TNT and 2,4'-dichlorobiphenyl (2,4'-DCB), on the growth of soybean plants, with the objective of assessing the potential of using energy crops (soybean) for combined benefit of land remediation and biofuel production. Growth inhibition tests showed that TNT and 2,4'-DCB exerted inhibitory effects on plant growth at concentrations of 50 and 100 mg / kg soil. Analysis of TNT and 2,4'-DCB in plant tissues showed average concentrations of 30 - 40 ng/g of TNT and 9,000 to 17,000 ng/g of 2,4'-DCB. Experiments conducted over 120 days showed in addition that exposure to TNT (50 mg / kg soil) significantly affected the number and biomass of beans produced by the plants, which may have an important consequence on the biofuel yield. The analyses of residual concentration of TNT and 2,4'-DCB in soil have been determine the potential of soybean plants for soil remediation. Further experiments will include whole genome expression analysis of soybean plants

exposed to TNT, PCB, and their potential metabolites (e.g., hydroxylated PCBs – OH-PCBs).

A **Conclusions Section** summarizes the major achievement of this research, discusses the significance of the work for science and engineering, and proposes further developments (Chapter 6).

1.6 Publications, Presentations, and Awards

The experimental work and literature review performed during this study have led to the following publications and presentations:

Publications:

a) R Kaveh, Y-S Li, S Ranjbar, R Tehrani, CL Brueck, and B Van Aken (Aug 2013). Changes in *Arabidopsis thaliana* gene expression in response to silver nanoparticles and silver ions. *Environ. Sci. Technol.* 47:10637-10644.

b) B Van Aken, R Tehrani and R Kaveh (Sep 2012). Uptake and metabolism of pharmaceuticals and other emerging contaminants by plants. Phytotechnologies, Remediation of Environmental Contaminants, CRC press.

c) R Tehrani, MM Lyv, R Kaveh, JL Schnoor, B Van Aken (Jan 2012). Biodegradation of mono-hydroxylated PCBs by *Burkholderia xenovorans*. *Biotechnol let*. 34(12): 2247-2252.

d) R Kaveh, S Ranjbar, B Van Aken. Changes in *Arabidopsis thaliana* gene expression in response to the antiviral drugs oseltamivir phosphate and zanamivir (*article in preparation*).

Presentations and Awards:

a) R Kaveh, B Van Aken (Feb 2014). Genetic response of plants exposed to anti-influenza drugs. Temple University School of Engineering Annual Poster Competition, Philadelphia, PA (third place).

b) R Kaveh (Jun 2014). Energy Path 2014 Convergence Conference, Allentown, PA. (Sustainable Energy Fund scholarship awardee).

c) R Kaveh, B Van Aken (Oct 2013). Transcriptional response of *Arabidopsis thaliana* exposed to the antiviral drugs oseltamivir and zanamivir. Student Scholar for the 10th International Phytotechnologies Conference, Syracuse, NY (travel grant awardee).

CHAPTER 2 LITERATURE REVIEW

2.1 Introduction

This chapter reviews the sources, fate, biodegradation, and ecotoxicological effects of the environmental contaminants selected for this study. It also reviews the characteristics of the plant species used in this investigation. The chapter provides an overview of the mechanisms, applicability, and limitation of phytoremediation for the treatment of soil and groundwater contaminated by environmental pollutants. Then, the fundamentals and usefulness of whole-genome expression analysis are briefly presented and discussed. Finally, a section about the production of biofuel from plant feedstock concludes the chapter.

2.2 Environmental Contaminants Selected for this Study

The toxic compounds selected for this study represent different classes of environmental contaminants, including conventional and so-called emerging contaminants, which include silver nanoparticles (AgNPs) and silver ion (Ag^{+}), the antiviral drugs, oseltamivir phosphate (OSP) and zanamivir (ZAN), and the more conventional contaminants, 2,4,6-trinitrotoluene (TNT) and polychlorinated biphenyls (e.g., 2,4'-dichlorobiphenyl - 2,4'-DCB).

2.2.1 Ecotoxicology and Fate of AgNPs in the Environment

Engineered nanoparticles (ENPs) are engineered structures with at least one dimension of less than 100 nm. Because of their small size and large surface area, NPs exhibit unique physicochemical properties leading to their utilization in an increasing number of products and processes, including textiles, electronics, pharmaceuticals,

cosmetics, and water treatment systems [2]. However, their special properties making ENPs attractive for technological applications, which make them interact with biological systems. ENPs have recently raised environmental concerns because they are released into the environment as a consequence of their widespread utilization and also because they have been shown to exert particle-size specific toxic effects on most living organisms [3, 4]. Regulations regarding the release of ENPs in the environment have been slow to emerge because of the relatively recent recognition of their environmental effects, the broad range of their application (e.g., industry, cosmetics, medicine), and the lack of characterization of their toxic effects [5, 6]. In the U.S., the utilization and potential release of ENPs are regulated by the Environmental Protection Agency (EPA), Toxic Substances Control Act (TSCA). Although the EPA is currently developing a Significant New Use Rule (SNUR) to ensure that nano-scale materials receive appropriate regulatory review, it appears that there is currently no specific regulation for the utilization, release, and maximum acceptable levels of ENPs in the environment [7].

ENPs interact with biological systems in very specific ways related to their small size, large surface area, and intrinsic reactivity [8, 9]. ENP sizes are of the same order of magnitude as most macromolecules (e.g., proteins, nucleic acids) and cellular organelles (e.g., ribosomes, mitochondria), which confer them special biological activities [10]. In addition of their nanosize, metallic ENPs possess specific properties that associated with the composing metal(s). In summary, there are four major ways by which ENPs can affect biological systems: (1) chemical processes, (2) mechanical processes, (3) catalytic processes, and (4) surficial processes [11]. (1) Metal ENPs have very large surface areas allowing them to dissolve easily in biological fluids. Resulting soluble species are toxic

ions that can bind thiol groups in proteins and are responsible of oxidative stress through the generation of ROS. (2) ENPs are also believed to have a purely mechanic effect by direct interaction with cellular structures and by obstructing pores in biological walls and membranes. (3) Soluble metal ions in the cell are frequently bound to specific molecules (chelators) and transporters and are subjected to cellular compartmentalization. On the contrary, metal species constituting NPs are not subjected to cellular regulation and can still exhibit catalytic activity, possibly resulting in generation of excessive amount of metabolic products. (4) Oxidized metal species at the surface of ENPs are negatively-charged and can strongly bind positive functional groups, which can lead to inactivation of biological molecules [11].

Prior research has shown that ENPs can significantly affect the growth of plant species. ENPs have been suggested to enter plant tissues through via pores in the cell wall and endocytosis. Once inside plant tissues, ENPs can be transported to other plant organs through the vascular system [2, 12]. Prior studies on the toxicity of ENPs for plants have been largely based on easily observable parameters, including germination rate, biomass growth, and transpiration volume, which have shown both positive effects at low exposure levels and negative effects at high exposure levels [13, 14, 15]. The mechanisms of toxicity of metal ENPs in plants include surface coating and pore obstruction which reduces the hydraulic fluxes and the uptake of nutrients, oxidative stress by the generation of ROS, toxic effects related to dissolved metal, inhibition of the photosynthetic activity, and potential negative effect on the microbial community in the root zone (rhizosphere) [2, 12].

Silver nanoparticles (AgNPs) are particles within the size range of approximately 1-100 nm and they have been shown to have specific physical and chemical properties different than soluble silver and/or bulk (not nanosized) silver particles [16]. Primarily because of their specific physicochemical properties and antimicrobial properties, AgNPs have been used in a wide variety of products, including textiles, bandages, deodorants, baby products, toothpaste, air filters, and house appliances [17, 18]. Benn and Westerhoff (2008) measured the amount of silver metal (Ag) in 6 types of socks and they reported that socks containing 1.36 mg-Ag/g-sock could release up to 0.65 mg Ag when soaked in 500 mL distilled water [19]. The predicted amount of AgNPs in soil treated with municipal sludge, in Europe, is 0.0015 mg / kg-soil and it shows an increase from 0.0023 to 0.0074 mg / kg-soil in the U.S. between years 2008 and 2012 according to Schlich1et al. (2013). According to their experimental investigations, 90% of AgNPs absorb into biosolids and will be transferred to the soil through biosolids land application [20].

The ecotoxicology of AgNPs is especially complex because it may be related simultaneously to silver-specific and/or nanoparticle-specific biological effects [21, 15]. Both AgNPs and dissolved silver have been shown to be toxic for bacteria, algae, aquatic organisms, plants, and humans [22, 23, 24].

Since plants constitute the basis of the terrestrial food chain, their exposure to AgNPs has potential implications for agriculture and human health [22]. Potential uptake of AgNPs by agricultural plants has raised concerns about the contamination of the food chain and consequently animals, including humans. AgNPs released from consumer products are likely to enter the wastewater. In wastewater treatment plants, AgNPs

partition between biosolids and treated water, which can both be used in agricultural fields through fertilization (biosolids) or irrigation (reclamation water) processes [25, 26].

2.2.2 Ecotoxicology and Fate of Antiviral Drugs in the Environment

Pharmaceuticals used in human and veterinary medicine have contributed to significantly increase the quality of life and life expectancy [27]. However, following their use, pharmaceuticals are released into the environment and they are increasingly considered as a new class of emerging contaminants because of their potential impact on wildlife and human health [28]. Because of their designated functions, these compounds have specific biological activities and are rather recalcitrant to biological degradation, making them potentially harmful for aquatic organisms. Recent developments of sensitive analytical methods has allowed the detection of very low concentrations of pharmaceuticals in various environmental samples [29, 28].

Following their intake in the body, pharmaceuticals are largely excreted (in their native form or as metabolites) into wastewater. Unused pharmaceuticals are also frequently disposed in wastewater: for instance ibuprofen, one of the most commonly used and detected over-the-counter anti-inflammatory drug, has been measured in wastewater influents at concentration as high as 22.7 µg/L during the dry months of the year [30]. Municipal sewage is therefore considered the main route of entrance of human pharmaceuticals into the environment. Conventional wastewater treatment processes are originally designed to remove degradable organic compounds (BOD) found in municipal wastewater and they are not necessarily well adapted to remove potentially toxic and recalcitrant pharmaceuticals [31]. Incomplete removal of pharmaceuticals in wastewater treatment operations leads to their persistence in treated water and accumulation in

municipal sludge. Gros et al. (2010) evaluated the removal efficiency of various pharmaceuticals, including ofloxacin, atenolol, and ibuprofen, from WWTP and they reported levels of 40, 59, and 91%, respectively [32]. Pharmaceuticals are then discharged in significant amounts in receiving waters and/or applied in land with organic fertilizers (i.e., municipal biosolids) [33]. Many studies about biodegradation of pharmaceuticals have focused on wastewater treatment processes and little is currently known about the environmental fate and transport of pharmaceuticals and hormones. Current research suggests that pharmaceuticals enter the environment and persist to a greater extent than it was first believed [28].

An increasing body of knowledge has been published about the capability of higher plants for the removal of pharmaceuticals and personal care products from wastewater, soil, and groundwater. As for other conventional pollutants, removal of pharmaceuticals by plants depends largely on the physical and chemical properties of the compound and the selected plant species. Even though many reports have documented the efficient uptake of pharmaceuticals by plants, information about the plant metabolism of pharmaceuticals by plants is scarce. Especially, very little is known about the metabolic pathways, enzymes, and molecular bases of the transformation of pharmaceutical compounds inside plant tissues. However, understanding the plant metabolism of pharmaceuticals is critical because in the absence of further transformation and detoxification, pharmaceuticals and/or their metabolites taken up by plants will enter the food chain or return to the soil, resulting in a potential hazard for human health. Moreover, the metabolism of xenobiotic pollutants by plants could, in some instances,

results in an increase of toxicity, further threatening human health and the environment [34].

Antiviral drugs are the medicines that help the body fight viral infections, including influenza. Among them, neuraminidase inhibitors are specifically effective on influenza viruses. Neuraminidase inhibitors deactivate the enzyme, neuraminidase, which allows the virus to enter and leave the host cell by hydrolyzing the cell membrane. Preventing viral particles to spread and infect other cells would slow down the dispersion of the virus in the body and, therefore, limit the infection and contagion [35].

Zanamivir (ZAN) was the first neuraminidase inhibitor drug commercially developed. It is currently marketed under the trade name, Relenza, and it is formulated as a powder for oral inhalation. Its chemical formula is $C_{12}H_{20}N_4O_7$ with a molar mass of 332.31 g/mol. ZAN has a water solubility of approximately 18 mg/mL at 20°C [36, 37]. ZAN is not significantly metabolized in human body and is mostly discharged in the urine as unchanged [38].

Oseltamivir phosphate (OSP), which is commercialized under the trade name Tamiflu, is another neuraminidase inhibitor antiviral drug. The chemical formula of oseltamivir is $C_{16}H_{28}N_2O_4$ and its molecular weight is 312.4 g/mol for the free base form and 410.4 g/mol for the phosphate salt [37]. Aqueous solubility of OSP is 588 mg/mL at 25°C [39]. Figure 2.1 shows the structures of OSP and ZAN.

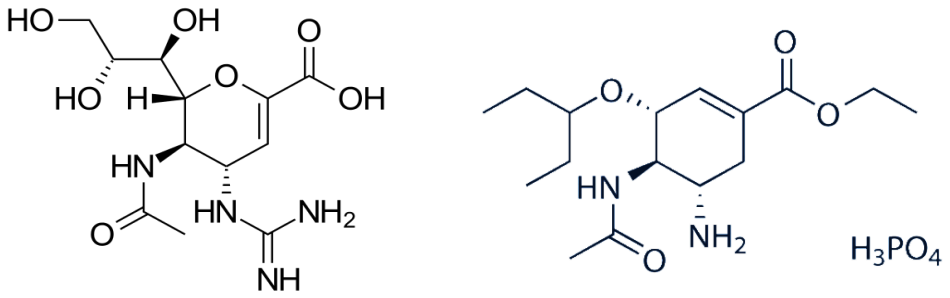

Figure 2.1. Chemical structure of zanamivir (ZAN - left) and oseltamivir phosphate (OSP - right)

OSP ingested is excreted from the human body primarily as OSP (15%) and OC (80%). OSP and OC are rather stable in water and through sewage treatment plants (STP) [41]. OSP is a prodrug: it is metabolized in the liver and transformed into OC which is the biologically active metabolite of the drug (Figure 2.2). Oseltamivir carboxylate (OC) carries both amine and carboxylate groups increasing the water solubility of the molecule [40].

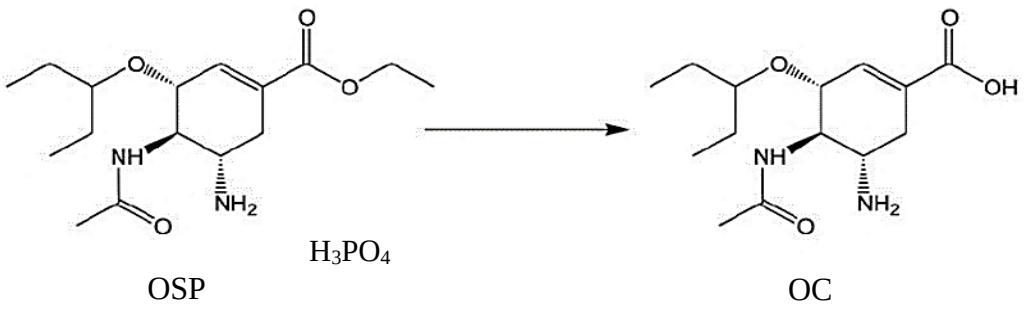

Figure 2.2. Hydrolysis of oseltamivir (OS) to its active metabolite, oseltamivir carboxilate (OC) [42]

Antiviral drugs reach the sewage system after they are excreted from the body. The release of neuraminidase inhibitor drugs into the environment increases markedly during the influenza season and it is expected to be the highest during an influenza pandemic. Japan has currently the highest consumption rate of antiviral drugs. In three

rivers in Japan, the concentration of OC was reported to change from non-detected level to a maximum of 58 ng/L after the flu season peak [43]. Singer et al. (2007) monitored 5 water catchments (drainage basin) in the UK and 11 catchments in the U.S. and they used the results to calibrate a hydrologic model to estimate the concentrations of OC in the water during an influenza pandemic [44]. The results indicate that OC concentrations in UK and U.S. catchments could reach 28 and 35 µg/L, respectively. (The model assumes that (1) all clinical cases were treated at the first sign of infection with a full course of Tamiflu, (2) Tamiflu was used only by clinically infected people, (3) 80% of the ingested Tamiflu was released as OC, and (4) all of the OC entering the catchment was flushed out in 1 day [44].) A study in the urban area of the Yodo River system in Japan by Azuma et al. (2013) showed that the highest median concentrations of OSP, OC, and ZAN in STP effluents were 86.7, 456, and 14 ng/L, respectively. The authors mentioned that the median values of ZAN were ten times lower than OSP and OC in all samples [41]. Based on the estimated toxicity and the reported concentrations in surface waters during seasonal or pandemic influenza outbreaks, OSP and its metabolites do not seem to pose a threat for the environment, although they may lead to the development of antiviral resistance [45, 46]. Similarly ZAN has not shown genotoxic or reproductive toxicity on animals at levels 17 to 197 times higher than the regular therapeutic dose (20 mg/day) [38]. Data about the acute and chronic toxicities of OSP on algae, daphnia, and fish in surface water is summarized in Table 2.1 [46, 47].

Table 2.1. OSP acute and chronic toxicity in surface water

Species	EC50 mg / L	NOEC mg / L
green algae	59	10
Daphnia	33	-
Fish	>100 HTC	-

HTC: highest tested concentration, NOEC: no observed effect concentration, EC50: half maximal effective concentration

Escher et al. (2010) observed that *Vibrio fisheri* bacterium shows more sensitivity to OC than OSP, although *Pseudokirchneriella subcapitata* microalga is more sensitive to OSP [48]. OSP and its photo-degraded metabolites showed no acute toxicity on the New Zealand marine copepod, *Quinquelaophonte* sp. [49]. To determine the potential effect of OSP on the microbial population in different water and wastewater samples, Fick et al. (2007) and Straub (2009) used gel electrophoresis and quantitative PCR analysis, which showed that the compound would not affect the microbial structure at the environmental concentrations [45, 47].

Antiviral drugs and their metabolites are rather stable in the environment. During the influenza seasons 2008-2009 and 2009-2010 in Japan, the removal of OC was monitored in selected STPs for all treatment processes, including primary, biological, and advanced treatments, showing removal efficiencies of 2-9%, 20-37% and up to 90%, respectively. OC concentration in STP influents ranged from 140 to 460 ng/L during the influenza season [50]. Regular sewage treatment systems are not able to remove OC, primarily because of the short retention time of these systems (less than 24 h). Longer incubation periods (40 days) have been shown to increase the mineralization of OC to up to 76% in biological tank and 37% in effluent water [51]. Studies have shown that OC can be used as carbon and energy source by two isolated bacterial strains, *Nocardioides* sp. and *Flavobacterium* sp. [45, 47]. Also Caracciolo at al. (2010) observed an increase in

Protobacteria abundance after adding OC to water samples, suggesting that the compound can be degraded by the bacteria [52]. Advanced oxidation techniques applied in STPs (e.g., ozonation [42] and photodegradation [49]) have shown relatively high removal efficiencies toward OSP.

2.2.3 Ecotoxicology and Fate of TNT in the Environment

The most commonly-found explosive in the environment is the nitroaromatic compound, 2,4,6-trinitortoluene (TNT). TNT is made of a toluene aromatic ring bearing three nitro groups with the chemical formula $C_7H_5N_3O_6$. It is a pale yellow, odorless chemical in the crystal form with a density of 1,654 kg/m^3. Figure 2.3 shows the TNT structure. TNT has a low solubility in water (130 mg / L at 20°C), but it is soluble in organic solvents. The hydrophobicity of TNT makes it less bioavailable and quite recalcitrant to biodegradation. TNT has an octanol-water partitioning coefficient (K_{ow}) of 1.6 and organic carbon-water partitioning coefficient (K_{oc}) of 1,100. Its vapor pressure at 20°C is 1.99×10^{-4} mm Hg [53].

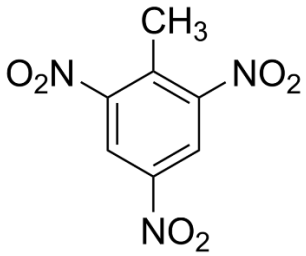

Figure 2.3. Chemical structure of 2,4,6-trinitortoluene (TNT)

Industrial uses of TNT, as an explosive in mining, road construction, and ammunition in military sites and ranges, have led to the widespread contamination of the environment over the years. Manufacturing, waste handling, improper storage, and

landfilling of TNT are the major causes of its release into the soil, groundwater, and air. TNT is also used as a chemical intermediate in the manufacture of photographic chemicals and dyes [54].

The highest TNT concentrations measured in soil at military sites were commonly within the range of 4,000 to 10,000 mg / kg [55, 56]. However, the concentration levels of explosive wastes in the soil at some ammunition production sites has been reported as high as 200 g/kg [57, 58]. A munition factory can produce 2×10^6 liters of contaminated wastewater per day from just one production line [59]. The concentration of TNT in a groundwater sample from an ammunition production facility was found to be 228 μg/L [60]. In the U.S. only, the soil contaminated by explosives as a result of military activities was estimated to be over 1.2 million tons [61].

Nitro-substituted explosives were shown to be toxic to most classes of living organisms [62, 63]. TNT exhibits acute and chronic toxicity towards different types of organisms, such as bacteria, algae, plants, animals, and humans. TNT has been reported mutagenic for both mammalian and prokaryotic cells [64]. According to the U.S. EPA, TNT is a potential human carcinogen (class C). Direct contact with TNT can cause anemia, liver disorder, skin irritation, and immune system damage [62].

Many different methods have been used to remove TNT from contaminated soil or water, including incineration, composting, activated carbon adsorption, bio-augmentation, and phytoremediation. Because of their toxicity and hydrophobicity, nitro-substituted explosives are rather resistant to biological degradation. However, biodegradation methods are attractive because they are cost-effective and less destructive to the environment. Microbes, fungi, and plants also have been used for TNT

bioremediation [61]. White-rot fungi were shown to mineralize TNT [64]. For instance, bioaugmentation of TNT-contaminated underground water with the enriched bacterial culture from a contaminated site showed an active degradation of TNT [66]. TNT in soil has the tendency to stay associated with the organic phase. TNT is more bioavailable in the aqueous phase, even though laboratory trials have showed efficient TNT uptake in both hydroponic and soil systems. TNT is typically tightly bound to the roots and can be efficiently transformed in plant tissues. For instance, it has been shown that up to 75% of TNT taken up into poplar plants stayed in the roots and more than 10% was translocated to the leaves. In plant tissues, TNT is fast transformed into 4-amino-2,6-dinitrotoluene (4-ADNT) and 2-amino-4,6-dinitrotoluene (2-ADNT) by plants [66]

2.2.4 Ecotoxicology and Fate of PCBs in the Environment

Polychlorinated biphenyls (PCBs) are composed of a biphenyl core substituted with chlorine atoms. PCB physical appearance varies from an oily liquid to a waxy solid. PCBs are hydrophobic and chemically stable [68]. PCBs that are liquid at room temperature have a density ranging from 1,182 to 1,566 kg/m^3. PCBs have low water solubility and are readily soluble in organic solvents. PCBs have extremely high thermal and chemical stability.

In general, the melting point and the lipophilicity of PCBs increase with the degree of chlorination and the vapor pressure and the water solubility decrease when increasing the degree of chlorination [69]. There are 209 different PCB congeners bearing one to ten chlorine atoms with a water solubility range from 7 to 0.12×10^{-5} mg / L [69]. The general PCB structure is shown in Figure 2.4.

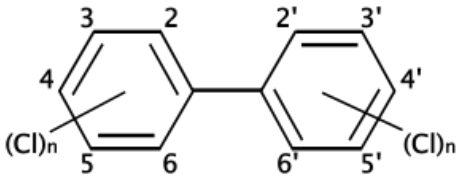

Figure 2.4. General structure of PCBs

Specific properties, such as chemical stability, resistance to fire, high dielectric constant, and high boiling point, have led PCBs to be utilized in many industrial applications, such as heat transfer and electrical equipment. PCBs have been also used in pigments and dyes, plasticizers in plastics, paints, rubber products, etc. Before the discontinuance of PCBs production in 1977, over 1.5 billion pounds were produced just in the U.S. [68]. PCB emissions can originate from different anthropogenic sources, such as usage, disposal, and accidental release [70].

Having a stable structure, PCBs are rather resistant to degradation and they are classified as persistent organic pollutants (POPs). PCBs are hydrophobic and tend to accumulate in fatty tissues in mammals. Toxicity of PCBs has been known since 1930s [70]. Chronic exposure to PCBs can cause severe neurobehavioral, immunological, reproductive, and endocrine disorders in children [71, 72], even though the acute toxicity for adults is somewhat low. Adults' exposure to PCBs can cause thyroid hormone depletion and they have been shown to decrease vitamin A in rodents [74]. Hung et al. (2012) used zebrafish as live biosensor and they reported that zebrafish was affected by PCBs at levels as low as 0.04 µg/L [75]. According to the Department of Health and Human Services (DHHS), U.S. EPA, and International Agency for Research on Cancer (IARC), PCBs are suspected to be carcinogenic in animals and humans [70, 75, 76].

PCBs are EPA Priority Pollutants (http://oaspub.epa.gov/) and they are ranked fifth in the 2007 CERCLA (Comprehensive Environmental Response, Compensation, and Liability Act) Priority List of Hazardous Substances (http://www.atsdr.cdc.gov/).

Removal of PCBs from the environment has been a challenging task due to their low concentration and the large variety of congeners characterized with different physico-chemical properties and their susceptibilities to biodegradation. Conventional methods of PCB remediation include incineration and landfilling. However, many alternative strategies have been proposed for the remediation of PCBs, such as solvent extraction, thermal desorption, chemical oxidation, and bioremediation. Bioremediation includes the use of bacteria or plants (e.g., phytoremediation) to degrade the PCBs. Plants, in particular, have been shown capable to achieve limited uptake, accumulation, and transformation of PCBs from soil and water [78].

Two major microbial metabolic pathways -- anaerobic and aerobic -- are known for PCB degradation depending on the chlorination degree of the PCB congener, the redox conditions, and the type of microorganisms [76]. PCBs with at least four chlorine atoms undergo anaerobic reductive dechlorination, a process in which PCBs play as electron acceptors to oxidize organic carbon [79]. Microorganisms that reductively dechlorinate PCBs are related to *Dehalococcoides* [80, 81]. Lesser chlorinated PCB congeners (three chlorine atoms or less) undergo co-metabolic aerobic oxidation mediated by specific biphenyl dioxygenases. This process results in ring-opening of the biphenyl core and can potentially lead to complete mineralization of the molecule [82, 83, 84]. Bacterial species capable of oxidative degradation of PCBs generally belong to the genera *Pseudomonas, Burkholderia, Comamonas, Rhodococcus,* and *Bacillus*. The

number and position of chlorine atoms in the PCB molecule is known to affect biodegradability of PCBs through both aerobic and anaerobic pathways [84, 83, 85]. Indeed, these parameters affect the bioavailability of PCB congeners and therefore their biodegradability. According to McFarland et al. (1996), the organic carbon content of soil and sediments also affects the bioavailability of PCBs [86]. In another study, Swackhamer et al. (1987) reported that, in addition to the total organic carbon (TOC), the organic carbon-water partitioning coefficient (K_{oc}) versus octanol-water partitioning coefficient (K_{ow}) relationship has to be considered to determine the partitioning characteristics of PCBs. The authors determined that the log K_{oc} of a range of PCBs in Lake Michigan ranged between 5.90 and 6.65, which affected the PCBs' fate in the water column [86].

2.3 Plant Species Used in this Study

The species selected for this study, *A. thaliana* and *G. max*, are well-studied, model plant species that have been used in extensively in both toxicological and phytoremediation studies [88, 89, 90]. *A. thaliana* is a small flowering plant native to Europe and Asia [91]. It is the favored model organism in plant biology and genetics (Figure 2.5). *A. thaliana* has a short growth period, making it a suitable model plant for laboratory experiments. Moreover, its genome has been fully sequenced and is publicly available. The Arabidopsis Information Resource (TAIR) is a web-based database that maintains genetic and molecular biology data for *A. thaliana* [92]. A higher flowering plant, *A. thaliana* has a comparatively small genome, which is approx. 135 megabase pairs (Mbp). The sequencing of the *A. thaliana* genome was completed in 2000 [92]. As a model plant, *A. thaliana* has been used in a variety of phytoremediation studies involving

transgenic plants. For instance, transgenic *A. thaliana* expressing a vacuolar proton pump was developed for the removal of the toxic fertilizer byproducts, phosphogypsum [88]. In another study, transgenic *A. thaliana* strains expressing an exogenous bacterial triphenylmethane reductase were shown to tolerate high levels of toxic triphenylmethane dyes [93]. In addition, *A. thaliana* was used as a model to study and improve crop tolerance to various stresses, including salt, cold, and drought [94]. Two species of *Arabidopsis* (*A. halleri* and *A. thaliana*) were used to develop a standardized test to determine the short-term tolerance of plants to zinc (Zn), cadmium (Cd), and nickel (Ni). The test was reported to provide a fast and reliable assay to assess heavy metal tolerance in plants [95].

Figure 2.5. *Arabidopsis thaliana* plants, final growth phase [96, 97].

Soybean (*G. max*) (Figure 2.6) is a legume species originating from East Asia. Soybean produces an edible bean with a multitude of uses. The soybean is an affordable and widely-used source of protein and it is classified as an oil seed plant by the UN Food and Agricultural Organization (FAO) [97]. The soybean genome was completely sequenced

in 2008 and contains approximately 950 Mbp [99]. Soybean is among the plants that are promising candidates for industrial-scale biofuel production [100].

Figure 2.6. Soybean (*Glycine max*) growth phases (left); soybean farm (right) [101, 102].

Besides these characteristics, soybean is an attractive candidate species for the phytoremediation of contaminated soils [103, 104, 70]. Soybean has been shown that actively take up and bioaccumulate pharmaceuticals (antibiotics) from different media. For instance, soybean plants were reported to accumulate up to 190 mg / kg (dry weight) oxytetracycline and 110 mg / kg of norfloxacin [105]. In another study, Cropp et al. (2010) used a two-compartment (soil/water) model to predict the uptake of the antibiotic norfloxacin by soybean plants. The authors predicted a maximum concentration of 52.5 mg / kg (dry weight) in plant tissues after 2.8 days of exposure [106]. Soybean was also shown to efficiently perform phytoextraction of lead (Pb) from soil contaminated with up to 25 mg / kg Pb [107].

2.4 Phytoremediation

Phytoremediation is one of the several biotechnologies that have been proposed for the removal of the environment contaminants from soil and groundwater. Phytoremediation is an emerging technology that makes use of plants and associated bacteria for the treatment of soil and groundwater contaminated by toxic pollutants.

Plants have been shown to efficiently take up and, to some extent, metabolize environmental pollutants and phytoremediation have been proven an efficient bioremediation strategy in many laboratory and filed studies [107, 108]. Mentioning phytoremediation efficiency for the treatment of oil-contaminated sites, Frick et al. (1999) called plants "organic pumps" for the removal of contaminants [110].

2.4.1 The Bioremediation Concept

Living organisms are commonly exposed to natural or xenobiotic toxic compounds. As a consequence, they have developed multiple detoxification mechanisms to prevent harmful effects from exposure to these compounds. Bacteria, more than higher life forms, are extremely versatile organisms, which allows them to constantly develop new metabolic pathways for the degradation of a large range of xenobiotic pollutants [111]. While provided with lower adaptation capabilities, higher organisms, such as plants and mammals, also possess detoxification mechanisms to counteract the harmful effects of toxic contaminants [112].

Bioremediation exploits the natural capability of living organisms to degrade toxic chemicals. Traditional remediation technologies of polluted sites requires soil excavation and transport, prior to treatment by incineration, landfilling or compositing, which is costly, damaging for the environment, and in many cases, practically infeasible due to the range of the contamination. There is therefore a considerable interest in developing cost-effective alternatives based on microorganisms or plants. Because of its potential for the sustainable mitigation of environmental pollution, bioremediation has been listed among the "top ten biotechnologies for improving human health" [112].

2.4.2 Bioremediation by Higher Plants (Phytoremediation)

The biodegradation of xenobiotic compounds by plants has been known for a long time. Land farming of wastewaters has been a treatment technology for at least 300 years, and wetland treatment of wastewater and the use of plants to control air pollution have been used for several decades [114]. Plant-mediated bioremediation of metal-contaminated soil was proposed first in the 1970s [114]. Because of their natural capability to absorb minerals, plants efficiently remove heavy metals from polluted soils [107]. Although the metabolism of xenobiotics by plants is known for a long time, the idea that plants can be used to detoxify organic compounds emerged in the 1970s with the discovery of the metabolism of 1,1,1-trichloro-2,2-bis-(4'-chlorophenyl) ethane (DDT) and benzo(a)pyrene [115]. Since then, phytoremediation acquired the status of a proven technology for the remediation of soil and groundwater contaminated by a variety of organic compounds, including pesticides, chlorinated solvents, explosives, polyaromatic hydrocarbons (PAHs), and polychlorinated biphenyls (PCBs) [107, 116]. Phytoremediation has been extensively reviewed in the literature (see for instance [89, 117, 107, 108])

2.4.3 Advantages and Limitations of Phytoremediation

Phytoremediation offers several advantages over other remediation strategies: low cost because of the absence of energy-consuming equipment and limited maintenance, no damaging impact on the environment because of the in situ nature of the process, and large public acceptance as an attractive green technology. In addition, phytoremediation offers potential beneficial side-effects, such as erosion control, site restoration, carbon sequestration, and feedstock for biofuel production [117]. As autotrophic organisms,

plants use sunlight and carbon dioxide as energy and carbon sources. From an environmental standpoint, plants can be seen as natural, solar-powered, pump-and-treat systems for cleaning up contaminated soils [119].

However, phytoremediation also suffers serious limitations that may impair the development of field applications [107, 108]. Phytoremediation is limited to shallow contamination of "moderately hydrophobic" compounds susceptible to sorption by/to the roots. More importantly, remediation by plants is often slow and incomplete. As a corollary to their autotrophic metabolism, plants usually lack the biochemical machinery to achieve full mineralization of many organic pollutants, especially the most recalcitrant, such as PAHs and PCBs [108]. Phytoremediation can therefore lead to non-desirable effects such as the accumulation of toxic pollutants and metabolites that may be released to the soil, enter the food chain, or be volatilized into in the atmosphere [119, 120].

2.4.4 Phytoremediation Processes

Phytoremediation encompasses a range of processes beyond direct plant uptake and metabolism, and it is best described as plant-mediated remediation. While definitions and terminology vary, the different processes involved as part of phytoremediation can be summarized (Figure 2.7). An extensive list of these physiological processes and their multiple names is presented in McCutcheon and Schnoor (2003) [113]. The simplified descriptions below are based on the recognition of the following mechanisms: phytotransformation, phytoextraction, rhizofiltration, phytovolatilization, phytophotolysis, rhizodegradation, phytostabilization, and hydrological control.

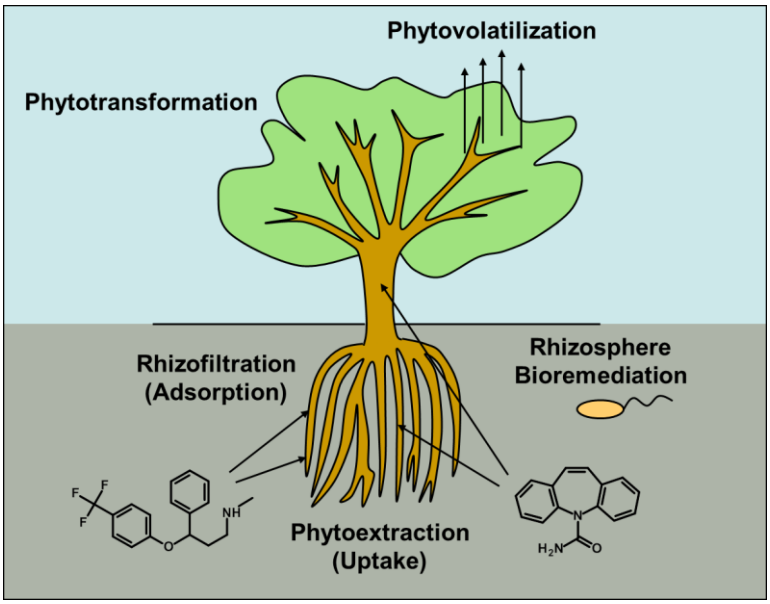

Figure 2.7. Phytoremediation involves several processes: Pollutants in soil and groundwater can be taken up inside plant tissues (phytoextraction) or adsorbed to the roots (rhizofiltration); pollutants inside plant tissues can be transformed by plant enzymes (phytotransformation) or can volatilize into the atmosphere (phytovolatilization); pollutants in soil can be degraded by microbes in the root zone (rhizosphere bioremediation) or incorporated to soil material (phytostabilization) (adapted from Van Aken, 2008) [121].

Phytotransformation refers to the metabolism of (organic) pollutants inside plant tissues [113, 108]. The process involves first the uptake of pollutants from soil or groundwater by the roots, which depends largely on the hydrophobicity of the chemical, represented by the octanol-water partition coefficient, log K_{ow}. Experimental relationships based on log K_{ow} can be used to predict the sorption of specific chemicals to the roots (root concentration factor, RCF) and the uptake and translocation of chemicals inside plant tissues through the transpiration stream (transpiration stream concentration factor, TSCF) [121]. Typical applications for phytotransformation include sites contaminated by organic biodegradable contaminants, such as explosives and energetic compounds, petrochemicals and PAHs, chlorinated solvents, pesticides and fertilizers, and landfill leachates [121, 108].

Phytoextraction refers to the use of plants for the uptake, translocation, and accumulation of contaminants from soil or groundwater inside the roots and aerial plant organs [123]. *Rhizofiltration* describes the sorption, concentration, or precipitation of metal contaminants from surface water or groundwater on the plant roots [107]. Phytoextraction and rhizofiltration typically apply to elemental contaminants (metals) not susceptible to biodegradation.

Volatile contaminants taken up inside plant tissues can be volatilized through the leaves via a process known as *phytovolatilization*. Volatile organic compounds, such as solvents and other chlorinated organic chemicals, are therefore susceptible to volatilization into the atmosphere [124, 121].

Phytophotolysis refers to the degradation of contaminants taken up and translocated to leaf tissues by exposure to light. Energetic UV radiation from sunlight has long been recognized as capable to breakdown a range of organic molecules. An indirect effect of sun light is the generation of free radicals and oxygen reactive species (ROS) that can further react with organic molecules [124].

Rhizodegradation (also known as *rhizosphere biodegradation*) refers to the enhancement of microbial activity and biodegradation of pollutants in the root zone [126, 111]. Root exudates and root turnover increase soil organic carbon, which is beneficial both for microbial growth and co-metabolic biodegradation. Root exudates also contain organic acids and catabolic enzymes, which can increase bioavailability and biodegradation of hydrophobic pollutants and complexation of heavy metals [127].

Phytostabilization is the use of vegetation to hold soil and sediments in place, immobilize toxic contaminants in soil, or stabilize dissolved phase plumes in order to

mitigate their impact on the environment [107]. Transpiration of large amounts of water by trees can prevent migration of plumes of toxic pollutants towards groundwater or receiving water (this process also refers as hydraulic control) [128].

2.4.5 Metabolism of Xenobiotic Compounds by Plants

Being exposed to a variety of natural allelochemicals and xenobiotic compounds, plants have developed diverse detoxification mechanisms of organic compounds [129]. Based on the early observations that plants were capable of metabolizing organic xenobiotic pollutants (pesticides), Sandermann 1994 introduced the *green liver* concept, which typically occurs in three phases (Figure 2.8) [111]. The initial activation (phase I) consists of the enzymatic oxidation, reduction, or hydrolysis of the xenobiotic compound (e.g., cytochrome P-450 monooxygenases). In phase II, the resulting activated product undergoes a transferase-catalyzed conjugation with a molecule of plant origin, forming a less toxic and more soluble than the parent pollutant (e.g., glutathione *S*-transferase or glycosyltransferases. Phase III typically involves the sequestration of the conjugate, which can be stored in plant organelles such as vacuoles, or incorporated into biopolymers such as lignin [115, 111].

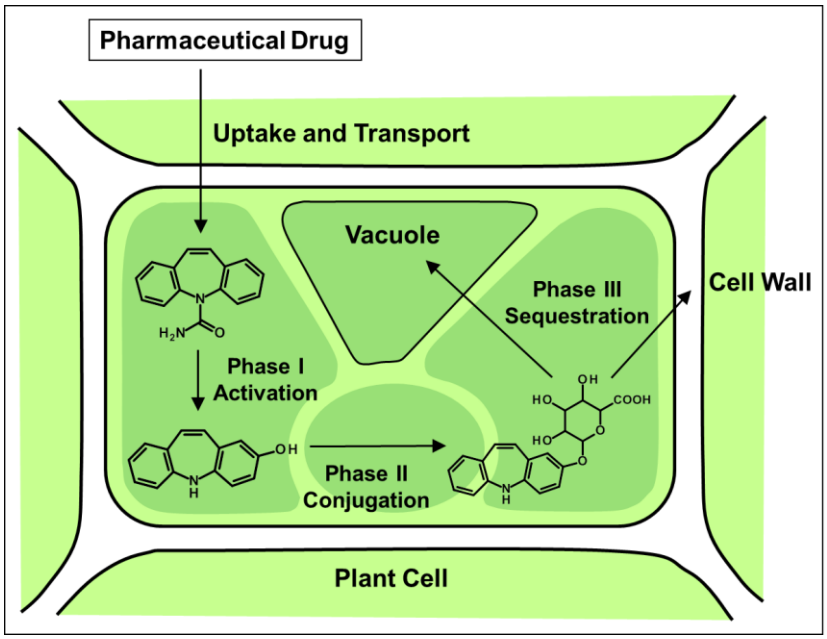

Figure 2.8. The three phases of the green liver model: Hypothetical pathway representing the metabolism of carbamazepine in plant tissues: phase I: Activation of carbamazepine by hydroxylation and hydrolysis to 2-hydroxyiminostilbene; phase II: Conjugation with a glucose to form a O-glucuronide; phase III: Sequestration of the conjugate into the cell wall or in the vacuole (adapted from Van Aken 2008 and Celiz et al. 2009) [121, 34].

2.4.6 Phytoremediation and Effect of AgNPs and Ag^+ on Plants

Previous studies have reported both positive and negative effects of AgNPs on plants. Investigating the impact of AgNPs of different sizes (from 2 to 20 nm) on barley (*Hordeum vulgare*), flax (*Linum usitatissimum*), and ryegrass (*Lolium perenne*), El-Temsah and Joner (2012) reported a significant reduction of the germination and growth rates, which were dependent on the plant species and concentration of AgNPs: e.g., 20 nm particles resulted in a noticeable reduction of the shoot length at 10 mg / L in flax and ryegrass and at 20 mg / L in all three species tested [130]. Another study reported a limited effect of AgNPs (30 nm) on cucumber (*Cucumis sativus*) and lettuce (*Lactuca sativa*). Germination rates were reduced by 24% and 5% and root elongation rates were reduced by 15% and 2% after exposure to 100 mg / L AgNPs in cucumber and lettuce,

respectively [131]. Kumari et al. (2009) studied the cytotoxicity and genotoxicity of 100-nm AgNPs on onion root tip cells (*Allium cepa*). Based on microscopic observations, cells exposed to increasing concentrations of AgNPs (from 25 to 100 mg / L) showed a decrease of the mitotic index (MI) from 60% to 28% and the occurrence chromosomal aberrations [18]. A recent report from Wang et al. (2013) showed that exposure of *A. thaliana* and poplar (*Populus deltoides* × *nigra* DN34) plants to AgNPs produced beneficial effects at low concentration: e.g., exposure to 25-nm AgNPs resulted in increased biomass and evapotranspiration in poplars at the concentration of 1.0 mg / L, although exposure to 10 and 100 mg / L resulted in decrease of these parameters [15].

Different studies have reported effective uptake of AgNPs by plants [132, 15]. Wang et al. (2013) recently reported accumulation of Ag in hydroponic A. thaliana and poplar plants exposed to AgNPs (1.0 mg /L, 5 nm) to levels of 1.0 to 4 μg/g fresh weight. In a recent study, we similarly reported a dose-dependent accumulation of Ag in *A. thaliana* plants exposed to various concentrations of AgNPs (20 nm) [133] (see next section). Interestingly, AgNPs have been shown to exert both positive and negative effects on plant growth [130, 131]. Investigating the impact of AgNPs of different sizes (5 and 20 nm) in barley, flax, and ryegrass, El-Temsah and Joner (2012) reported a significant reduction of the germination and growth rates, which were dependent on the plant species and the concentration of AgNPs [131]. Wang et al. (2013) showed that exposure of poplar plants to AgNPs enhanced plant growth and transpiration rates at low concentration (e.g., 1.0 mg / L) although higher concentrations (e.g., 10 and 100 mg / L) resulted in decrease of these parameters [15]. In addition, our study on the exposure of A.

thaliana to AgNPs has identified transcriptional changes that are consistent with the inhibition of growth and increase of lignin synthesis (see next section) [14].

2.4.7 Phytoremediation and Effect of TNT on plants

The idea of using plants to remediate explosive-contaminated soil and water started in the mid-1990s [134]. Many studies have shown the plant potential for the bioconcentration and biotransformation of nitro-substituted explosives [135]. Lewis et al. (2004) reported that TNT contamination does not penetrate very deeply into the soil, which makes phytoremediation a potentially efficient strategy [61], although it is slower than conventional physicochemical processes [58, 57]. The initial concentration of TNT and the plant tolerance seem to be the limiting factors of TNT uptake by plants [58]. The toxic effect of explosives toward plants has been reported in many researches [136]. For instance, exposure of duckweed (*Lemna perpusilla* Torr) to 1 mg / L of TNT was reported to result in lethal effects [137]. In a similar study by Palazzo and Leggett (1986), TNT was shown to be toxic to yellow nutsedge (*Cyperus esculentus* L.) at 5 mg / L and to duckweed at above 1 mg / L [138]. Pavlostathis et al. (1998) examined the toxicity of TNT on the aquatic plant Eurasian watermilfoil (*Myriophyllum spicatum*): chlorosis[1] was observed after exposure to concentrations between 1.3 and 5.22 mg / L [139]. TNT causes less toxic effect in soil than in hydroponic media presumably because of its lower bioavailability due to binding to humic materials [136].

The uptake and/or metabolism of TNT by plants, including switchgrass, are well documented [134, 66]. TNT is known to be efficiently taken up inside plant tissues through the roots and then largely translocated to the leaves. Inside plant tissues, TNT is

[1] A condition in which leaves produce insufficient chlorophyll.

quickly reduced into aminodinitrotoluenes and diaminonitrotoluenes, which are less toxic and persistent than the parent TNT molecule [135, 140]. TNT has been shown to exert phytotoxicity at rather low doses. Thompson et al. (1998) reported that exposure of hydroponic poplar plantlets to TNT resulted in a dose-dependent reduction of both the transpiration rate and plant biomass at concentrations equal or above 5 mg / L [66]. Peterson et al. (1998) observed that the growth rate of roots and shoots of hydroponic switchgrass plants was significantly reduced by exposure to 15 and 30 mg /L TNT, respectively [142]. Gene expression studies (SAGE and microarrays) have revealed that exposure of A. thaliana to TNT (2.3 to 15 mg / L) resulted in up-regulation of several genes involved in lignin biosynthesis, including phenyl ammonium lyase, cinnamate 4-hydroxylase, 4-coumarate:CoA ligase, cinnamyl alcohol dehydrogenase, and UDP-glucosyltransferase [140, 141].

2.4.8 The effect of PCBs on Plants

The effects of PCBs and their metabolites have been studied on different species, such as mammals, plants, and bacteria. Plants show species-specific susceptibilities when exposed to PCBs. Uptake and potential transformation in plant tissues are the processes involved in phytoremediation. PCB congeners with less chlorine atoms are expected to be translocated at higher rate in plant tissues than higher chlorinated congeners [142]. Besides the uptake, PCBs have been shown to be, to some extent, metabolized inside plant tissues. For instance, Kucerova at al. (2000) studied the transformation of 22 PCB congeners by garden nightshade (*Solanum nigrum*) and showed that hairy root cultures can metabolize almost all of the congeners up to 72%. The authors mentioned that the position and number of chlorine atoms plays an important role in the conversion of the

compounds [144]. Using nine plant species[2], Zeeb et al. (2006) observed PCB concentrations ranging from 47 to 6,700 µg/g in root tissues and from 1 to 470 µg/g in shoot tissues (the PCB level of the contaminated soil ranged from 90 to 4,200 µg/g) [142].

PCBs tend to bind to soil particles and they are generally slowly taken up inside the plant tissues because of their high hydrophobicity. On the other hand, microorganisms of rhizosphere[3] may play an important role in PCB remediation in soil [145]. Microbes in the soil are more effective for the biodegradation of PCBs when they are in association with plants. Therefore, both rhizosphere biodegradation and plant uptake are processes involved in the phytoremediation of PCBs [117].

The first metabolites of PCBs that are formed in living organisms are hydroxylated PCBs (OH-PCBs). Backman et al. (2006) reported the presence of OH-PCBs in the plasma of Great Lakes fishes exposed to PCBs for 30 days [146]. Moza et al. (1979) described the production of mono-OH metabolites of PCB-4 (2,2′-dichlorobiphenyl) in sugar beet and carrot plants [147]. The authors also identified mono- and di-OH metabolites of PCB-31 (2,4',5-trichlorobiphenyl) in exposed carrot plants. Similarly, OH-metabolites of PCB-77 (3,3',4,4'-tetrachlorobiphenyl) have been detected in cultures of rose, tomato, sunflower, and lettuce plants by Bock et al. [147].

[2] *Festuca arundinacea, Glycine max, Medicago sativa, Phalaris arundinacea, Lolium multiflorum, Carex normalis,* and three varieties of *Cucurbita pepo* ssp. Pepo.
[3] The region of the soil in contact with the roots of a plant. It contains many microorganisms and its composition is affected by root activities.

2.5 Genetic Methods for Studying the Plant Response to Environmental Contaminants

Exposing plants to chemicals induces responses at physiological and molecular levels. Plants need to constantly adapt the new conditions and stresses. These chemical-induced changes are, for the most part, regulated at the transcriptional level. The increasing knowledge of the genetic factors that are likely to play a role in the uptake and metabolism of environmental pollutants provides a support for genetic modification of plants to in an attempt to improve phytoremediation efficiency. For example, the study of the genes involved in the biology of metals in plants can show the mechanisms of metal accumulation [149]. The introduction of exogenous genes to increase tolerance to bioaccumulation of heavy metals in plants has been the object of several studies. For instance, Kramer (2005) introduced specific genes from *Escherichia coli*, yeast, and *Arabidopsis* into tobacco and *Arabidopsis* plants, which was shown to enhance trace elements accumulation in the shoots [150]. The genetic response of plants to a variety of environmental factors, such as cold, drought, and metal toxicity, can provide valuable information that can help enhance the phytoremediation processes.

Although RNA sequencing emerges as the method of choice for genome-wide gene expression analysis (RNA-Seq), it is still expensive, especially considering the number of samples that we have analyzed in this study. The microarray approach is significantly cheaper and constitutes today a widely-accepted, reliable technology. Microarray experiments are conducted to identify genes potentially involved in the metabolism of environmental contaminants. A microarray is a slide onto which a large number of oligonucleotide probes specific to a set of genes (or the entire genome) are

spotted. Messenger RNA (mRNA) is extracted from plant tissues exposed and non-exposed (control) to contaminants. mRNA is labeled with a fluorophore and hybridized to the array probes. The slide is then be scanned using laser emission. Computer-assisted analysis of the fluorescence intensities allows identifying the genes that are induced, repressed, or unaffected by exposure to the contaminants. However, although attractive as high-throughput screening tools, microarrays provide only "semi-quantitative" results. Expression of selected genes involved in the plant response to contaminants has to be further confirmed using RT-qPCR.

Recently, the changes in gene expression in plants exposed to various environmental contaminants, including explosives, PCBs, and nanomaterials, have been studied using the microarray technology, providing a better understanding of the molecular mechanisms of the plant responses [151, 152, 133]. As an illustration, a few studies have been conducted to study the metabolism of the explosives, TNT and RDX, in the model plant *A. thaliana*. These studies consistently reported the overexpression of phase-I and phase-II genes known or suspected to be involved in the metabolism of xenobiotics by plants: e.g., cytochrome P-450 monooxigenases and transferases [152, 153, 154].

2.6 Prior Gene Expression Analysis in Plants Exposed to Environmental Contaminants

Most relevant to the present research are investigations focusing on transcriptional changes in plants exposed to metal nanoparticles. To the best of our knowledge, no studies have been conducted on the effects of pharmaceuticals on plants.

Gene expression studies on the effects of ENPs on plants revealed primarily changes in gene expression in relation with biotic and abiotic stimuli. Using whole-genome microarray analysis, Landa et al. (2012) reported that exposure of *A. thaliana* to ZnO NPs and fullerene soot (FS) (100 mg / L) – but not titanium dioxide (TiO_2) NPs – caused phytotoxic effects (biomass reduction) associated with up-regulation of genes involved in biotic and abiotic stress response (e.g., oxidative stress, draught, pathogens) and down-regulation of genes involved in cell biosynthesis, cell organization, electron transport, and energy pathways (indicative of general cellular stress) [154]. Other reports indicated that ENPs may also impact photosynthetic pathways. For instance, Ma et al. (1999) investigated the effects of cerium oxide (CeO_2) and indium oxide (In_2O_3) NPs on *A. thaliana*, showing that high levels of CeO_2 – but not In_2O_3 – NPs (≥1,000 mg / L) negatively impacted plant growth and chlorophyll production [99]. Exposure to both types of NPs also caused induction of genes involved in glutathione metabolism (oxidative stress response) and metal stress response. In an attempt to understand the positive effect of TiO_2 NPs on plant growth, Ze et al. (2012) investigated the photosynthetic efficiency of exposed *A. thaliana* plants. Plant exposure to TiO_2 NPs induced a light-harvesting complex II (LHCII) gene, resulting in higher LHCII content in the thylakoid membrane and increased light absorption efficiency in the chloroplast [156].

Few reports have been published on the transcriptomic response of other plant species exposed to metal ENPs. Exposure of wheat (*Triticum aestivum*) to Ag NPs resulted in reduction of plant biomass and accumulation of oxidized glutathione (indicative of oxidative stress) [157]. In addition, over-expression of metallothionein

gene suggested that the plant responded to Ag NPs by metal ion sequestration. Two studies conducted with the model plant tobacco (*Nicotiana tabacum*) showed that exposure to aluminum oxide (Al_2O_3) and TiO_2 NPs resulted in a range of phytotoxic effects (e.g., reduction of germination rate and plant biomass) associated with up-regulation of a suite of microRNAs (miRNAs) [158]. Small endogenous noncoding RNAs are gene regulators known to be involved in plant development and tolerance to abiotic stresses, including drought, salinity, cold, and heavy metal.

In summary, plant exposure to ENPs seems to induce genome-wide responses, affecting multiple transcription factors and genes involved in various cellular stresses (referred to as "biotic and abiotic stimuli"), which may reflect complex and highly networked transcriptional pathways.

2.7 Biodiesel Production from Plant Feedstock

Biodiesel production from vegetable oil is considered as a promising option for reducing the dependency on fossil fuel and mitigating greenhouse gas emission and atmospheric pollution. However, the cultivation of agricultural crops for bioenergy production has raised serious concerns because of the competition with the increasing food demand. Large areas in the U.S. are heavily contaminated by industrial and agricultural wastes and are considered improper to residential or agricultural uses (e.g., brownfields and Superfund sites). Often, these areas are lost for local business and communities because of the high cost associated with their reclamation. In this application, we propose to conduct greenhouse experiments to test whether exposure of soybean plants cultivated on contaminated land would affect biomass productivity and lipid content.

A major critic addressed to the production of biofuel from plants is the competition with agricultural land used for food production. By studying the feasibility of growing energy crops on brown fields and contaminated lands unusable for traditional agricultural applications, this project is expected to contribute significantly to the Program Area Priority, including "feedstock development, production, and delivery to ensure the sustainable production of biomass to be used for conversion to advanced liquid transportation fuels".

Because our project proposes to combine the benefits of biofuel production with land bioremediation, it is expected to contribute to the sustainability of U.S. agriculture through the four goals of the National Research Council Committee on Twenty-First Century Systems, i.e., "satisfy human food, feed, and fiber needs and contribute to biofuel needs; enhance environmental quality and the resource base; sustain the economic viability of agriculture; and enhance the quality of life for farmers, farm workers, and society as a whole."

Biodiesel as Economically and Ecologically Sustainable Energy: Biodiesel produced from biomass is renewable, biodegradable, non-toxic, and safer (classified as a non-flammable liquid) than petroleum-based diesel. Environmentally, biodiesel results in significantly fewer noxious emissions than petrodiesel and gasoline (e.g., ~80% less CO_2 and ~100% less SO_2). In addition, biodiesel is the only alternative fuel that is readily usable in conventional, unmodified diesel engines (ASTM D 6751). Economically, biodiesel has almost the same mileage per gallon (MPG) rating as petrodiesel.

Consequently the production of biodiesel in the U.S. has increased from 75 million gallons in 2005 to 650 million gallons in 2008, with a projected total capacity

well over 1 billion gallons in the next few years [159]. According to a World Bank report in 2008, 6.5 billion liters of biodiesel were produced worldwide in 2006, including 75% in the European Union and 13% in the U.S. [162] Biodiesel production is expected to increase 5 times by 2020 according to Courchesne et al. (2009) [162].

Biodiesel consists of fatty acid methyl esters (FAMEs) that can be produced from various lipid sources (i.e., triacylglycerols) by transesterification reaction with an alcohol (methanol) in the presence of a catalyst [158, 159]. Traditional feedstocks for biodiesel production include vegetable oil, such as soybean and canola, which are expensive (70% - 85% of the total biodiesel production cost) and compete with the increasing food demand [161]. If used in totality for biofuel production, corn and soybean harvested in the U.S. would meet only 12% of gasoline (bioethanol) and 6% of diesel (biodiesel) demand as Csavina et al. (2011) mentioned [166]. There is therefore an urgent need to develop sustainable lipid sources that do not compete with agricultural land for food production.

A few studies have investigated the potential of using energy crop for bioremediation applications. Shi and Cai (2009) have demonstrated the potential of eight energy crops, including soybean, peanut, and rapeseed, grown in the greenhouse to tolerate and accumulate high levels of cadmium [166]. In a 6-year field experiment, Faessler et al. (2010) investigated the potential of growing maize, sunflower, and tobacco in crop rotation in order to remove zinc and cadmium [168]. Meers et al. (2010) conducted a study to assess the potential use of maize plants for the phytoremediation of large land areas in Campine (Belgium) mildly contaminated with metals. The authors concluded that cultivation of energy maize could result in the production of 33,000 -

46,000 kWh of renewable energy (electrical and thermal) per hectare per year associated with significant removal of zinc from soil (0.4 - 0.7 mg/ kg) [162].

Even though plants have been shown to actively take up organic contaminants from soil, including the compounds that we plan to use in this investigation, PCBs, TCE, and TNT [163], no studies have been conducted to date on the potential of using plants for the bioremediation of organic contaminants and bioenergy production. In addition, the studies cited above on phytoremediation of metals have not focused on the effect of soil pollutants on bioenergy production. The innovative aspect of our seed proposal is to test the effect of common toxic soil contaminants on the plant lipid content and fatty acid composition, which are known to affect both biodiesel yield and quality. In order to be utilizable in conventional diesel engine, biodiesel must satisfy ASTM D6751 standards, which ultimately depends on the fatty acid composition of the lipid feedstock. For instance, biodiesel quality (i.e., low temperature operability and oxidative stability) increases with the content of 16 and 18 carbon monounsaturated acids, palmitoleic acid (C16:1) and oleic acid (C18:1) as mentioned in Fallen et al. (2011) [171]. In addition, our study will focus on the accumulation of organic contaminants in lipids, which, if present in biodiesel, could lead to undesirable noxious emissions during combustion (e.g., combustion of PCBs generates dioxins).

CHAPTER 3 EXPOSURE OF *ARABIDOPSIS THALIANA* TO SILVER NANOPARTICLES

3.1 Introduction

The release of silver nanoparticles (AgNPs) in the environment has raised concerns about their effects on living organisms, including plants. There is therefore a critical need to collect more experimental data about the ecotoxicity of engineered nanoparticles (ENPs) in general. AgNPs are the most widely used ENPs. Most toxicological studies on the effects of AgNPs have been conducted through acute toxicity testing (short time exposure to high doses) while environmental effects are more adequately assessed by chronic toxicity testing (long time exposure to low doses). Although chronic toxicity is typically difficult to observe in laboratories, molecular studies (e.g., proteomic or transcriptomic methods) can provide useful information about the potential long term effects of exposure to environmental contaminants [164]. This chapter includes the objective of the study, experimental methods applied for medium and seed preparation, seed germination, chemicals and concentrations used in the tests also about plants exposure and harvesting procedures. This chapter also details the molecular techniques and related data processing. Results of the toxicity testing and the transcriptional responses of the plants are presented and discussed at the end.

Results and data processing presented in this section have been published in Kaveh et al. (2013).

3.2 Objective

The objective of this study is to provide new insights on the transcriptional response of the model plant, *Arabidopsis thaliana*, exposed to AgNPs and Ag^{+} through the use of whole genome cDNA microarrays.

3.3 Materials and Methods

3.3.1 Chemicals

AgNPs (99.99%, 20 nm) were obtained from U.S. Research Nanomaterials (Houston, TX) (See Figure 3.1). Silver nitrate ($AgNO_3$) (99.9%) and polyvinylpyrrolidone (MW = 40,000 Dalton, PVP40) were purchased from Sigma Aldrich (St-Louis, MO). Phytoagar and Murashige & Skoog (MS0) Basal Salt were bought from Plant Media in Dublin, OH and Carolina™ Biological Supply Company in Burlington, NC, respectively. RNAlater storage solution was from Ambion (Foster City, CA) and nitric acid used for silver metal (Ag) digestion was analytical grade.

3.3.2 Nanoparticle Characterization

For AgNP characterization, fresh particle suspensions were prepared in 0.5-strength Murashige and Skoog (MS) medium (at concentration of 5 to 20 mg / L with an equal concentration of PVP40) and dispersed by sonication for 30 min in a water bath (150 W). Particle suspensions were analyzed immediately after preparation and after 24 h of agitation at 55 °C, 150 rpm. Particle suspensions were characterized by visible spectrometry, dynamic light scattering (DLS), and transmission electron microscopy (TEM). Visible spectra (300 to 800 nm) of particle suspensions were recorded using an Agilent 8453 spectrophotometer (Agilent, Santa Clara, CA). The particle size distribution

and zeta potential of the suspensions were determined by DLS using a Zetasizer Nano (Malvern, Worcester, MA) with the following parameters: wavelength 632.8 nm, angle 173 °, temperature 25 °C. The particle size and morphology were characterized by TEM using a JEM-1400 (JEOL, Peabody, MA) with a HT voltage of 120 kV and a beam current of 66 mA. Samples were prepared by applying and air drying 4 µL of particle suspension onto a 400-mesh copper grid covered with ultrathin carbon film on Holey carbon support film (Ted Pella, Redding, CA).

3.3.3 Plant species and culture conditions

A. thaliana, ecotype Columbia (Col-0/Redei-L211497) was obtained from the *Arabidopsis* Biological Resource Center (Ohio State University, Columbus, OH). Seeds were then surface-sterilized by immersion successively in DI water for 1 h, in 95% ethanol for 5 min, and 0.6% sodium hypochloride for 5 min, and after they were rinsed 3 times in sterile DI water, the seeds were germinated under sterile conditions in Magenta boxes (10×10 cm) under sterile conditions (4 boxes per treatment and 5 seeds per box). The boxes were filled with 75 mL nutrient agar medium and capped with vented lids. The medium consisted of half strength MS0 basal salt solution supplemented with 2% sucrose and 0.7% phytoagar (pH 5.7) and it was sterilized by autoclaving (121°C, 15 min). Plants were grown at 25 ºC under white (cool) fluorescent light (5,000 K, 0.38 ± 0.02 W ft^{-2}) with a 16 h light/8 h dark photoperiod.

3.3.4 Growth inhibition experiment

The inhibitory effect of AgNPs and Ag^{+} was tested by cultivating *Arabidopsis* plants in the presence of increasing concentrations of the toxicants (1.0, 2.5, 5.0, 10, and 20 mg / L) added to the nutrient medium. After sterilization, the medium (prepared as

described above) was cooled to 55 ºC and supplemented with the AgNPs or Ag^+ (formulated as aqueous stock solutions). AgNP stock solution was prepared by mixing 1.0 g AgNPs/L (0.1% w/v) and 1.0 g PVP40/L (0.1% w/v) with DI water and dispersing AgNPs by sonication for 30 min in a water bath (150 W). Ag^+ stock solution was prepared by dissolving 1.575 g $AgNO_3$/L (0.1% w/v Ag) and 1.0 g PVP40/L (0.1% w/v) in DI water. Two sets of non-exposed control plants were grown in nutrient medium (MS) only and in nutrient medium supplemented with 20 mg PVP40/L (i.e., equivalent to the highest concentration of PVP40 applied in the experiments with AgNPs). After 10 days of growth, plants were removed from the medium, washed with water to remove the excess of medium, dried by blotting, and weighted. Twenty plants were used for each treatment. The significance of differences between treatments was evaluated using one-way ANOVA (Prim 6.0, GraphPad, La Jolla, CA) followed by Tukey's multiple comparison tests at 95% confidence level ($p < 0.05$).

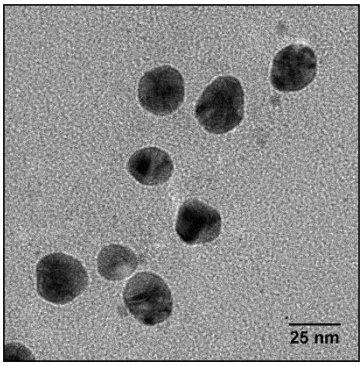

Figure 3.1. A TEM image of 20-nm AgNPs used in this study

3.3.5 Analysis of AgNP and Ag^+ in plants tissues

To measure the amount of Ag in the tissues exposed to AgNPs and Ag^+, plants were washed with deionized water to remove the adsorbed AgNPs or Ag^+ ions to the

plant tissue [2]. Then their roots and leaves were separated, dried at 70°C for 24 h and digested in 4:1 (v/v) concentrated HNO_3:30% H_2O_2 at 70°C for 8 h. After dilution and filtration (0.2 µm) the supernatant[4] was analyzed using an Agilent 7500i Benchtop ICP-MS (Santa Clara, CA). Fifteen plants were used for each treatment. Leaves and roots of 5 plants were pooled together to make three biological replicates. Analyses were performed by the Material Characterization Laboratory, York Center for Environmental Engineering & Science, New Jersey Institute of Technology (Newark, NJ).

3.3.6 Gene expression analysis using microarray method

Plants that were exposed to 5 mg / L AgNPs and 5 mg / L Ag^+ (both containing 5 mg / L PVP40) were chosen for RNA extraction. Ten days after sowing the seeds, plantlets were removed from the medium, rinsed, and were kept in RNAlater solution at 4ºC for 24 h to preserve the RNA in the tissue. After 24 h, plants were dried by blotting and stored at -80 ºC for future RNA extraction. RNA was extracted from the whole plant tissues (leaf and root together) using TRIzol Plus RNA Purification kit. An additional step of tissue homogenization was performed after addition of the TRIzol® reagent using bead beating (1-mm glass beads, 4,200 rpm, 40 sec). Purified RNA was kept at -80 °C. RNA was quantified by the OD_{260} using a NanoDrop™ ND-2000 spectrophotometer (Vernon Hills, IL). The quality of RNA was assessed by the ratios OD_{260}/OD_{280} and OD_{260}/OD_{230} and using an Agilent 2100 Bioanalyzer (Santa Clara, CA). RNA samples used for microarray analysis had OD_{260}/OD_{280} ratios of 2.12 – 2.17, OD_{260}/OD_{230} ratios of 2.16 – 2.36, and RNA integrity numbers (RIN) of 8.3 – 9.1.

[4] Supernatant of a solution of 1,000 mg / L AgNP after centrifugation was used as a growth medium.

To study the transcriptional response of the plants to AgNPs and Ag^+, Affymetrix whole-transcript genome expression microarrays were used. RNA samples were transcribed to cDNA and the cDNA was labeled and hybridized to the Affymetrix Arabidopsis Gene 1.0 ST Arrays. For each treatment, three biological replicates were used for microarray experiments. Scanned microarray images were analyzed using the Affymetrix Gene Expression Console with Robust Multi-array Average normalization algorithm. Microarray processing and analysis were performed with the technical support of Dr. Yue-Sheng Li at the Gene Expression Core (Fox Chase Cancer Center, Fox Chase, PA). Statistical analyses were performed using BRB-ArrayTools package [165]. Gene classification into gene ontology (GO) categories was performed using BLAST2GO online database version 2.6.4 (Biobam Bioinformatics, Valencia, Spain).

3.3.7 Reverse-transcription real-time PCR

Quantitative analysis of gene expression was performed for selected genes using reverse-transcription real-time PCR (RT-qPCR). Four genes significantly down-regulated (fold change < 0.25), 4 genes significantly up-regulated (fold change > 4.0), and 4 genes with moderate expression differences (fold change between 0.4 and 2.0) upon exposure to both AgNPs and Ag^+ were selected (see Appendix A). The internal standard was the housekeeping gene, mitogen-activated protein kinase 6 (MPK6) (AT2G43790) [152]. RT-qPCRs were conducted for three biological replicates per treatment using the same RNA as used for the microarray experiments. RNA was reverse-transcribed into cDNA using SuperScript® III First-Strand Synthesis system and oligo-dT primers (Invitrogen, Foster City, CA). Negative controls were generated by running the reactions without reverse-transcriptase. Gene sequences were obtained from the National Center for

Biotechnology Information (NCBI) and used to design gene-specific real-time primers using PrimerQuest (IDT, Coralville, IA). When possible (for 10 of the 12 selected genes), primers were designed with one of the primer sequence spanning an exon-intron boundary (Table 3.1).

Table 3.1. List of primers used for the reverse-transcription real-time PCR (RT-qPCR) amplification of selected genes

TAIR ID	Gene Description	Fold Change		Primer Sequence	
		AgNP	Ag^+		
AT3G59900	ARGOS protein (ARGOS)	0.08	0.09	Forward	CAAGAGTTACGGCGGAGTTT
				Reverse	TGCCGTTAGACCAACCAATAG
AT4G25750	ABC transporter G family member 4 (AT4G25750)	0.11	0.11	Forward	CGGTCTTGTCTTAGGCACTATC
				Reverse	TAGTGGAGGAGAGGAGGAATG
AT3G16770	Ethylene-responsive transcription factor RAP2-3 (EBP)	0.15	0.19	Forward	CCAACCAAGTTAACGTGAAAGAG
				Reverse	AATCTCAGCCGCCCATTT
AT1G69490	NAC domain-containing protein 29 (NAP)	0.20	0.19	Forward	CGTAACGGTTCCATGAGGTTAG
				Reverse	CTTCGTCCATGAAACCCTCTT
AT1G62380	1-Aminocyclopropane-1-carboxylic oxidase	0.46	0.43	Forward	AGAAGTCGAAGATGTCGATTGG
				Reverse	TTCATGGCCGTCCTGTATTC
AT2G37640	Alpha-expansin gene family	0.58	0.56	Forward	GATCTCGCCATGCCTATGTT
				Reverse	AAGGTACCCTGCGATAGGA
AT2G27080	Late embryogenesis abundant (LEA) hydroxyproline- rich glycoprotein	1.85	2.01	Forward	GCTCCTTTATTGCAAGTGACTC
				Reverse	CTGAAGTTGCCGGAGAATTG
AT5G26330	Cupredoxin superfamily protein	2.08	2.13	Forward	CACATTGGTGATACTGTCTTGTTC
				Reverse	TAGAGATTGGCTTTGAGGTGTT
AT5G42590	Cytochrome P450 71A16 (CYP71A16)	3.85	4.03	Forward	GGAGGAACGTTAAGAGTCTATGC
				Reverse	CTTCCAGCGTCTCCATCAATAG
AT5G26260	TRAF-like family protein	4.76	7.25	Forward	ACCGATACTGGAGACTAGGATT
				Reverse	TAACAACTGCGTTTGCCTTATG
AT4G11320	Putative cysteine proteinase.	4.76	6.39	Forward	GCTTTATGAATCGGGAGTGTTTG
				Reverse	AATCCAGTAGTCACGACCATTC
AT2G01520	MLP-like protein 328 (MLP328)	5.56	7.67	Forward	AGGAGTGAGAACCACCTCTT
				Reverse	TTTCCCATCGCATGTGTAGTT
AT2G43790	Mitogen-activated protein kinase 6 (MPK6) (Internal standard)	N.A.	N.A.	Forward	GCATCGTTTGTTCGGCTATG
				Reverse	GATCTCACGGAGAGTCCTCTTA

Real-time PCR quantification of cDNA was performed on a StepOnePlus™ Real-Time PCR System using SYBR® Green PCR Master Mix (Applied Biosystems, Foster City, CA). The amplification efficiency for each primer set was determined by using $\log_{10}$-dilutions of cDNA according to standard protocols. C_T (cycle threshold) data were computed by the StepOnePlus™ Software (version 2.1; Applied Biosystems). The mean

relative levels of amplification of the target genes and standard deviations were calculated based on C_T values and amplification efficiencies using REST 2009 (version 2.0.13; Qiagen, Foster City, CA) [166].

MIAME compliance: This article is written in compliance with the Minimum Information About a Microarray Experiment (MIAME) guidelines (http://www.mged.org/miame). Microarray data have been submitted to the Gene Expression Omnibus (http://www.ncbi.nlm.nih.gov/geo) with the accession number E-MEXP-3950.

3.3.8 Data validation and statistical analysis

In all experiments the significance of differences between treatments was evaluated using one-way ANOVA (Prism 6.0, GraphPad, La Jolla, CA) followed by Tukey's multiple comparison tests at 95% confidence level ($p < 0.05$).

3.4 Results and Discussion

3.4.1 Nanoparticle characterization

Particle suspensions were characterized in fresh preparation (MS medium) and after 24 h of agitation at 55 °C, 150 rpm to detect potential aggregation and/or change in properties. The spectrum of the fresh AgNP suspension (5 mg AgNPs/L, 5 mg PVP40/L in 0.5-strength MS medium) showed a single peak at 405 nm, which is consistent with uniform-sized nanoparticles with a diameter of approx. 20 nm. No significant change of the spectrum was observed after agitation of the suspension for 24 h at 55 °C, 150 rpm (Figure 3.2). DLS analysis of the fresh AgNP suspension (20 mg/ L) showed a narrow size distribution with a hydrodynamic diameter of 27.1 ± 0.3 nm, which shifted to 29.6 ±

0.1 nm after 24 h of agitation at 55 °C. The zeta potential of the fresh suspension was -38.1 ± 0.3 V, which shifted to -30.9 ± 0.6 V after 24 h of agitation at 55 °C (Figure 3.3). TEM pictures of AgNP suspensions showed mostly spherical particles of uniform size (Figure 3.1). No observable change was recorded after agitation at 55 °C for 24 h. After adding AgNPs to the culture medium, phytoagar solidifies the medium in a short time, which stops AgNPs from agglomeration.

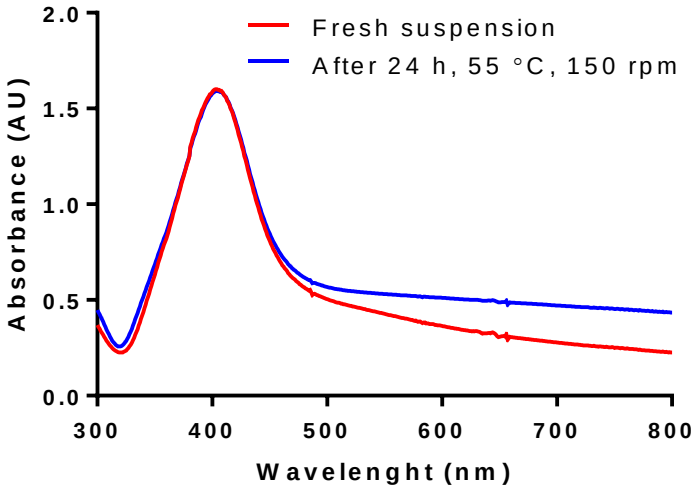

Figure 3.2. Absorption spectra (300 – 800 nm) of 20 nm silver nanoparticle (AgNP) suspensions prepared in 0.5 strength Murashige and Skoog (MS) medium with polyvinylpyrrolidone (molecular weight 40000 Dalton, PVP40). **Red spectrum**: fresh suspension. **Blue spectrum**: suspension after agitation at 55 °C, 150 rpm for 24 h.

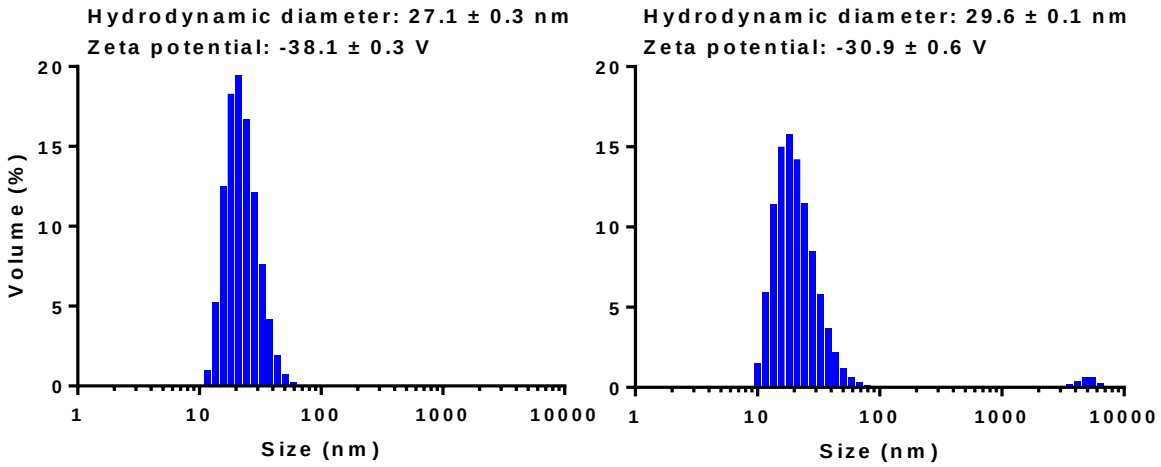

Figure 3.3. Size distribution of 20 nm silver nanoparticle (AgNP) suspensions prepared in 0.5 strength Murashige and Skoog (MS) medium with polyvinylpyrrolidone (molecular weight 40000 Dalton, PVP40). **Panel A**: fresh suspension. **Panel B**: suspension after agitation at 55 °C, 150 rpm for 24 h.

3.4.2 Effect of AgNPs and Ag^+ on *A. thaliana* growth

To determine the potential toxic effect of AgNPs and Ag^+ on *A. thaliana*, the plants fresh biomass was measured after 10 days of exposure. Figure 3.4 presents the average fresh biomass of plants exposed to each treatment. No significant difference in biomass was observed between the two sets of non-exposed control plants (i.e., growing in medium with MS0 only and in MS0 medium containing 20 mg-PVP40/L).

Exposure of plants to 1.0 and 2.5 mg AgNPs/L for 10 days resulted in significant increase of the biomass, although exposure to higher concentrations (from 5.0 to 20 mg / L) resulted in reduction of the biomass. Although no significant effect was recorded in the presence of 1.0 and 2.5 mg-Ag^+/L, the biomass after 10 days was significantly reduced upon exposure to 5.0 mg / L and above. Comparatively, low levels (1.0 and 2.5 mg / L) of exposure to AgNPs resulted in a significantly higher plant biomass than

exposure to Ag^+. No significant differences were recorded between the two treatments at higher levels (5.0, 10, and 20 mg / L).

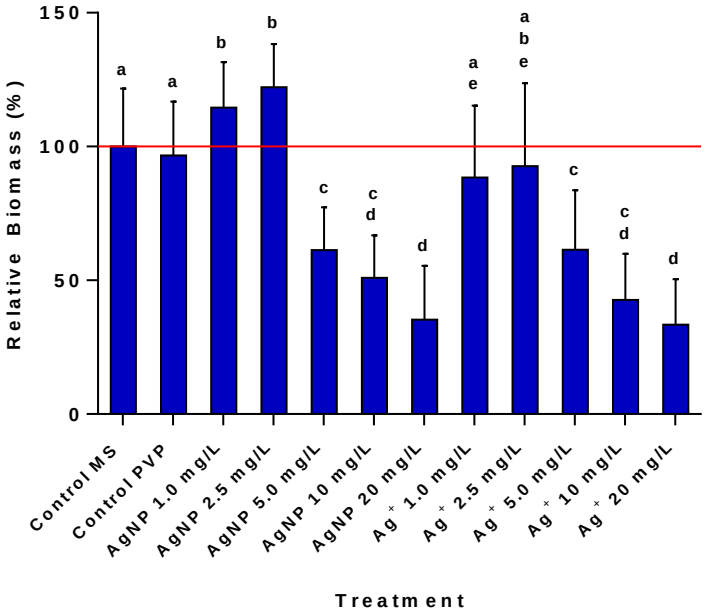

Figure 3.4. Relative fresh biomass of *A. thaliana* exposed to AgNP and Ag^+

3.4.3 Analysis of Ag content in plant tissues

The samples that were considered for Ag extraction were dried and digested in nitric acid. Then, the Ag content was determined by an ICP-MS. The Ag concentration was significantly higher in plants dosed with Ag^+ than in plants dosed with AgNPs for each concentration. The Ag concentration was also significantly higher in the root than in leaves (Figure 3.5).

There is a stronger correlation between the exposure dosage and the Ag content in the root tissues compared to the leaves. Overall, these results are consistent with previous studies described in the literature. For instance, recently reported a higher Ag content in *A. thaliana* leaves exposed to Ag^+ (about 8 µg/g) than exposed to AgNPs (about 2 µg/g)

[15]. As observed in our study, the Ag concentration detected in roots was higher than aerial parts of the plants: 68% of total Ag^+ and 24% of total AgNPs were found in root tissues while only 2% of total Ag^+ and 1% of total AgNPs were detected in the aerial parts.

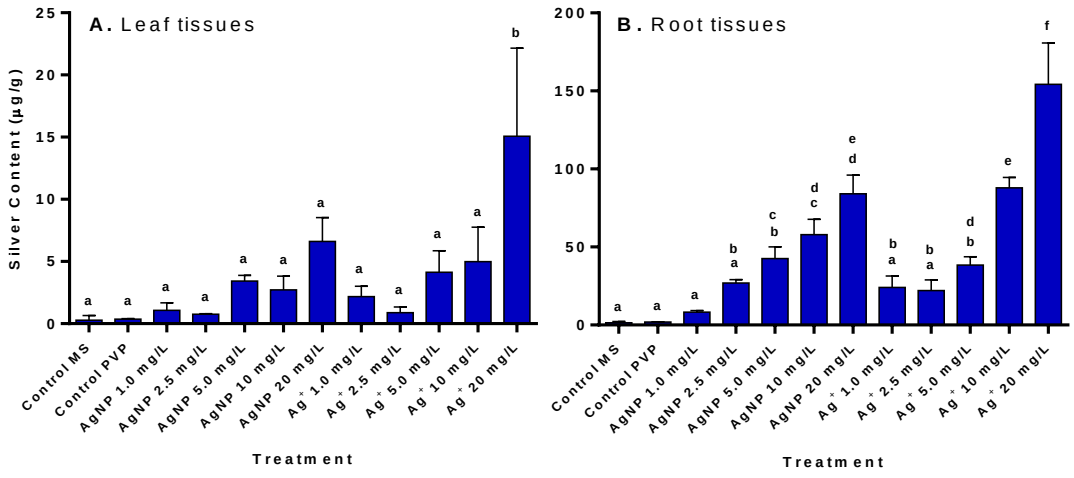

Figure 3.5. Ag content measured in tissues of *A. thaliana* exposed to AgNP and Ag^+. Panel A: Leaves. Panel B: Roots. Error bars represent standard deviations of 3 biological replicates.

3.4.4 Gene expression microarrays

The transcriptional response of plants exposed to AgNPs and Ag^+ was investigated using Affymetrix whole-transcript expression microarrays. AgNP and Ag^+ concentration of 5 mg/ L, which resulted in moderate reduction of the plant biomass (37%), was chosen for microarray experiments. After filtering out the genes with low-quality signals and conducting univariate *t*-tests ($p < 0.001$; BRB-ArrayTools), 446 and 405 genes showed consistent expression levels after exposure to AgNPs and Ag^+, respectively. Of these, 375 and 141 genes were expressed at significantly different levels (change fold < 0.5 or > 2.0) by exposure to AgNPs and Ag^+, respectively: 286 genes (78%) were up-regulated and 81 genes (22%) were down-regulated at significant levels

by exposure to AgNPs; 84 genes (60%) were up-regulated and 53 genes (40%) were down-regulated at significant levels by exposure to Ag^+. A significant overlap of differentially-expressed genes was observed upon exposure to AgNPs and Ag^+: 15 genes were up-regulated and 29 genes were down-regulated in response to both AgNPs and Ag^+ (representing 13% and 21% of the total up- and down-regulated genes, respectively).

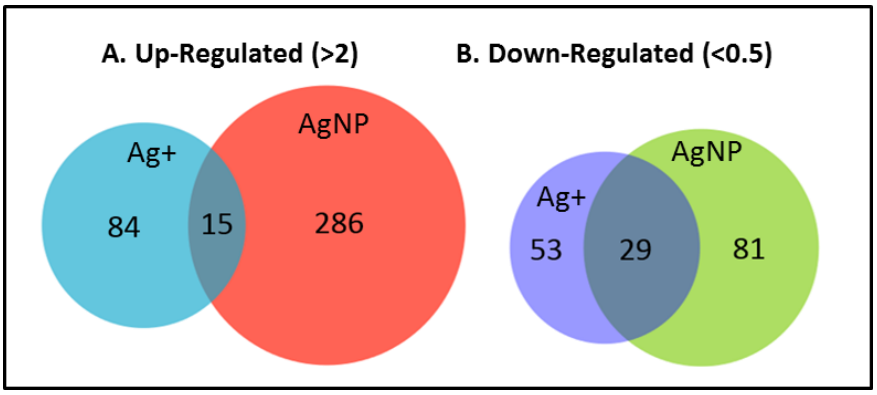

Figure 3.6. Venn diagrams showing the number of genes significantly up-regulated (**Panel A**) and down-regulated (**panel B**) by exposure to AgNPs and Ag^+ individually, and by both compounds simultaneously.

This observation suggests that some of the AgNP effects on gene expression originate from Ag^+ released by AgNPs, which was previously observed or proposed by other authors [157, 15]. As in several other studies [15, 167, 168], we chose to expose the plants to the same concentrations of AgNPs and Ag^+ (expressed as mg Ag/L). This approach was motivated by the lack of information about the nature of the toxic effects and cellular targets of both Ag forms. Soluble Ag is known to be cytotoxic and AgNP toxicity likely originates partly from the release of soluble Ag. Besides, nanoparticles are known to exert specific 'particulate' effects that may not be related to Ag^+ toxicity. Dimkpa et al. (2013) reported that exposure of sand-grown wheat plants (*Triticum aestivum*) to both 10-nm AgNPs and soluble Ag (Ag^+) (2.5 mg /kg) resulted in comparable biomass reduction. Interestingly, exposure to Ag^+ equivalent to soluble Ag

released from AgNPs (63 μg/kg) did not result in observable effect [159]. Moreover, using TEM, the authors observed accumulation of AgNPs inside plant tissues, suggesting that AgNPs exert toxic effects that are, at least in part, unrelated to the release of soluble Ag [157]. In order to determine the respective effect of AgNPs and Ag^+, Stampoulis et al (2009) exposed zucchini plants (*Cucurbita pepo*) to bulk (powder) Ag, AgNPs (100 nm), and Ag^+ (both supernatant of AgNP suspension and $AgNO_3$). The authors reported that exposure to bulk Ag at 1,000 mg / L did not significantly affect the plant biomass, while exposure to 1,000 mg/ L AgNPs reduced the biomass by approx. 75%. On the other hand, AgNP supernatant and Ag^+ ($AgNO_3$) at concentration as low as 1.0 mg / L reduced the biomass by approx. 25%, suggesting that about half the observed phytotoxicity originated from the elemental nanoparticles themselves [21]. Few studies have been conducted on the transcriptional response of organisms exposed to AgNPs. Analyzing gene expression in human cells (HeLa) exposed to AgNPs and Ag^+, Xu et al (2011) reported a higher number of genes up-regulated (62%) than down-regulated (38%) with Ag nanoparticle exposure, which is consistent with our results. The authors also observed that a large number of genes were differentially expressed in response to both AgNPs and Ag^+ (85% of up-regulated genes and 68% of down-regulated genes) [24]. The complete list of *Arabidopsis* genes up- and down-regulated by exposure to AgNPs and Ag^+ is provided in Appendix A.

In order to validate the microarray results, quantitative analysis of gene expression was performed on selected genes using RT-qPCR. Figure 3.7 shows the plots of the expression levels of the selected genes as recorded using microarrays against their expression levels recorded using RT-qPCR. Correlations were generally satisfactory with

Pearson's correlation coefficient of 0.96 and 0.97 for exposure to AgNPs and Ag^+, respectively. The RT-qPCR amplification levels were corrected for the amplification efficiencies of different primer sets (ranging from 97.9% to 109.9%, R^2 = 0.99 to 1.0) using REST 2009.

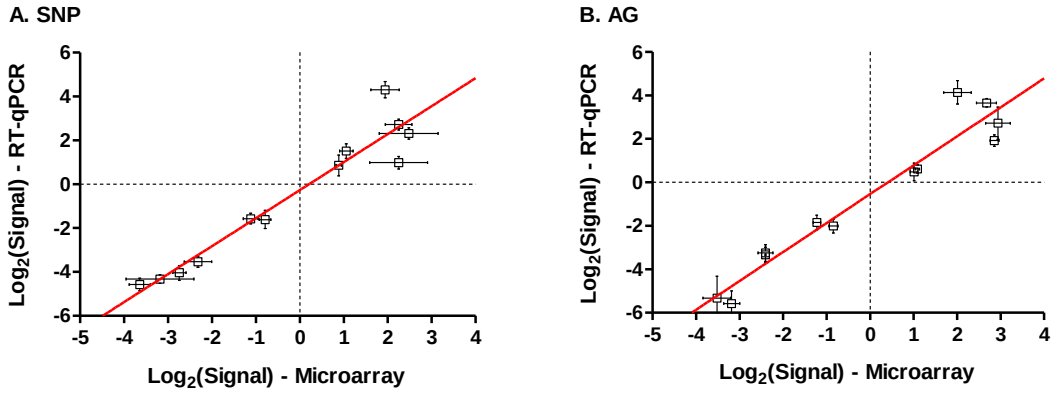

Figure 3.7. Log_2 microarray relative expression levels versus log_2 RT-qPCR relative expression levels for exposure to panel A: AgNPs and panel B: silver ions (Ag^+). Error bars represent the standard deviations between three biological replicates.

3.4.5 Functional categories of differentially expressed genes

Differentially expressed genes were classified by gene ontology (GO) categories using BLAST2GO® software. Distribution of major processes and also functional categories in GO at parental level 2 showed little differences between genes up- and down-regulated by exposure to AgNPs and Ag^+. Most represented process categories for both up- and down-regulated genes were metabolic process, cellular process, response to stimulus, and biological regulation (see Figure 3.8). Most of the represented functional categories for both up- and down-regulated genes were catalytic activity, binding, nucleic acid binding transcription factor activity, and transporter activity (see Figure 3.9).

Two remarkable exceptions are the *signaling* process category involving only down-regulated genes (25% and 30% of total down-regulated genes by exposure to AgNPs and Ag^+, respectively) and the *electron carrier* functional category involving (almost) only up-regulated genes (11% and 16% of total up-regulated genes by exposure to AgNPs and Ag^+, respectively). Genes in the *signaling* category are mostly involved in hormone signaling pathways and cellular response to hormone stimuli, which may be related to the reduction of plant growth in response to the toxicity of AgNPs and Ag^+ [169]. On the other hand, heavy metals are known to interact with electron carriers. Up-regulation of genes in this category may reflect the response of the plant to the decreased electron transport efficiency in the presence of AgNPs and Ag^+ [170].

A significant proportion of genes differentially expressed by exposure to AgNPs and/or Ag^+ is involved in *response to stimuli* (GO level 2) (49% of total up-regulated genes and 68% of total down-regulated genes). Among them, most up-regulated genes (63% and 78% of genes in this category up-regulated by AgNPs and Ag^+, respectively) are involved in response to abiotic stimuli (GO level 5), including metal ions, salts, light, starvation, oxidative stress, osmotic stress, and radiation. On the other hand, most down-regulated genes (74% and 62% of genes in this category down-regulated by AgNPs and Ag^+, respectively) are involved in response to pathogens and hormonal stimuli (GO level 5), including abscisic acid, auxine, cytokinin, ethylene, gibberellin, jasmonic acid, and steroid hormones (Figure 3.9). Up-regulation of genes related to abiotic stimuli likely reflects the response of the plant to AgNP/Ag^+-induced stress. On the other hand, down-regulation of genes related to hormones and biological stimuli can be seen as a plant strategy to prioritize the response to AgNP and Ag^+-induced stress [169]. Alternatively,

hormones are involved primarily in the regulation of plant development and down-regulation of hormone-responsive genes may simply reflect attempts of the plant to limit the growth under toxic conditions. In addition, beside their role in plant development, hormones are known to be involved in response to biological and abiotic stresses. For instance, the down-regulation of abscisic acid and auxin signaling pathways has been shown to play a role in various plant defense responses [169].

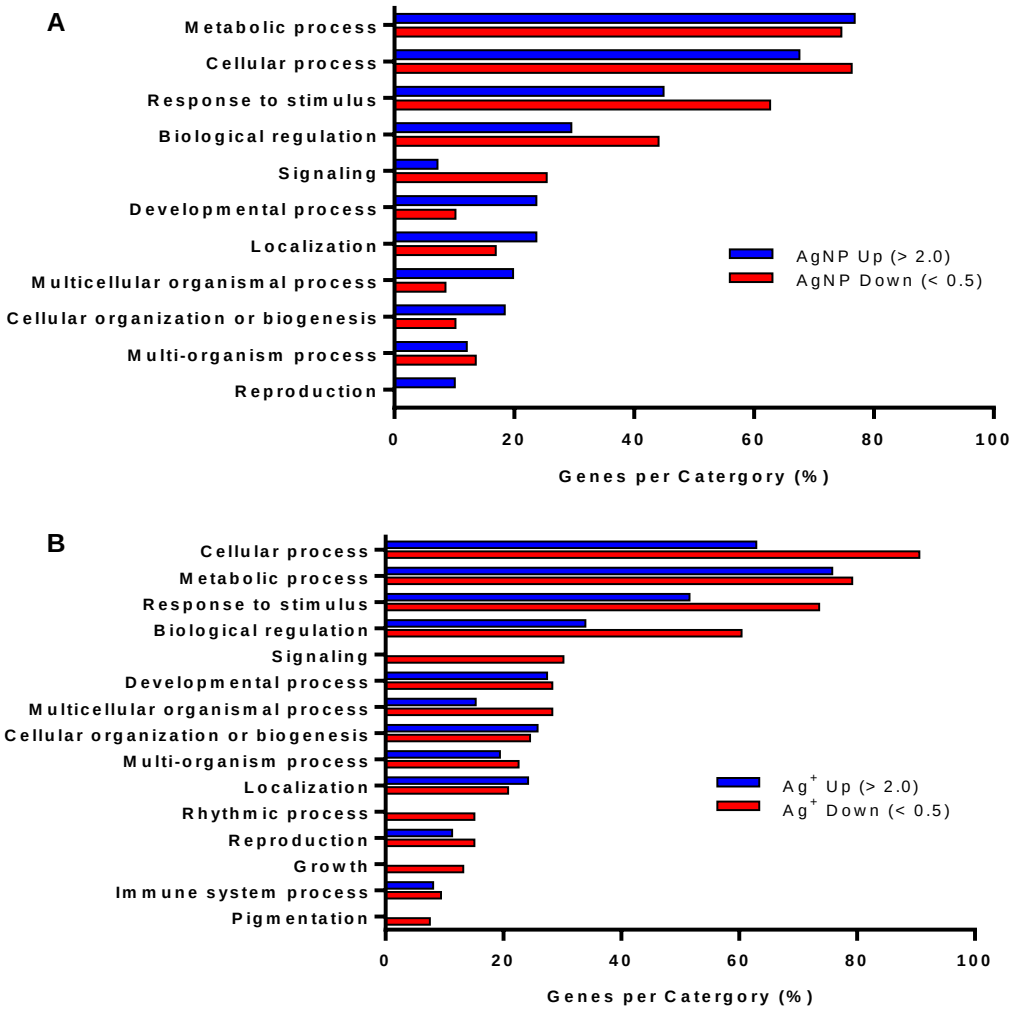

Figure 3.8. Major gene ontology (GO) process categories of genes up (fold change > 2.0) and down-regulated (fold change < 0.5). Panel A: Genes differentially expressed by exposure to AgNPs. Panel B: Genes differentially expressed by exposure to Ag+.

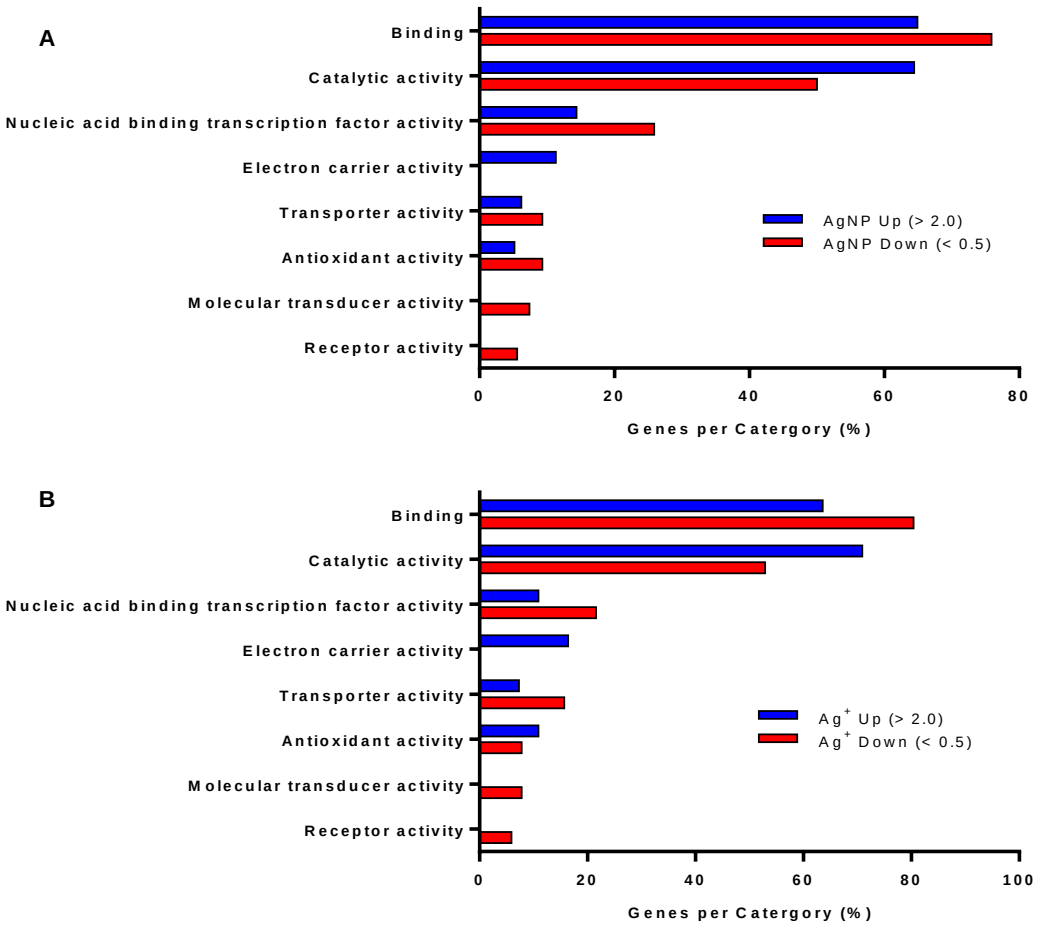

Figure 3.9. Major gene ontology (GO) functional categories of genes up (fold change > 2.0) and down-regulated (fold change < 0.5) Panel A: Genes differentially expressed by exposure to AgNPs. Panel B: Genes differentially expressed by exposure to Ag^{+}.

Remarkable genes discussed in this section were differentially expressed in response to both AgNPs and Ag^{+} (reflecting the effects of Ag^{+}) or in response to AgNPs only (reflecting nanoparticle-specific effects). Genes highly up-regulated (fold change > 4.0) in response to both AgNPs and Ag^{+} are involved in response to metal and oxidative stresses. These genes encode the following proteins: a vacuolar cation/proton exchanger involved in root development under metal stress (AT5G01490), a miraculin-like protein

(MLP) (AT2G01520), two copper/zinc superoxide dismutases (AT2G28190 and AT1G08830), two cytochrome P-450-dependent monooxygenases (AT5G42590 and AT3G28740), and a peroxidase (AT3G21770). MLPs have been suggested to be involved in response to wounding and pathogen infection in other plant species [171]. Superoxide dismutases and peroxidases are involved in protection against reactive oxygen species (ROS), which are frequently associated with metal and ENP toxicity [2]. Although they are involved in many physiological processes, cytochrome P-450 genes have been reported to be induced by metal stress in *Arabidopsis* [172]. Genes most down-regulated in response to both AgNPs and Ag^+ (fold change ≤ 0.25) include a gene encoding an ARGOS (auxin-regulated gene involved in organ size) protein (AT3G59900), three genes involved in the ethylene signaling pathway (AT3G16770, AT5G25350, and AT2G40940), and two genes involved in systemic acquired resistance (SAR) against fungi (AT4G12470) and bacteria (AT5G46330). The ARGOS gene (the most down-regulated gene by both AgNP and Ag^+, 0.08- and 0.09-fold change, respectively) regulates the size of lateral organs and its down-regulation likely reflects attempts of the plant to limit its expansion under stressed conditions. As suggested above, down-regulation of genes involved in ethylene signaling pathway and SAR can be understood as a prioritization of plant defense mechanisms under AgNP and Ag^+-induced stresses [169]. Genes differentially expressed in response to both AgNPs and Ag^+ are likely to be implicated in response to Ag^+, either directly added or released from AgNPs.

On the other hand, a number of genes were differentially expressed in response to AgNPs only, which reflects their involvement in nanoparticle-specific responses. The most remarkable genes up-regulated (fold change > 4.0) specifically by AgNPs include

two genes involved in salt stress (AT3G28220 and AT1G52000), a gene encoding a myrosinase-binding protein involved in defense against insects and pathogens (AT1G52040), three genes involved in the thalianol biosynthetic pathway (AT5G48010, AT5G48000, and AT5G47990), and a gene encoding a MLP involved in response to wounding (AT2G01520). The most up-regulated gene in our study (28.6-fold change) encodes a TRAF (tumor necrosis factor receptor-associated factor)-like protein involved in salt stress response. Although the relationship between salt and AgNP-induced stress is not readily apparent, similar functional genes were found to be induced in *Arabidopsis* exposed to other kinds of ENPs [152]. The induction of genes responsive to pathogens and wounding may be related to mechanical damages caused by AgNPs to plant tissues. [4]. The three genes of the *thalianol* pathway belong to a cluster of four genes, which constitutes a rare case of gene clustering in higher plants [173]. Although gene clusters are common in bacteria (i.e., operons), they are less frequent in eukaryotes and were thought until recently to be restricted to paralogs originating from repeated tandem genes. Only a few clusters of non-homologous, functionally-related genes have been detected in fungi and plants. In plants, these clusters are all involved in biosynthesis of stress-induced secondary metabolites that are (or are believed to be) required for survival under specific conditions, such as the exploitation of new environments [174].

Interestingly, the most down-regulated gene by exposure to both AgNP and Ag^{+} in our study (ARGOS) was also reported down-regulated in *Arabidopsis* plants exposed to zinc oxide and fullerene nanoparticles [152]. Other remarkable genes up-regulated by both AgNPs (our study) and zinc oxide nanoparticles according to Landa et al (2012) are genes encoding a superoxide dismutase (AT1G08830) and two peroxidases, which are

involved in response to oxidative stress (AT3G21770, AT2G18150), and a phytosulfokine-beta growth factor involved in response to wounding (AT3G49780) [154].

This work presents the first whole-genome expression microarray experiment focusing on *A. thaliana* plants exposed to AgNPs and Ag^{+}. Results from this study are believed to provide new insights into the molecular mechanisms of plant response to AgNPs and Ag^{+}.

CHAPTER 4 EXPOSURE OF ARABIDOPSIS THALIANA TO ANTIVIRAL DRUGS

4.1 Introduction

The neuraminidase antiviral drugs, oseltamivir phosphate (OSP) and zanamivir (ZAN), are major medications currently used for the treatment of influenza. These pharmaceuticals have been detected in municipal wastewater, especially during the influenza season. Because OSP and ZAN are not efficiently removed by wastewater treatment and partly adsorb to municipal sludge, so they are may contaminate agricultural plants by irrigation or utilization of biosolids. Although limited information has been published about the toxicity of OSP and, to a lesser extent, ZAN, on aquatic organisms, the potential effects of neuraminidase antiviral drugs on plants has received little attention. In this study, the effects of OSP and ZAN on the model plant, *A. thaliana*, were investigated at the physiological and transcriptional levels. Results from this study are expected to provide insights on the molecular effects of the antiviral drugs, ZAN and OSP, on plants.

The present chapter describes the objective of the study, the experimental methods (plant growth and exposure techniques, analytical methods, gene expression analysis, and related data processing), and the results and discussion.

Results and data processing described in this section will be published in a manuscript, which is in preparation: "R Kaveh, S Ranjbar, B Van Aken. Changes in *Arabidopsis thaliana* gene expression in response to the antiviral drugs oseltamivir phosphate and zanamivir. *Int. J. Phytoremediation*".

4.2 Objective

The purpose of this section is to understand the potential physiological and transcriptional responses of the model plant, *A. thaliana* exposed to different concentrations of the antiviral drugs, OSP and ZAN, using whole-genome expression microarrays.

4.3 Materials and Methods

4.3.1 Chemicals

Oseltamivir phosphate (Tamiflu®) was obtained from Genentech (South San Francisco, CA). Zanamivir (Relenza®) was obtained from GlaxoSmithKline (Philadelphia, PA). Phytoagar was obtained from Plant Media (Dublin, OH). Other chemicals were of analytical grade, solvents were of HPLC grade, and they were obtained from Acros Chemicals (Geel, Belgium), Fischer Scientific (Pittsburgh, PA), or Sigma-Aldrich.

4.3.2 Plant species and culture conditions

A. thaliana seeds, ecotype Columbia (Col-0/Redei-L211497), were obtained from the Arabidopsis Biological Resource Center (Ohio State University, Columbus, OH). Seeds were sterilized and germinated as we described in Kaveh et al. (2013). Briefly, the seeds were placed on a wet filter paper at 4ºC in the dark for 24 h and then surface-sterilized by immersion successively in DI water, 95% ethanol, and 0.6% sodium hypochloride (NaClO). After rinsing with sterile DI water, the seeds were germinated under sterile conditions in vented Magenta boxes (10 × 10 cm) containing 75 mL of semi-solid medium. The medium consisted of half strength Murashige and Skoog (MS)

solution with 2% sucrose and 0.7% phytoagar (pH 5.7) and it was sterilized by autoclaving (121 °C, 15 min). Plants were grown at 25 ºC under white fluorescent light (5,000 K, 0.38 ± 0.02 W ft^{-2}) with a 16 h light/8 h dark photoperiod.

4.3.3 Growth inhibition experiment

The potential inhibitory effect of OSP and ZAN was tested by cultivating the plants in medium containing increasing concentrations of the target compounds: 0, 5, 20, 100 mg / L. After sterilization, the medium (prepared as described above) was cooled to 55ºC and supplemented with OSP and ZAN aqueous stock solutions. After 3 weeks of growth, plants were removed from the medium, washed with DI water, and weighted. A minimum of twenty plants were used for each treatment. The significance of differences between treatments was evaluated using one-way ANOVA and Tukey's multiple comparison tests (Prim 6.0, GraphPad, La Jolla, CA) at 95% confidence level ($p < 0.05$).

4.3.4 Gene expression analysis using microarray method

Microarray experiments were conducted as we described in Kaveh et al. (2013). In brief, plants were exposed to 20 mg / L of OSP or ZAN added in the growth medium as described above. Control plants were grown without OSP or ZAN. After three weeks, plants were removed from the medium, washed, and immediately immerged in RNA Later™ (Life Technologies, Foster City, CA). The plant material was incubated at 4ºC for 24 h and stored at -80ºC until RNA extraction. RNA was extracted from whole plant tissues using TRIzol® Plus RNA Purification kit with on-column PureLink® DNAase (Life Technologies) treatmen. Tissue homogenization was performed using a bead beater (1-mm glass beads, 4,200 rpm, 40 sec). RNA was analyzed using a NanoDrop™ ND-2000 (Vernon Hills, IL) and a 2100 Bioanalyzer (Agilent, Santa Clara, CA). RNA

samples used for microarray analysis had OD_{260}/OD_{280} ratios of 2.17 – 2.21, OD_{260}/OD_{230} ratios of 1.76 – 2.38, and RNA integrity numbers (RIN) of 7.6 – 8.9. RNA samples were labeled and hybridized to the Affymetrix Arabidopsis Gene 1.0 ST Array (Santa Clara, CA). For each treatment, three biological replicates were used for microarray experiments. Scanned microarray images were analyzed using the Affymetrix Gene Expression Console with RMA (Robust Multi-array Average) normalization algorithm. Further statistical analyses were performed using BRB-ArrayTools software (Simon, 2007). Gene classification into ontology categories (GO) was performed using BLAST2GO® version 2.6.4 (Biobam Bioinformatics, Valencia, Spain). The data obtained in this study were compared with microarray data in Genevestigator database (plant biology version; www.genevestigator.com/gv/plant.jsp). The Genevestigator database contains quantitative expression microarray data (2,100 ATH1 full-genome arrays) obtained from AtGenExpress Consortium, NASCArrays, GEO (NCBI), ArrayExpress, and Functional Genomics Center Zurich databases [175]. The Condition Search Tool Perturbations was used to obtain genes expression data related with various stimuli, including abiotic stresses, biotic stresses, toxic chemicals, and response to hormones.

4.3.5 Reverse-transcription real-time PCR

Microarray expression data were confirmed for selected genes using reverse-transcription real-time PCR (RT-qPCR). Twelve genes covering a large range of expression levels were selected (Table 4.1). The housekeeping gene, mitogen-activated protein kinase 6 (MPK6) (AT2G43790) was used as internal standard [152]. RT-qPCRs were conducted as we described in Kaveh et al. (2013) using the same RNA as used for the microarray experiments. In short, RNA was reverse-transcribed into cDNA using

SuperScript® III First-Strand Synthesis system and oligo-dT primers (Invitrogen, Foster City, CA). Real-time primers were designed based on gene sequences obtained from the National Center for Biotechnology Information (NCBI) using the software PrimerQuest (IDT, Coralville, IA). One of the primer sequences was designed for spanning an exon-intron boundary (Table 4.1).

Table 4.1. List of primers used for the reverse-transcription real-time PCR (RT-qPCR) amplification of selected genes

TAIR ID	Gene Description	Fold Change		Primer Sequence	
		OSP	ZAN		
AT1G74890	Two-component response regulator ARR15 (ARR15)	2.19	2.25	Forward	CTTCTTCTTCTTCACCGGAGTT
				Reverse	CACTCTCAACAGTCGTCACTTTA
AT2G37640	Expansin-A3 (EXP3)	N.A.	2.5	Forward	GATCTCGCCATGCCTATGTT
				Reverse	AAGGTACCCTGCGATAGGA
AT2G33830	Dormancy/auxin associated protein	N.A.	2.87	Forward	AAACTGTAGCCGGACCTAAAC
				Reverse	CCCTTCTCCTACACCTTTGATG
AT1G21890	Nodulin MtN21 /EamA-like transporter-like protein	N.A.	4.01	Forward	TCTCGGAAGTGTGATTGGAAC
				Reverse	CTTCGTCATCATCCGTCATTCT
AT5G36220	Cytochrome P450 81D1 (CYP81D1)	N.A.	N.A.	Forward	CGTCTCGCAGGAACCAAA
				Reverse	CGGTTGTTTCTTCACCGTAGTA
AT4G17660	Protein kinase family protein	0.46	0.53	Forward	GGTGGCTTTGGTAGTGTCTATAA
				Reverse	CTTGTGACCCTGTAGACTTTGT
AT5G45830	protein DELAY OF GERMINATION 1	N.A.	1.75	Forward	TGTATGGTTGACACCGAAGTAATA
				Reverse	GCCACGTAAACACACAAATCTC
AT1G12570	Glucose-methanol-choline (GMC) oxidoreductase-like protein	2.4	1.93	Forward	TGACAAAGCTCCGAACTACTC
				Reverse	CCCACCACCGATGATGATATAG
AT3G21500	1-deoxy-D-xylulose 5-phosphate synthase 1 (DXPS1)	0.29	0.1	Forward	TCTTCAGATTGGGAGAGGTAGG
				Reverse	CGCGTTCGCTTAGCATAGAT
AT3G44860	Farnesoic acid carboxyl-O-methyltransferase (FAMT)	0.33	0.22	Forward	CGTGTCCGGTGGATTACTATTG
				Reverse	GTTGATCTATGAGACCCTGGTTAG
AT4G25000	Alpha-amylase (AMY1)	0.47	0.24	Forward	CCACAACTCCATTGACGACATA
				Reverse	CTTTCCCGGTAAGTAACCTTCAG
AT3G46660	UDP-glucosyl transferase 76E12 (UGT76E12)	0.32	0.3	Forward	CAAGCTCCCTTGAAAGAAACTAAAG
				Reverse	GCAAACCGTGAAACTGGAAAG

Real-time PCR was performed on a StepOnePlus™ Real-Time PCR System using SYBR® Green PCR Master Mix (Applied Biosystems, Foster City, CA). The amplification efficiency for each primer set was determined by using $\log_{10}$-dilutions of cDNA according to standard protocols. C_T (cycle threshold) data were calculated using

the StepOnePlus™ Software (version 2.1; Applied Biosystems). The normalized amplification levels and standard deviations were calculated using REST 2009 version 2.0.13 (Qiagen, Foster City, CA) [166].

This article is written in compliance with the Minimum Information About a Microarray Experiment (MIAME) guidelines (http://www.mged.org/miame). Microarray data have been submitted to the Gene Expression Omnibus (http://www.ncbi.nlm.nih.gov/geo) (accession number pending).

4.4 Results and Discussion

4.4.1 Effect of OSP and ZAN on *A. thaliana* growth

In order to determine the potential adverse effect of the antiviral drugs, OSP and ZAN, on *A. thaliana*, seeds were germinated and grown for 3 weeks on semi-liquid medium containing increasing concentrations of OSP and ZAN (ranging from 5 to 100 mg / L). *A. thaliana* plants after 21 days of growth are shown in Figure 4.1.

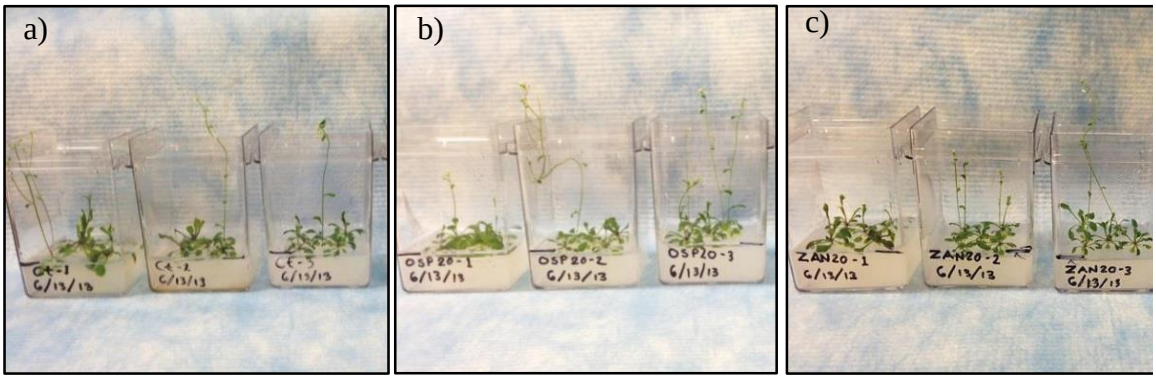

Figure 4.1. *A. thaliana* plants exposed to OSP and ZAN after three weeks. Panel a) Non-exposed controls, Panel b) OSP 20 mg / L, and Panel c) ZAN 20 mg / L.

The biomass of plants exposed to each treatment is represented in

Figure 4.2. A statistically significant reduction of the biomass was observed in plants exposed to OSP at the concentrations of 20 and 100 mg / L, although no significant effect was recorded at the concentration of 10 mg / L. On the contrary, exposure of *A. thaliana* to ZAN did not result in any significant effect on the plant biomass at all concentrations tested.

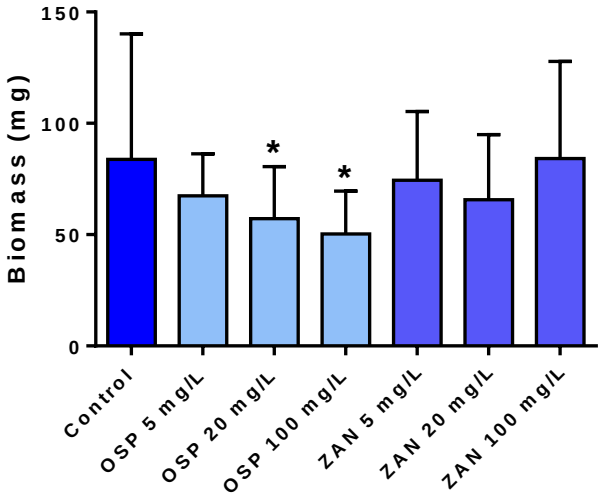

Figure 4.2. *A. thaliana* plants fresh weight biomass after exposure to OSP and ZAN for three weeks. Error bars represent standard deviations. Asterisks (*) show Statistically significant differences.

The low toxicity or absence of toxicity of the antiviral drugs, OSP and ZAN, on *Arabidopsis* plants were expected based on prior toxicology studies. Although there are no data available regarding the toxicity of OSP and ZAN on plants, toxicology studies conducted with other organisms, including algae, invertebrates, and fishes, have concluded that these compounds exhibit moderate toxicity [46, 47]. However, based on the OSP concentrations in surface water measured during the flu season (18 – 58 ng/L) or even the concentrations predicted during an influenza pandemic (98 μg/L), the toxic

levels of OSP that we recorded for *A. thaliana* suggest that this compound is unlikely to constitute a significant threat for plants [46, 43, 50]. The absence of phytotoxic effects detected with ZAN is consistent with prior animal studies concluding that ZAN does not exert significant toxicity at therapeutic doses [38].

4.4.2 Gene expression analysis using microarrays

Using Affymetrix whole-transcript expression microarrays (Arabidopsis Gene 1.0 ST Array), we analyzed the transcriptional response of plants exposed to 20 mg / L of OSP and ZAN. This concentration was chosen because it was shown to result in significant plant biomass reduction upon exposure to OSP. After filtering out the genes with low-quality signals and conducting univariate *t*-tests ($p < 0.001$; BRB-ArrayTools), 76 and 306 genes showed statistically different expression levels after exposure to OSP and ZAN, respectively. Exposure to OSP resulted in more than 2-fold up-regulation (> 2 fold) in 15 genes (32%) and less than 0.5-fold down-regulation (< 0.5 fold) of 32 genes (68%). Exposure to ZAN resulted in more than 2-fold up-regulation of 40 genes (20%) and more than 2-fold down-regulation of 165 genes (80%). Exposure to each target compound resulted in a larger proportion of down-regulated genes than up-regulated ones (68% and 80% in response to OSP and ZAN, respectively), suggesting that OSP and ZAN introduce a more negative regulatory effect on plants. Three genes were up-regulated (> 2 fold) and 20 genes were down-regulated (< 0.5 fold) in response to both OSP and ZAN (Figure 4.3), which represents 6% and 13% of the total up- and down-regulated genes, respectively. The complete list of *A. thaliana* genes up- and down-regulated by exposure to OSP and ZAN is provided in Appendix B.

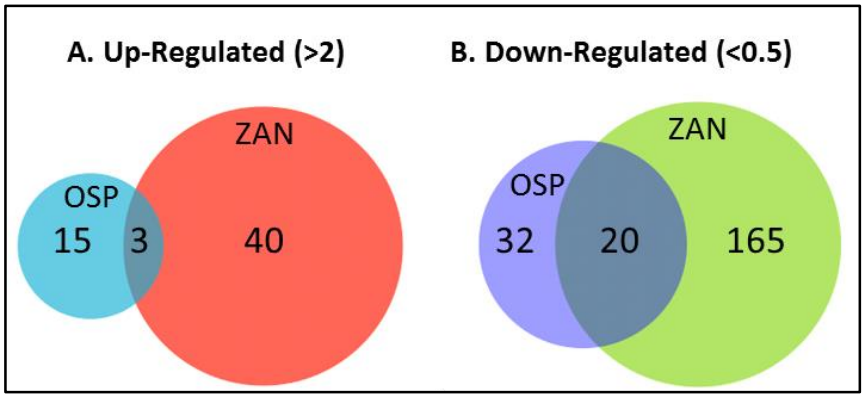

Figure 4.3. Venn diagrams showing the number of genes significantly up-regulated (**Panel A**) and down-regulated (**panel B**) by exposure to the antiviral drugs, oseltamivir phosphate (OSP) and zanamivir (ZAN) individually, and by both compounds simultaneously.

Reverse-transcription real-time PCR. In order to validate the microarray results, quantitative analysis of gene expression was performed on selected genes using RT-qPCR. Figure 4.4 shows the plots of the expression levels of the selected genes as recorded using microarrays against their expression levels recorded using RT-qPCR. Correlations were satisfactory with Pearson's correlation coefficient of 0.74 and 0.96 for exposure to OSP and ZAN, respectively. The RT-qPCR amplification levels were corrected for the amplification efficiencies of different primer sets (ranging from 98% to 110%, $R2 \geq 0.99$) using the software REST 2009.

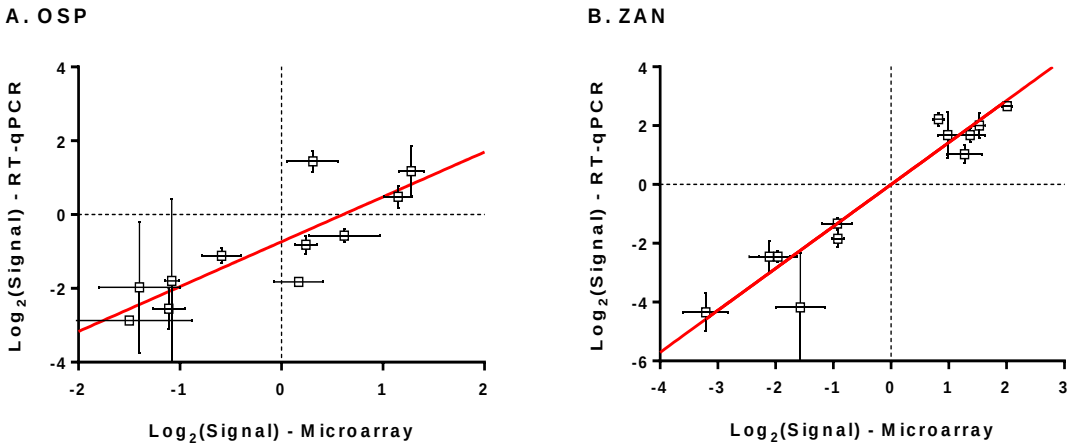

Figure 4.4. Log2 microarray relative expression levels versus log2 RT-qPCR relative expression levels for exposure to panel A: oseltamivir phosphate (OSP) and panel B: zanamivir (ZAN). Error bars represent the standard deviations between three biological replicates.

4.4.3 Functional categories of differentially expressed genes

Genes showing statistically different expression levels were classified in gene ontology (GO) categories using the application BLAST2GO®. Distribution of differentially expressed genes into major categories (GO level 2) showed that the most represented process categories for up- and down-regulated genes in response to OSP were metabolic process, single-organism process, response to stimulus, and cellular process. The most represented process categories for both up- and down-regulated genes in response to ZAN were cellular process, single-organism process, metabolic process, response to stimulus, and biological regulation (Figure 4.5). The most represented functional categories for differentially expressed genes were binding and catalytic activity for exposure to OSP and catalytic activity for exposure to ZAN (Figure 4.6). The process category, *response to stimulus*, included approx. 17% of the expressed genes upon exposure to OSP (ranked 1st) and 13% in ZAN (ranked 2nd), which seems to reflect

a toxicity on exposed plants. A more detailed examination of the distribution of differentially-expressed genes in ontology GO categories (GO level 3) showed that exposure to both OSP and ZAN affected primarily the expression of genes involved in response to stresses and stimuli. Interestingly, the three most represented process categories (GO level 4) for both OSP and ZAN were *response to organic substances*, *response to oxygen-containing compounds,* and *response to hormones*. Another important category involving mostly down-regulated genes was the *organic compound synthesis,* which may also reflect a toxic effect of OSP and ZAN on the plants. One of the most represented processes (GO level 2) for genes simultaneously up-regulated by exposure to OSP and ZAN was *response to stimulus*. The most represented categories for the genes simultaneously down-regulated by exposure to OSP and ZAN were *catalytic activity*, *response to stimulus*, and *metabolic process* at GO level 2, and *organic substance metabolic process*, *single-organism metabolic process*, *cellular metabolic process*, *response to chemical stimulus*, and *biosynthetic process* at GO level 3. The induction of genes involved in response to stimulus and the down-regulation of genes involved in the metabolism of organic compounds also supports the hypothesis that high doses of OSP and ZAN may negatively impact the plants growth.

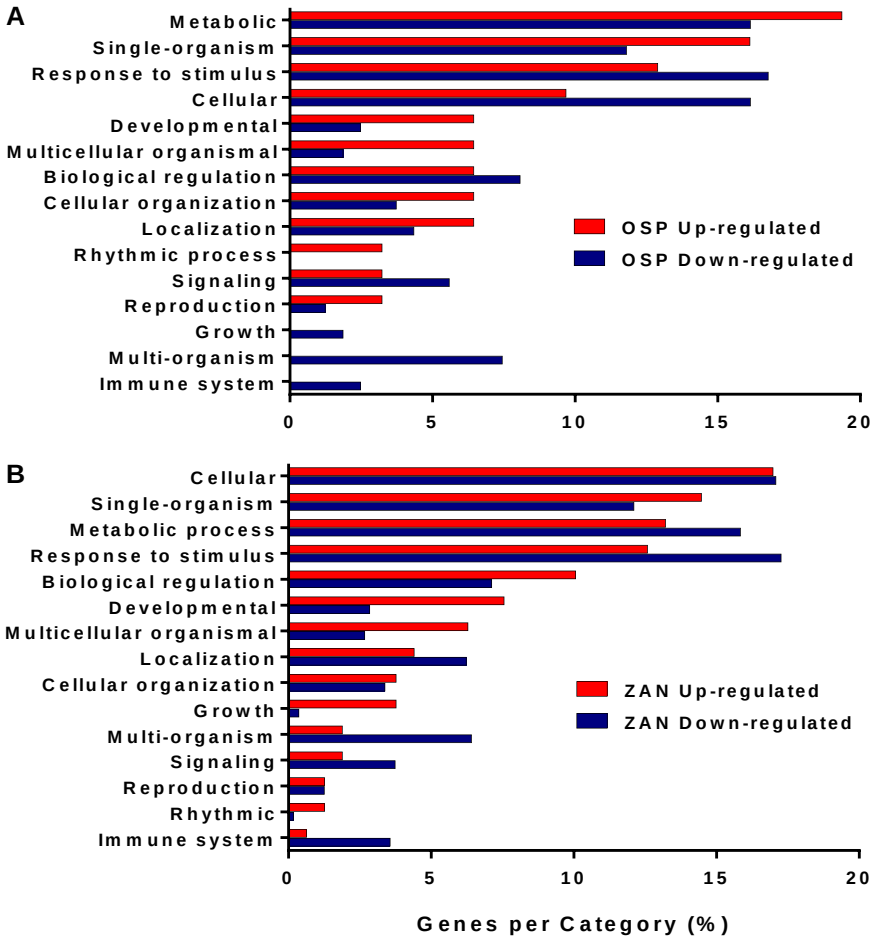

Figure 4.5. Major gene ontology (GO) process categories of up- and down-regulated genes. Distribution of genes into GO categories was performed using BLAST2GO® (GO level 2). Panel A: Genes differentially expressed by exposure to ZAN, Panel B: Genes differentially expressed by exposure to OSP.

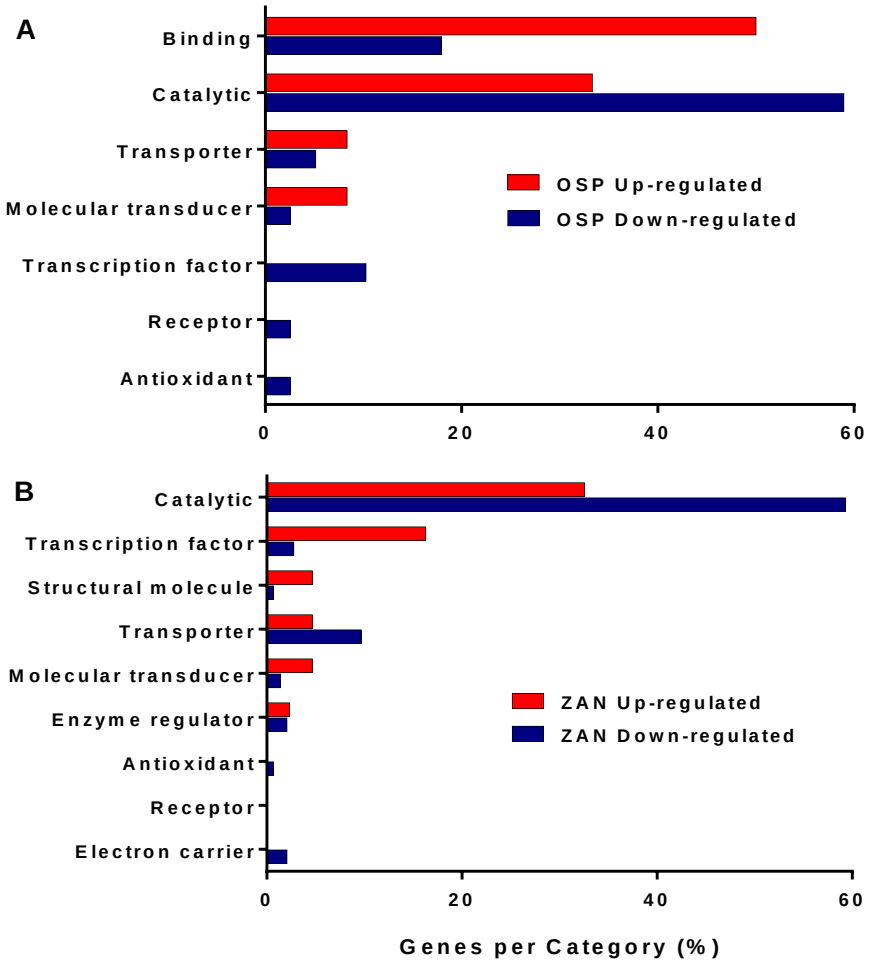

Figure 4.6. Major gene ontology (GO) functional categories of genes up (fold change > 2.0) and down-regulated (fold change < 0.5) Panel A: Genes differentially expressed by exposure to ZAN. Panel B: Genes differentially expressed by exposure OSP.

Differential expression of remarkable genes. The genes that are up- and down-regulated at the highest level in response to OSP and ZAN are listed in Appendix B. Exposure to OSP strongly stimulated five genes encoding a *S*-adenosylmethionine-dependent methyltransferase (AT5G37970, fold change 10.35), a cell wall protein precursor (AT2G20870, fold change 10.04), a midchain alkane hydroxylase (AT1G57750, fold change 5.93), a pollen ole e 1 allergen/extensin (AT5G22430, fold change 5.45), and a lipid transfer protein 4 (AT5G59310, fold change 5.32). Methyltransferases mediate

DNA methylation, which has been shown to regulate gene expression in response to environmental factors, such as exposure to toxic compounds. On the other hand, stimulation of cell wall biosynthesis has also been recognized as a mechanism of plant defense against various biotic and abiotic stresses. Similarly, extensin is a protein that has been associated with the reduction of organ size, which is also a recognized plant defense process. The genes the most up-regulated in response to ZAN include a dormancy/auxin associated protein (AT2G33830) involved in response chilling, heat shock, and salt treatment. A beta-glucosidase (BXL2) involved in response to pathogens, and again, an expansin-A3 (EXP3) involved in reduction of organ expansion. The genes the most down-regulated in response to ZAN include two genes involved in the biosynthesis of terpenes and terpenoids, 1-deoxy-D-xylulose 5-phosphate synthase 1 (DXPS1) and terpene synthase 04 (TPS04), which are known to be involved in plant response to various biotic and abiotic stresses and plant signaling. The genes the most down-regulated in response to OSP include again a terpene synthase 04 (TPS04), an 2-oxoglutarate (2OG) and Fe(II)-dependent oxygenase-like protein (AT2G38240) involved in response to salt stress and karrikin, and a defensin-like protein 17 (PDF1.2c) involved in response to various biotic and abiotic stresses.

Genes significantly up-regulated by exposure to both OSP and ZAN (fold change > 2) are coding for an uncharacterized protein (AT3G04721), a glucose-methanol-choline (GMC) oxidoreductase-like protein (AT1G12570) involved in alcohol metabolism, a CBL-interacting serine/threonine-protein kinase 20 (CIPK20, AT5G45820), and a two-component response regulator ARR15 (AT1G74890) acting as negative regulator in cytokinin-mediated signal. A majority of genes significantly down-regulated by exposure

to both OSP and ZAN (fold change < 0.5) are involved to biosynthesis processes: 1-deoxy-D-xylulose 5-phosphate synthase 1 (DXPS1, AT3G21500), UDP-glucosyl transferase 76E12 (AT3G46660), leucoanthocyanidin dioxygenases (LDOX, AT4G22880, AT4G22870), tryptophan synthase beta chain (AT5G28237), dihydroflavonol-4-reductase (DFR, AT5G42800), and stress and defense processes: 2-oxoglutarate (2OG) and Fe(II)-dependent oxygnase-like protein (AT2G38240), terpene synthase 04 (TPS04, AT1G61120), receptor like protein 53 (RLP53, AT5G27060), beta-amylase 5 (BAM5, AT4G15210).

Prior studies published on the transcriptional response of *A. thaliana* plants exposed to organic contaminants, such as TNT and PCBs reported gene expression changes of genes involved in metabolism of the contaminants in plant tissues [181, 153, 144, 182]. Xenobiotic organic compounds, such as pesticides, nitroaromatic explosives, and chlorinated solvent and aromatic chemicals, have been shown to undergo plant-mediated biodegradation inside plant tissues. Based on the observation that plants can metabolize pesticides, Sandermann (1994) introduced first the green liver model, which suggests a three-step metabolic sequence similar to the one that occurs in the liver of mammals involving initial activation by oxidation or reduction (phase I), transferase-catalyzed conjugation of the activated compound (phase II), and sequestration of the conjugate in plant tissues (phase III) [111]. Exposure to antiviral drugs, ZAN and OSP, was also shown to induce several genes potentially involved in biodegradation pathways of the compounds. Although there is currently no information about the biodegradability of ZAN and OSP by plants, potential genes involved in phase I of the green liver model include various oxidoreductases (e.g., fatty acyl-CoA reductase, glucose-methanol-

choline oxidoreductase, 2-alkenal reductase), and cytochrome p-450 monooxygenases. Potential phase II genes include different transferases (e.g., *S*-adenosyl-*L*-methionine-dependent methyltransferase). Several genes potentially involved in phase III of the green liver model include genes involved in carbohydrate metabolism and transport (e.g., nodulin MtN21/EamA-like transporter, xanthine dehydrogenase, β-glucosidase 33, and peptide transporters).

Genes differentially-expressed in response to OSP and/or ZAN (fold-change >2 or <0.5) were then searched against the Genvestigator *Arabidopsis* microarray database (Hruz et al. 2008) for their potential responsiveness to other stimuli, including abiotic stress (e.g., salt, drought, temperature, light), toxic stress (e.g., metals, pesticides, antibiotics), biotic stress (e.g., bacteria, fungi, nematodes), and phytohormone stimulus (e.g., auxin, zeatin, ethylene). Figure 4.7summarizes the number of times *Arabidopsis* OSP and/or ZAN-responsive genes were reported to be overexpressed in response to stimuli in other microarray investigations. For instance, a gene coding for a non-specific lipid-transfer protein 4 (LTP4) (AT5G59310) up-regulated by exposure to OSP (fold change 5.32) was shown to be also up-regulated (fold change > 2.0) in multiple microarrays experiments including exposure to abiotic stress, toxic species, pathogens, and phytohormones. Other OSP-responsive genes shown to be stress-inducible include a CBL-interacting serine/threonine-protein kinase 20 (CIPK20) (AT5G45820) with unknown function, a response regulator ARR15 (AT1G74890) that acts as a negative regulator in cytokinin-mediated signal transduction, and a fibrillarin 2 (FIB2) protein (AT4G25630) involved in protein synthesis. Two of these genes (AT5G45820 and AT1G74890) were also significantly up-regulated by exposure to ZAN. Gene

significantly up-regulated by ZAN, which were reported to be induced by various abiotic stresses, include a dormancy/auxin associated protein (AT2G33830), an aluminum induced protein with YGL and LRDR motifs (unknown function) was shown to be induced by ZAN.

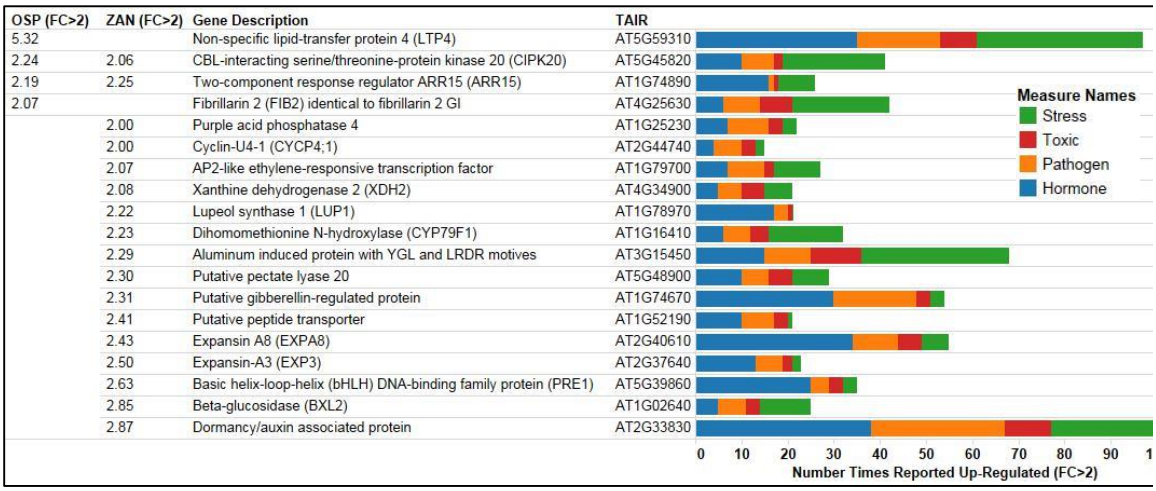

OSP (FC>2)	ZAN (FC>2)	Gene Description	TAIR
5.32		Non-specific lipid-transfer protein 4 (LTP4)	AT5G59310
2.24	2.06	CBL-interacting serine/threonine-protein kinase 20 (CIPK20)	AT5G45820
2.19	2.25	Two-component response regulator ARR15 (ARR15)	AT1G74890
2.07		Fibrillarin 2 (FIB2) identical to fibrillarin 2 GI	AT4G25630
	2.00	Purple acid phosphatase 4	AT1G25230
	2.00	Cyclin-U4-1 (CYCP4;1)	AT2G44740
	2.07	AP2-like ethylene-responsive transcription factor	AT1G79700
	2.08	Xanthine dehydrogenase 2 (XDH2)	AT4G34900
	2.22	Lupeol synthase 1 (LUP1)	AT1G78970
	2.23	Dihomomethionine N-hydroxylase (CYP79F1)	AT1G16410
	2.29	Aluminum induced protein with YGL and LRDR motives	AT3G15450
	2.30	Putative pectate lyase 20	AT5G48900
	2.31	Putative gibberellin-regulated protein	AT1G74670
	2.41	Putative peptide transporter	AT1G52190
	2.43	Expansin A8 (EXPA8)	AT2G40610
	2.50	Expansin-A3 (EXP3)	AT2G37640
	2.63	Basic helix-loop-helix (bHLH) DNA-binding family protein (PRE1)	AT5G39860
	2.85	Beta-glucosidase (BXL2)	AT1G02640
	2.87	Dormancy/auxin associated protein	AT2G33830

Figure 4.7. Genes up-regulated by exposure to OSP and/or ZAN in *A. thaliana* and the number of times they were reported similarly overexpressed by various stresses in other microarray experiment (Genevestigator).

Figure 4.8 summarizes the number of times *Arabidopsis* OSP and ZAN-responsive genes were reported to be down-regulated in response to stimuli in other microarray investigations. Among the genes down-regulated by OSP and/or ZAN the most frequently reported down-regulated by various stresses are a tetratricopeptide repeat family protein (involved in salt tolerance and osmotic stress), a myrosinase binding protein 1, and several transferases, such as acyl-CoA N-acyltransferases-like protein, tyrosine aminotransferase 3 (TAT3), and glutathione *S*-transferase phi 12 (GSTF12).

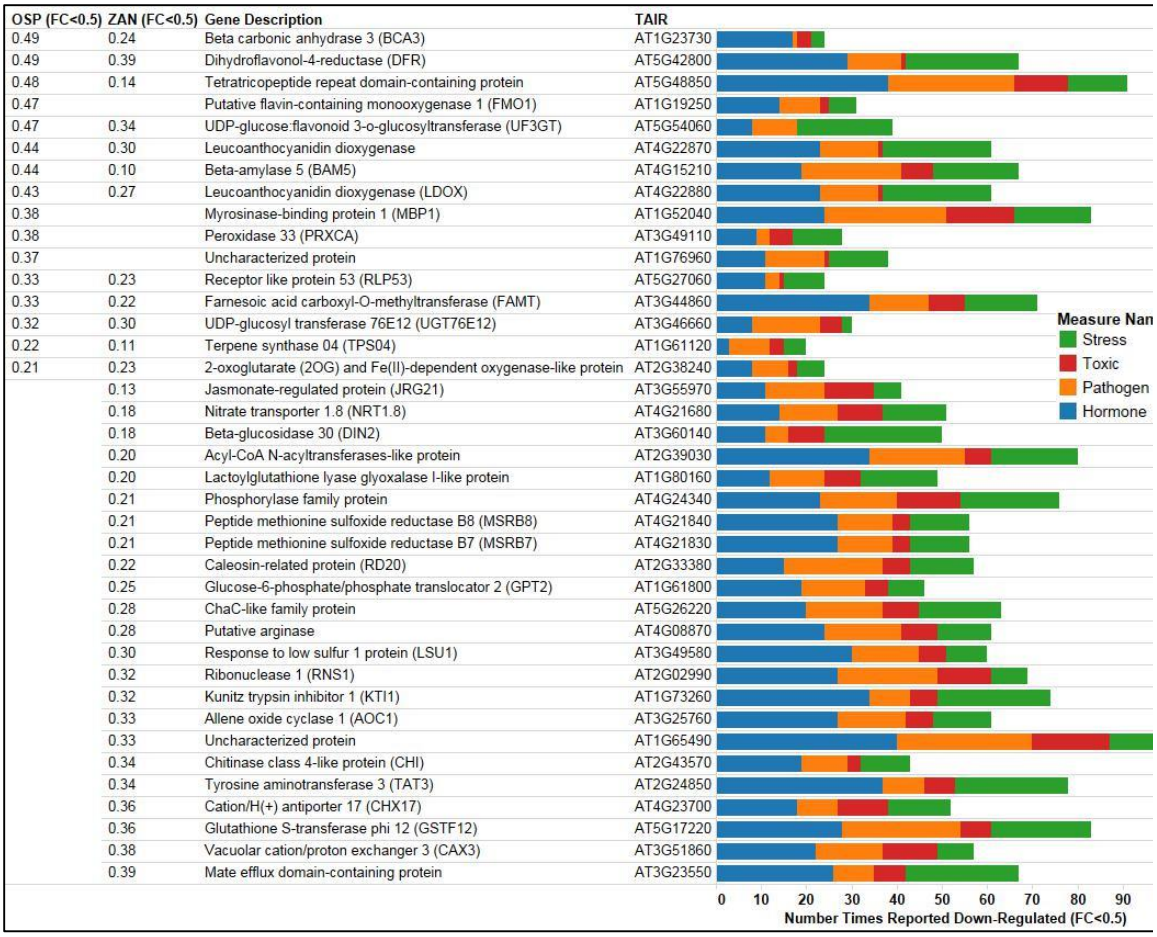

Figure 4.8. Genes down-regulated by exposure to OSP and/or ZAN in *A. thaliana* and the number of times they were reported similarly repressed by various stresses in other microarray experiments (Genevestigator).

Overall, these results suggest that exposure to OSP and ZAN change the expression level of several important genes involved in plant response to stress and external stimuli. Often, lack of knowledge of the gene function limits the interpretation of the results. Comparison of our gene expression results with other microarray data on *Arabidopsis* exposure to toxic compounds, biotic and abiotic stress, and hormonal stimuli reveals that many genes significantly impacted by exposure to the antiviral drugs are generally involved in response to stress, therefore suggesting a negative impact of the target compounds on plants development.

This article presents the first whole-genome expression microarray experiment focusing on *A. thaliana* plants exposed to the neuraminidase antiviral drugs, OSP and ZAN. Results from this study suggest that OSP and ZAN may exert a negative effect on the model plant *A. thaliana*, but only when exposed to very high levels that are unlikely to be found in the environment. Although the effects of pharmaceutical compounds on plants chronic toxicity of chemicals toward plants is typically difficult to observe in the laboratory, gene expression analysis can provide useful information about the potential long-term potential effects of exposure to contaminants [164]. Gene expression results are believed to provide new insights into the molecular mechanisms of plant response to antiviral drugs.

CHAPTER 5 EXPOSURE OF SOY PLANTS TO PCBS AND TNT

5.1 Introduction

Industrial and military utilization of explosives, such as 2,4,6-trinitrotoluene (TNT), and chlorinated organics, such as polychlorinated biphenyls (PCBs), for many years have left numerous polluted sites, which have led to further contamination of soil and water. Different physical, chemical, and biological methods have been used to remove these contaminants from the environment, including phytoremediation. Many studies have been conducted to determine the plant tolerance and uptake capability of explosives and PCBs [58, 62]. Plants are known to be able to take up and, to some extent, metabolize organic contaminants from soil and groundwater. Because plants grown on land contaminated with toxic pollutants for phytoremediation purposes are unsuitable for food production, we proposed to test the possibility to use energy feedstock plants whose biomass could be valorized for bioenergy production. In this chapter, we report an experimental investigation on the potential of growing the bioenergy crop, soybean, on soil contaminated by the toxic organic chemicals, PCBs and TNT, for the combined benefits of land phytoremediation and biofuel production. Results from this study are then expected to promote the development of sustainable bioenergy programs that do not compete with land used for food production. Although a few studies have been conducted on the potential of using energy plants for phytoremediation of metal-contaminated land, little information is available about the effect of organic pollutants, such as TNT and PCBs, on the feedstock biomass production and bioenergy yield in plants grown in contaminated soil.

This chapter includes the Objective of the study, the Experimental Methods (soybean growth, exposure experiments, analytical methods for TNT and PCBs), and the Results section, and the Discussion section.

5.2 Objectives

The objective of this study was to evaluate the potential of growing an important energy crop, soybean, on soil contaminated by the organic pollutants, TNT and PCBs (e.g., 2,4'-dichlorobiphenyl - 2,4'-DCB), for the combined benefits of land phytoremediation and sustainable biofuel production.

5.3 Materials and Methods

5.3.1 Chemicals

TNT was obtained from Chem Service (West Chester, PA). 2,4'-DCB was obtained from AccuStandard (New Haven, CT). RNAlater solution was purchased from Ambion (Foster City, CA). Solvents used in the extraction processes were HPLC grade and were bought from different sources.

5.3.2 Plant species and culture conditions

Soybean seeds, *Glycine max* L. cv. Enrei, were obtained from the Missouri Foundation Seed at the University of Missouri (Columbia, MO). Synthetic soil was prepared by mixing 50:50 (v:v) sieved coarse sand (4 mm) and organic seeding mix (peat moss). Soybeans were planted 1 inch deep in soil with two seeds per pot. Seeds were incubated at room temperature under cool (white) fluorescent light (4100 K) with a 16 h light/8 h dark photoperiod and a light intensity of 0.2-0.4 W/ft^2.

5.3.3 Growth inhibition experiments

Stock solutions of 5,000 and 10,000 mg / L of TNT or PCB were prepared in acetone. The desired volume of stock solution was then added to 10 to 12 mL acetone before mixing with an aliquot of dry soil for the purpose of wetting the soil evenly and distributing the contaminant homogeneously into the soil body. The amount of stock solution was calculated to reach the final desired concentrations after mixing with the soil. The non-exposed (control) soil was spiked with an equivalent volume of acetone. The stock solution was added first to one third or one fourth of the final soil amount, mixed and homogenized in glass beakers, and allowed to dry overnight in a chemical hood with frequent manual soil mixing. The contaminated soil aliquot was then mixed with the remaining soil in a glass jar by vigorous shaking and was placed in the growing pots (individual 500-mL pots or 150-mL cell tray). The experiments were conducted with 24 to 48 replicate plants per treatment.

Germination rate and plant growth were monitored during the time of exposure. After 1 to 2 weeks of growth (after development of leaves and reaching at least 7 inches height), plantlets were sacrificed. Plantlets were carefully removed from the soil without damaging the roots. The roots were washed under running tap water, DI water, and 20% ethanol to remove potential contaminant adsorbed to the root surface. The roots were dried by blotting and the plants were then separated into different organs, including roots, aerial parts, stems, leaves, and –in the case of long-term experiments – beans. The different organs were then weighed, and their size was measured. Plant tissues and soil aliquots were stored at -80°C for further analyses. The tissues for RNA extraction and

microarray experiments were kept in RNAlater™ solution for 24 hours at 4°C to preserve the RNA quality and then were stored at -80°C.

5.3.4 Analysis of TNT and PCBs

For TNT analyses, the roots and aerial parts of the plants were ground separately in liquid nitrogen using mortar and pestle. The samples were transferred into vials and their weights were recorded. The samples were extracted with 10 mL of acetonitrile/g sample (fresh weight). The vials were then placed in an ultrasonic bath for 18 hours. The extracts were filtered with 0.45 µm nylon membrane filters. TNT analysis was performed on an Agilent 1100 (LC) - 6140 (MS) equipped with an Ascentis Express C18 (150×3 mm, 5 µm) column. Operating conditions were as follows: mobile phase: water:acetonitrile 45:55 (v/v); flow rate: 0.2 mL/min; column temperature 20°C; injection volume: 10 µL. MS detector parameters were as follows: SIM mode (M-1 = 226); mode ESI negative; drying gas flow: 13.0 L/min; nebulizer pressure: 35 psi; drying gas temperature: 300°C; capillary voltage: 4,000 V.

To extract TNT from soil, soil samples were first dried in a chemical hood at room temperature with mixing several times over 24 h. Three replicates from each soil sample were collected from 6-10 different locations. Each soil replicate was weighted (approx. 3 g) and introduced in a glass tube sealed with Teflon caps. 1,2-Dinitrobenzene was added to the soil sample as surrogate to determine the recovery of the extraction. The final concentration of the surrogate was 20 mg / kg in soil. The soil was then extracted with 3 mL of acetone by vortexing for 30 seconds and shaking horizontally at 125 rpm for 18 h at room temperature. The tubes were centrifuged for 1 minute at 2,500 rpm and the supernatant was filtered using 0.2 µm PTFE syringe filters. TNT analysis was

conducted using an Agilent HPLC 1200 series. The system was load with a reverse-phase C18 column (75 × 4.6 mm, 3 μm). The detection was performed using a UV-visible photodiode array detector at 230 nm. The mobile phase was water:ACN (50:50 v/v). The column temperature was maintained at 27°C.

For PCB analysis, the roots and aerial parts of the plants were ground separately in liquid nitrogen using mortar and pestle. The samples were transferred into vials and weighed. 200 ng of 4,4'-DCB was added to each sample as an internal standard. The samples were then extracted with 5 mL mixture of hexane:acetone 1:1 (v/v) and ultrasonicated for 5 hours. The samples were centrifuged at 3,000 rpm for 5 min and the organic phase was collected. A second extraction was performed with 5 mL of hexane for 0.5 hours. The combined extracts were dried under a flow of nitrogen and re-dissolved in 1 mL hexane. The samples were treated with 1 mL of concentrated H_2SO_4 for 0.5 hours. The samples were centrifuged at 3,000 rpm for 5 min and the organic phases were transferred to a new vial. The acidic phase was re-extracted with 1 mL of hexane. The extracts were combined and applied on a column containing 1 g of acid silica gel over 0.1 g of activated silica gel. PCBs were eluted with 10 mL of hexane and the eluents were concentrated with a gentle nitrogen flow to 1 mL before GC-ECD analysis.

5.3.5 Data validation and statistical analysis

The statistical significance of the results will be assessed by performing one-way ANOVA test followed by Tukey's multiple comparison test at 95% confidence level ($p < 0.05$) (Prism 6.0, GraphPad, La Jolla, CA). When no statistical differences were observed, the data were screened for the presence of outliers using the ROUT method (Q = 1 to 5%). When outliers were found, they were removed from the data set and one-way

ANOVA (with Tukey's multiple comparison test) was performed again (Prism 6.0, GraphPad, La Jolla, CA).

5.4 Results and Discussion

5.4.1 Soybean exposure to TNT

Short-term experiments:

Soybean plants were first exposed to low TNT concentrations: 0.0, 2.5, 5.0, and 10 mg / kg soil (dry weight). No significant effect was observed between the treatments (Figure 5.1) after 10 days of growth suggesting that these doses were below the lowest-observable-adverse-effect level (LOAEL) for TNT.

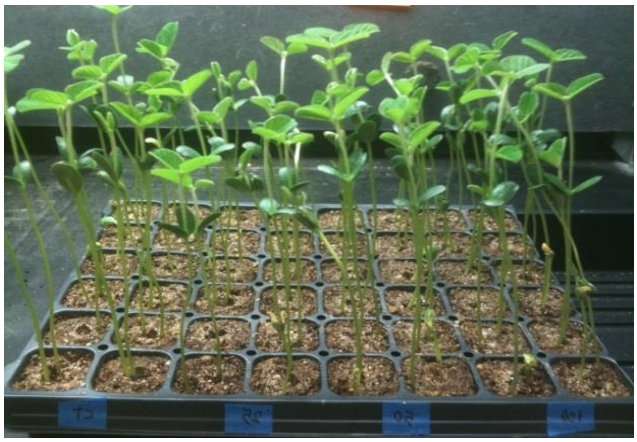

Figure 5.1. Soybean plantlets exposed for 10 days to TNT at concentration from 0.0 to 10 mg / kg soil (fresh weight).

The experiment was then repeated using 10-time higher concentrations: 0.0, 25, 50, and 100 mg / kg soil (dry weight). Germination rates were 91.7% in control plants, 95.8% in plants exposed to 25 mg / kg, 91.7% in plants exposed to 50 mg / kg, and 83.3% in plants exposed to 100 mg / kg, suggesting a slight toxic effect of TNT at high dose.

Delay in plant growth was then recorded with the plants exposed to 50 and 100 mg / kg (Figure 5.2).

Figure 5.2. Soybean plantlets exposed for 10 days to TNT at concentration from 0.0 to 100 mg / kg soil (fresh weight).

Figure 5.3 Soybean harvested after 15 days of exposure for the determination of plant metrics.

Surprisingly, after 15 days of growth, no significant differences at 95% confidence level in the weight of roots or leaves were recorded between the treatments (one-way ANOVA) (Figure 5.3).

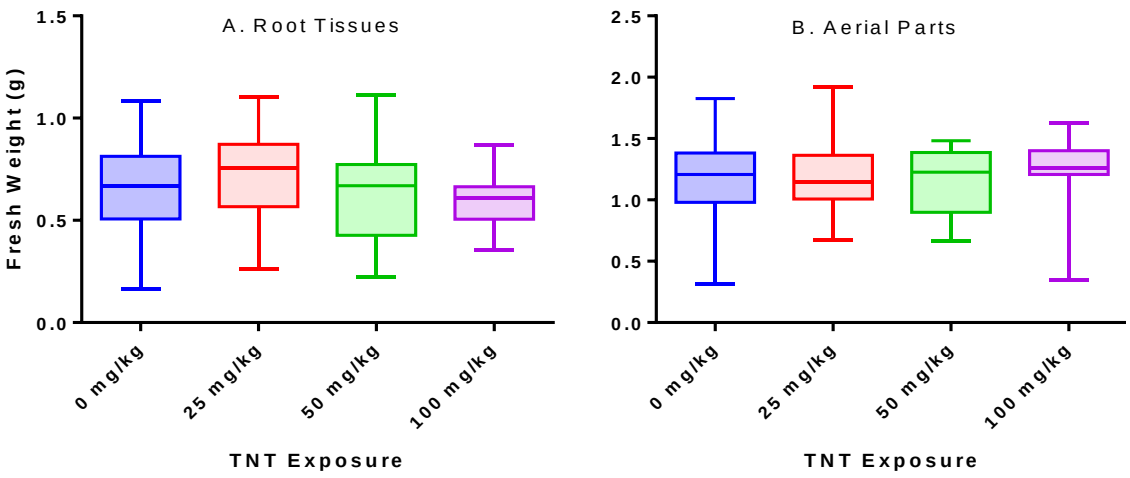

Figure 5.3. Organ weight of soybean plantlets exposed for two weeks to TNT at concentration ranging from 0.0 to 100 mg / kg soil (fresh weight). Panel A: Root weight. Panel B: Aerial part weight.

In order to further test the effect of TNT on the germination and growth rates of soybean plants, higher concentrations of TNT were applied: 0.0, 50, 100, and 250 mg / kg soil. However, only exposure to the highest concentrations (250 mg / kg) resulted in statistically significant differences in root biomass. No significant differences in shoot/leaf biomass were observed even at the highest concentration applied. On the other hand, exposure to TNT resulted in a significant dose-dependent decrease of root length from 50 to 250 mg / kg. Interestingly, the shoot length showed a significant increase upon exposure to 250 mg / L (Figure 5.4).

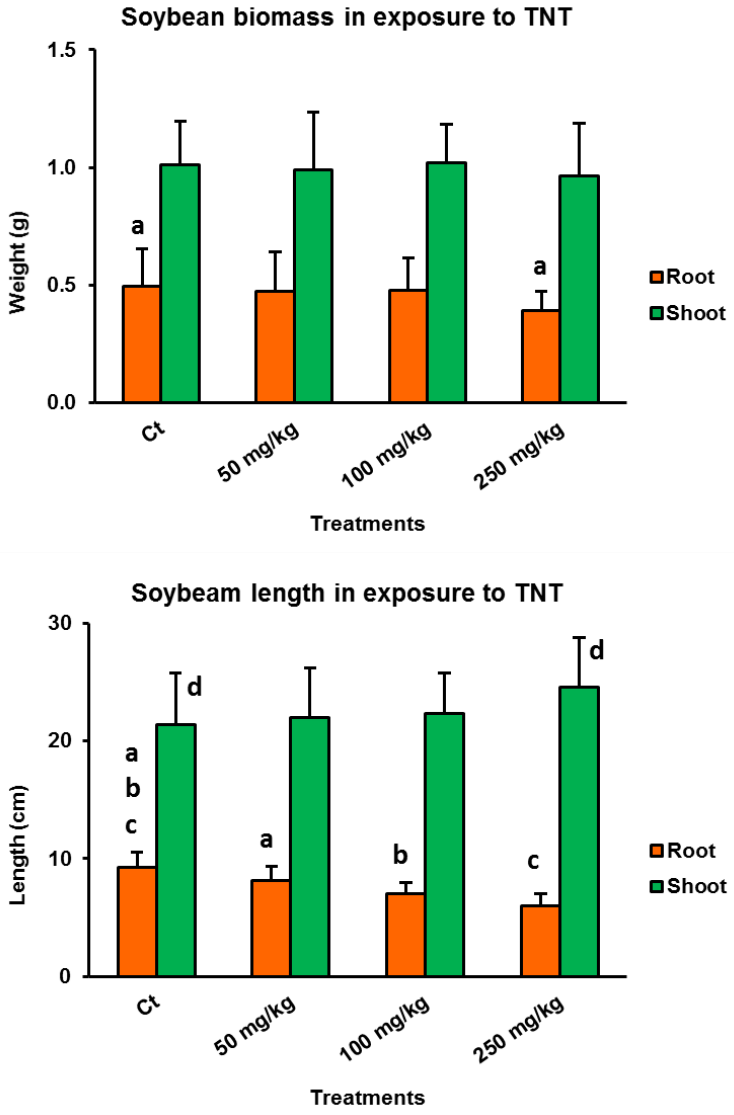

Figure 5.4. Exposure of soybean plants to TNT at concentration ranging from 0.0 to 250 mg / kg soil. Weight and length of plants are presented. Data sets labeled with similar letters are significantly different.

5.4.1 Analysis of TNT in plant tissues

TNT was then analyzed in the tissues (roots and shoots/leaves) of exposed plants (0.0, 25, 50, and 100 mg / kg soil), showing a TNT accumulation proportional to the dose applied. After 28 days of exposure, TNT content in the root tissues was approx. 15, 60, and 160 ng/g tissue for exposure doses of 25, 50, and 100 mg / kg soil, respectively. TNT

content in roots was 48, 20 and 18 times higher than in shoots for exposure doses of 100, 50 and 25 mg / kg soil, respectively (Figure 5.5). These results suggest a significant, but limited translocation of TNT within the plant tissues. Analysis of residual TNT in soil, show very low concentration by comparison the initial application, strongly suggesting that TNT in soil was fast transformed (reduced) into different metabolites (Figure 5.6). In order to determine the effect of the vegetation on TNT stability in soil, we analyzed the residual TNT in contaminated soil (50 mg / kg soil dry weight) vegetated with soybean plants (V) and in control, non-vegetated soil (NV) after 15 days of incubation. Results show that TNT concentration in samples without plants was almost two times higher than in soil vegetated with soybean, suggesting that the presence of plants increases the microbial activity and TNT reduction in soil.

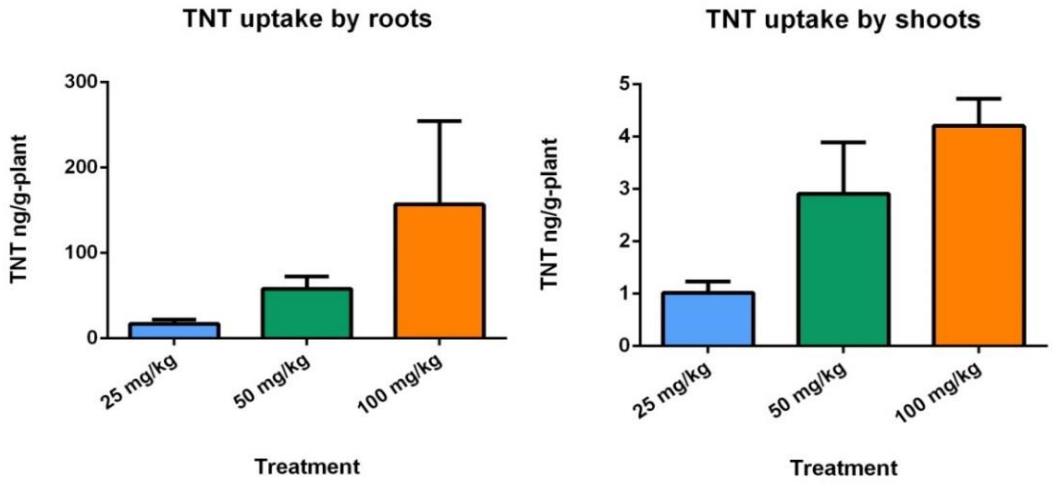

Figure 5.5. TNT detected in soybean tissues after 28 days of exposure in soil containing supplemented with 25, 50, and 100 mg TNT/kg soil.

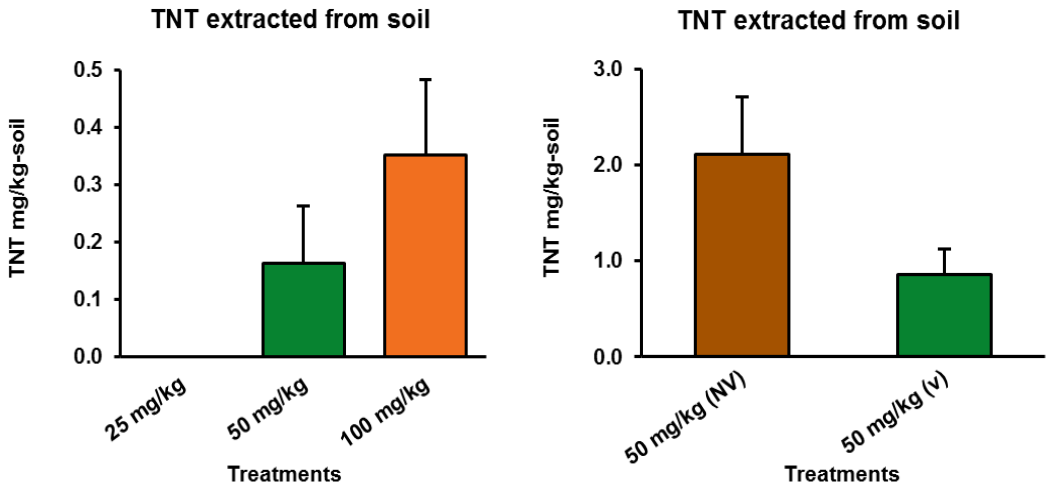

Figure 5.6. Residual concentration of TNT in soil. Left: soil vegetated with soybean plants and supplemented with 25, 50, and 100 mg TNT/kg soil after 28 days of exposure. Right: soil supplemented with 50 mg TNT/kg soil vegetated and non-vegetated (NV) with soybean plants (V) after 15 days of exposure.

The average amount of TNT detected in plant tissue and in soil was used for mass balance calculations of soybean plants exposed to 25, 50, and 100 mg / kg of TNT in order to estimate the phytoremediation ability of plants and calculate the bioaccumulation factors (Table 5.1).

Table 5.1. TNT mass balances in soil and soybean plants. Total TNT amounts used for each treatment are shown. Corresponding percentages are shown in parentheses. Bioaccumulation factors are defined as the ratios of TNT concentration in plant tissues over its concentration in soil.

	Treatment		
	25 mg / kg	50 mg / kg	100 mg / kg
Initial TNT in soil (µg)	13,500 (100)	27,000 (100)	54,000 (100)
Root uptake (µg)	0.304 ($2.25\ 10^{-3}$)	0.968 ($3.59\ 10^{-3}$)	3.000 ($5.56\ 10^{-3}$)
Aerial parts uptake (µg)	0.030 ($2.24\ 10^{-4}$)	0.086 ($3.19\ 10^{-4}$)	0.127 ($2.35\ 10^{-4}$)
Final TNT in soil (µg)	0.0 (0 %)	88 ($3.26\ 10^{-1}$)	190 ($3.52\ 10^{-1}$)
Uptake by plant (%)	$2.5\ 10^{-3}$	$3.9\ 10^{-3}$	$5.8\ 10^{-3}$
Bioaccumulation factor in roots	$6.74\ 10^{-4}$	$1.16\ 10^{-3}$	$2.04\ 10^{-3}$
Bioaccumulation factor in aerial parts	$4.08\ 10^{-5}$	$5.82\ 10^{-5}$	$4.21\ 10^{-5}$

The mass balances were based on all replicate plants and the average TNT content in each part of the plant (root or shoot) in each treatment. Bioaccumulation factor were defined as the ratio of TNT concentration in plant tissue:TNT concentration in soil. The mass balances seem to indicate a high level of biodegradation of TNT in soil and/or plant tissues. TNT was presumably reduced into its metabolites (2-amino-4,6-dinitrotoluene (2ADNT) and 4-amino-2,6-dinitrotoluene (4ADNT).

Long-term experiments:

The prolonged effect on TNT on soybean plant was investigated in the long-term, in order (1) to detect potential chronic effects on plant health and (2) to identify potential effects on bean production. This aspect of the research was critically important as beans are the plant organs from which triacylglycerols (TAGs) are extracted for transesterification into fatty acid methyl esters (FAMEs) and biodiesel production. Soybean plants were then cultivated over four months in soil supplemented with 0.0 (controls), 25, and 50 mg / kg soil of TNT. After 10, 12, and 32 days of exposure (Figure 5.7), soybean plants exposed to 25 and 50 mg TNT/kg soil show a slower growth by comparison to control, non-exposed plants. After 72 days, no significant difference in plant sizes across the different treatments was observable (Figure 5.8).

Figure 5.7. Long term soybean exposure to TNT during the first month of growth. Germination started exposed to TNT concentrations of 0, 25, and 50 mg / kg (left to right). Plants showed a lag in the plants' growth rate after A) 10 days, B) 12 days, and C) 24 days.

Plants were then maintained through a period of 120 days (bean stage) before they were harvested. As the soybean plants were growing taller, they needed a type of support that was provided as 1-m bamboo poles (Figure 5.8).

The plant produced first pods with green beans on the four top nodes on the main

Figure 5.8. Bamboo poles to hold the bean stalk upright for the long term experiment. Picture is taken after 72 days from planting the seeds.

stem. Rapid yellowing of the leaves began shortly after this stage. Three to six trifoliolate leaves might fall from the lowest nodes after the yellowing began (Figure 5.9). Soybean plants are known to continue seed filling the pods until the full seed stage is completed [176].

Figure 5.9. A) Beginning seed period for soybean plants happen at this stage. Lower leaves fall and yellowing starts. At this time pods start filling with seeds. B) Beginning seed C) Full seed.

After 120 days, the plants were sacrificed and plant metrics were determined, including leaf size and weight, root size and weight, and plant size and weight (Figure 5.10). Beans were collected, counted and weighed. Figure 5.11 presents specific plant metrics, showing that exposure to TNT resulted in reduction of the aerial parts and root's weight and size.

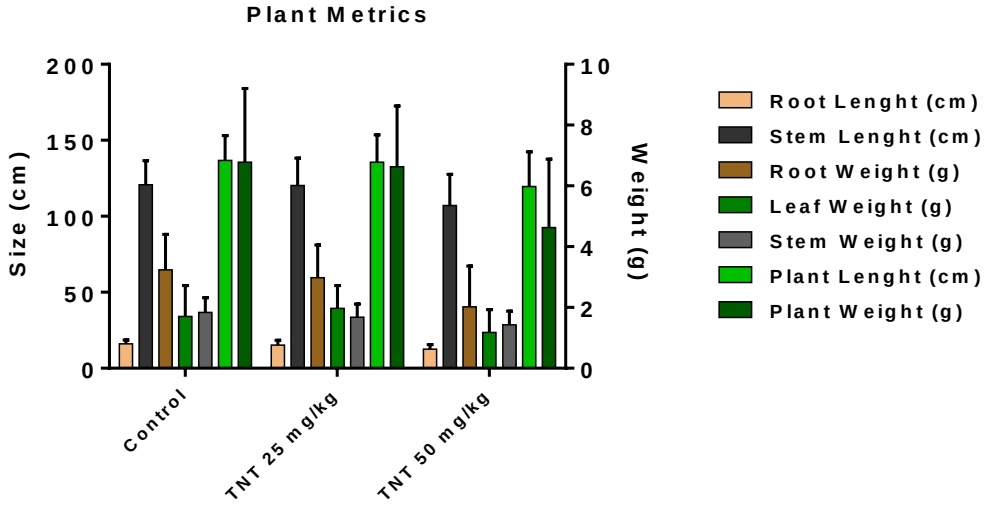

Figure 5.10. Effects of TNT applied at concentration of 0.0, 25, and 50 mg / L on various metrics of soybean plants. Plants metrics were recorded after 120 days of exposure.

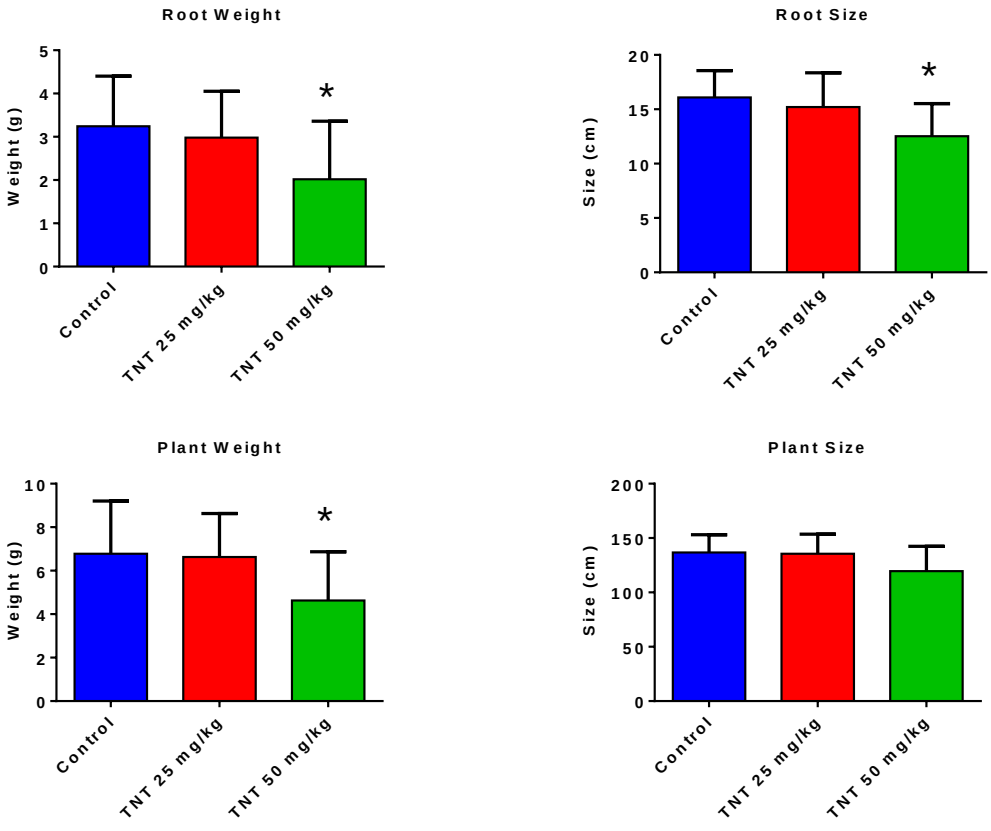

Figure 5.11. Effects of TNT applied at concentration of 0.0, 25, and 50 mg / L on the size and biomass of soybean plants. Plants metrics were recorded after 120 days of exposure. Asterisks (*) indicate statistically significant differences ($p < 0.05$) by comparison to control plants.

Exposure of the plants to TNT also resulted in effects on the number and weight of the beans produced. Figure 5.12 shows that exposure to 50 mg / L TNT resulted in a statistically significant decrease of the number of beans harvested per plant. Interestingly, TNT at the highest dose (50 mg / L) also increased to average weight of individual beans. The combined effects, i.e., decrease of bean number and increase of bean weight, in exposed plant, however, resulted in an overall reduction of the biomass of soy bean that was harvested from each plant (bottom panel). Even though in prior short-term experiments, exposure of soybean plants to TNT did not seem to have a significant effect of the plant size and biomass (only a lag in the plant growth was observed), long-term exposure was shown to affect plant size and biomass in a more marked way.

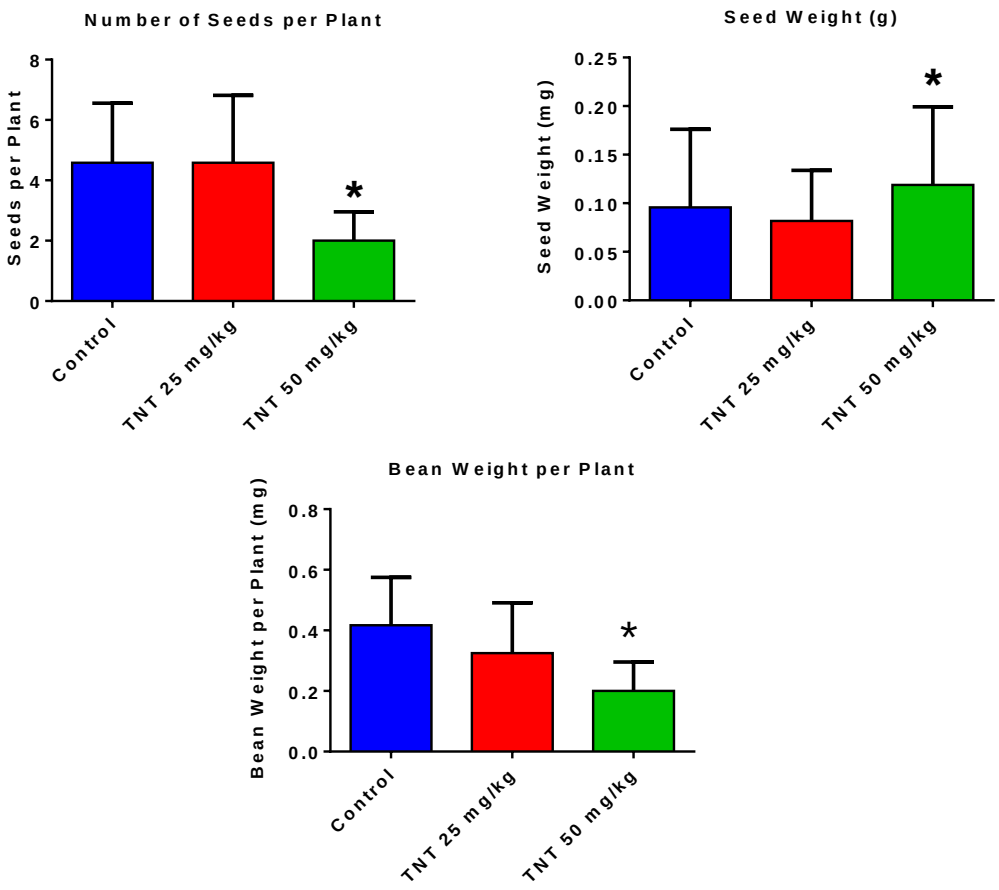

Figure 5.12. Effects of TNT applied at concentration of 0.0, 25, and 50 mg / L on the number and weight of bean produced. Plants metrics were recorded after 120 days of exposure. Asterisks (*) indicate statistically significant differences ($p < 0.05$) by comparison to control plants.

These observations may have significant consequences on the use of bioenergy plants for the combined benefit of bioremediation and biodiesel production. Indeed, our results suggest that growing soybean plants on soil containing 50 mg / L TNT may results in more than 50% reduction of the bean biomass per plant (i.e., from 0.42 ± 0.16 to 0.20 ± 0.10 g bean/plant).

5.4.2 Soybean exposure to PCBs and OH-PCBs

The second part of this study focused on the exposure of soybean plants to polychlorinated biphenyls (PCBs). The first congener chosen was 2,4'-dichlorobiphenyl (2,4'-DCB or PCB 8) because of its widespread occurrence in Aroclor mixtures. Our results show that exposure of soybean plants to 2,4´-DCB at concentrations ranging from 0.0 to 25 mg / kg soil resulted in changes in the growth rate of the plant, as shown in Figure 5.13. However, after 15 days of exposure, the determination of plant metrics did not reveal statistically significant effects in plant biomass.

Figure 5.13. Effect of 2,4'-DCB on soybean plants. The picture shows that exposure to 12.5 and 25 mg / L caused a visible lag phase in soybean growth. From left to right, applied treatments are 0.0 (control), 6.25, 12.5, and 25 /kg-soil.

Another experiment was then conducted with higher concentration of 2,4'-DCB, ranging from 0.0 to 50 mg / L. The results showed again a very mild effect of the PCB on plants growth as only a significant increase of root biomass was observed for exposure to the lowest concentration (Figure 5.14 and Figure 5.15).

Figure 5.14. Soybean exposed to 2,4'-DCB at concentrations of 0.0, 10, 25, and 50 mg / kg soil after 17 days of growth.

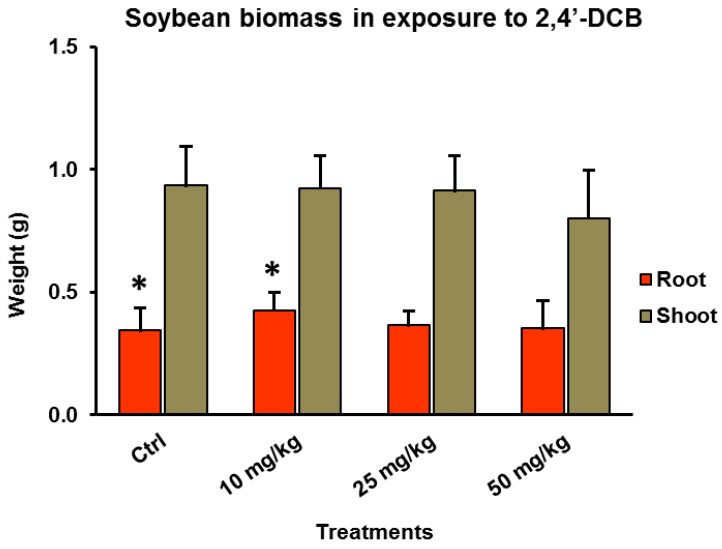

Figure 5.15. Effect of 2,4'-DCB on the root and shoot biomass in soybean plants exposed to concentrations of 0.0, 10, 25, and 50 mg / kg. The asterisks (*) shows the statistical significance of the changes in the treatments versus control (at 95% confidence level).

Hydroxylated PCBs (OH-PCBs) are PCB metabolites that are formed in the environment through both biotic and abiotic pathways. Because they carry a hydroxyl group attached to the biphenyl ring, OH-PCBs are more hydrophilic, more bioavailable, and often more toxic to various organisms than the parent PCBs. OH-PCBs are also the first PCB metabolites detected in the tissues of plants exposed to PCBs. Several experiments were then conducted to assess the toxicity of PCB OH-metabolite on soybean plants. The OH-PCBs used in our experiments are shown in Table 5.2.

Table 5.2. PCB compounds and Hydroxylated PCBs tested on soybean or *A. thaliana*.

No.	PCB number	PCB abbreviation	PCB full name
1	PCB 3	4-CB	4-chlorobiphenyl
2		4-OH-4'-CB	4-hydroxy-4'-chlorobiphenyl
3	PCB 8	2,4'-DCB	2,4'-dichlorobiphenyl
4		4-OH-2,4'-DCB	4-hydroxy-2,4'-dichlorobiphenyl
5	PCB 9	2,5-DCB	2,5-dichlorobiphenyl
6		4-OH-2',5'-DCB	4-hydroxy-2',5'-dichlorobiphenyl
7	PCB 18	2,2',5'-TCB	2,2',5'-trichlorobiphenyl
8		4-OH-2,2',5'-TCB	4-hydroxy-2,2',5'-trichlorobiphenyl

In a first experiment, soybean plants were exposed to increasing concentrations of 2,4'-DCB and 4-OH-2',4-DCB: 0.0, 10, and 25 mg / kg soil. Plant shoot/leaf biomass showed a significant decrease upon exposure to 25 mg / L in to both the parent PCB (2,4'-DCB) and the OH-metabolite (4-OH-2',4-DCB) (Figure 5.16 and Figure 5.17).

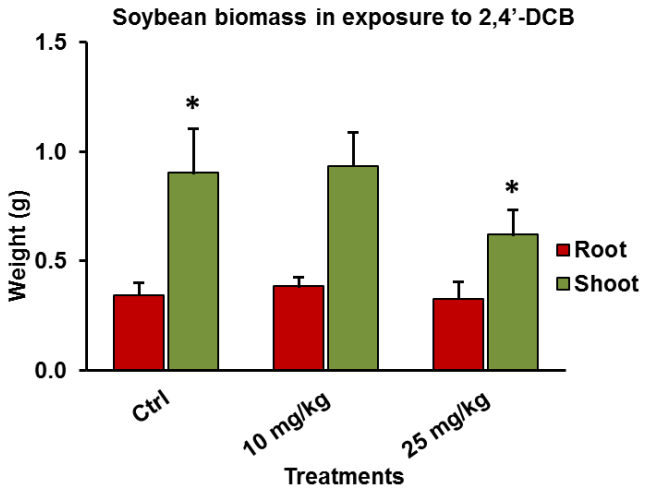

Figure 5.18. Weight of soybeans' roots and aerial parts after 11 days of exposure to 0.0, 10, and 25 mg / kg 2,4'-DCB. Asterisks (*) indicate statistically significant differences ($p < 0.05$) by comparison to control plants.

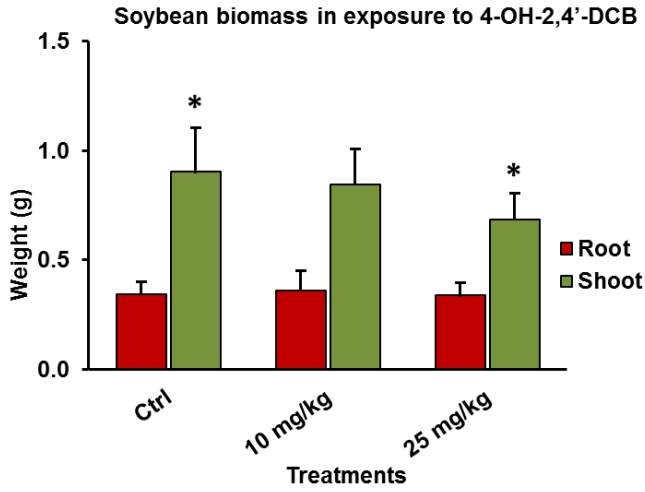

Figure 5.19. Weight of soybeans' roots and aerial parts after 11 days of exposure to 0.0, 10, and 25 mg / kg 4-OH-2,4'-DCB. Asterisks (*) indicate statistically significant differences ($p < 0.05$) by comparison to control plants.

In a further experiments, soybean plants were exposed to another PCB congener and its 4'-OH-metabolite, 2,5-DCB and 4'-OH-2,5-DCB. In this case, the absence of noticeable toxic effect lead us to expose the plants to concentrations up to 250 mg / kg

soil of PCB and 50 mg / kg soil of OH-PCB. Surprisingly, exposure to the highest level of both parent PCB (250 mg / kg) and its OH-metabolite (50 mg / kg soil) did not show any observable effect on plants growth (Figure 5.20). These results again tend to indicate that PCBs and OH-PCBs exert limited toxic effect on the growth of soybean plants.

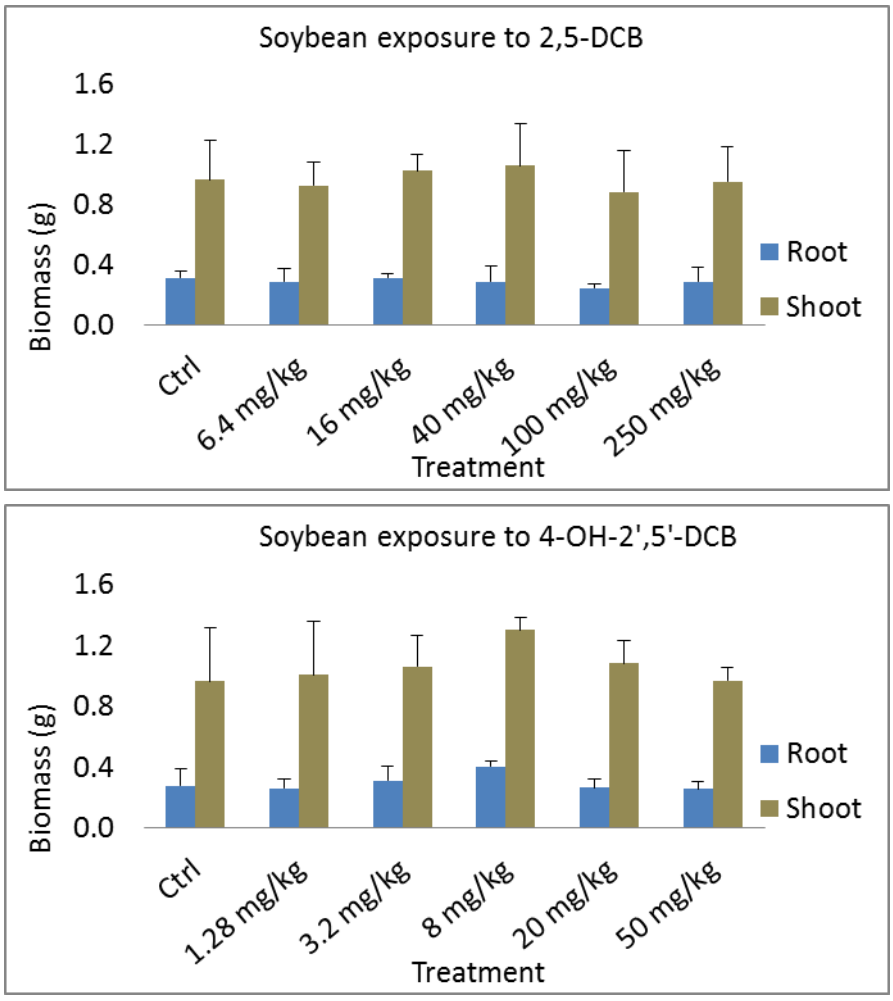

Figure 5.20. Biomass of soybean plants exposed to 2,5-DCB (6.4, 16, 40, 100, and 250 mg / kg soil) and 4-OH-DCB (0.0, 1.3, 3.2, 8, 20, and 50 mg / kg soil) after two weeks of growth. Data showed no statistical significance across the different treatments.

5.4.3 Analysis of PCBs inside plant tissues

The analysis of 2,4'-DCB inside plant tissues showed an accumulation of 1.5, 14.0, and 56.6 µg/g-plant (fresh weight) in roots of plants exposed to 10, 25, and 50 mg / kg soil, respectively. The analysis of 2,4'-DCB inside the plant shoots/leaves showed an

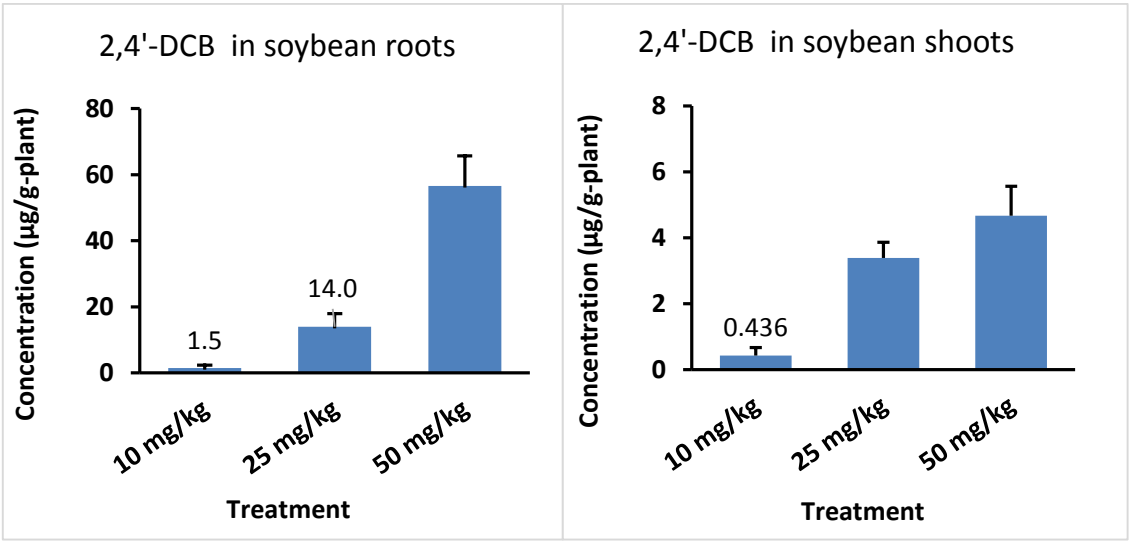

Figure 5.21. The amount of 2,4'-DCB in roots (right) and shoots (left) for different exposure concentrations.

accumulation of 0.44, 3.4, and 4.7 µg/g-plant (fresh weight) in plants exposed to 10, 25, and 50 mg / kg soil, respectively. Results show that the amount of 2,4'-DCB in roots was 12, 4, and 3.3 times higher than what was extracted from the shoots in 50, 25, and 10 mg / kg samples, suggesting that PCB undergoes limited, but significant translocation in soybean plants.

The average amount of 2,4'-DCB detected in plant tissues was used for mass balance calculations on soybean plants exposed to 10, 25, and 50 mg / kg. Mass balances were performed to estimate the phytoremediation ability of plants and to calculate the bioaccumulation factors (Table 5.3).

Table 5.3. 2,4'-DCB mass balances in soil and soybean plants. Total 2,4'-DCB amounts used for each treatment are shown. Corresponding percentages are shown in parentheses. Bioaccumulation factors are defined as the ratio of 2,4'-DCB concentration in plant tissues over its concentration in soil.

	Treatment		
	10 mg / kg	25 mg / kg	50 mg / kg
Initial calculated PCB in soil (µg)	5,400 (100)	13,500 (100)	27,000 (100)
Root uptake (µg)	0.015 ($2.85\ 10^{-4}$)	0.123 ($9.11\ 10^{-4}$)	0.557 ($2.06\ 10^{-3}$)
Shoot uptake (µg)	0.010 ($1.81\ 10^{-4}$)	0.075 ($5.56\ 10^{-4}$)	0.091 ($3.37\ 10^{-4}$)
Uptake by plant %	$5\ 10^{-4}$	$1.5\ 10^{-3}$	$2.4\ 10^{-3}$
Bioaccumulation factor in roots	$2.85\ 10^{-6}$	$9.11\ 10^{-6}$	$2.06\ 10^{-5}$
Bioaccumulation factor in aerial parts	$1.81\ 10^{-6}$	$5.56\ 10^{-6}$	$3.37\ 10^{-6}$

5.5 Discussion

Our results show that in the short term (2 - 3 weeks), exposure to TNT even at very high doses (up to 250 mg / kg soil) resulted in mild adverse effects on soybean plants. However, exposure to TNT (50 mg / kg soil) for a longer period of time (120 days) resulted in significant reduction of plant biomass and size. Also, exposure to 50 mg / kg soil for 120 days caused an approx. 50% decrease of the average bean biomass produced by individual plants, which may have a significant impact on biodiesel yield by plants grown on TNT-contaminated soil.

Analysis of TNT in exposed plant roots showed average concentrations of 30 - 40 ng/g tissue (exposure 50 mg / kg). Uptake of TNT by soybean was up to 12 times higher in roots than aerial parts (exposure to 50 mg / kg) showing significant uptake and translocation of TNT inside the plant. This observation suggests that soybean plants may be a promising candidate for phytoremediation of TNT-contaminated soil. The relatively low level of TNT observed in soybean tissues by comparison to the PCB levels (see below) may be explained by the fast metabolism of TNT in plant tissues. Indeed,

reduction of TNT in plant tissues results in the formation of hydroxylaminodinitrotulenes (OHADNTs), aminodinitrotulenes (ADNTs), and small amounts of diaminonitrotulenes (DANTs) [176].

Similarly, the almost complete disappearance of TNT from soil is likely to be explained by the microbial reduction of TNT, which was shown to be enhanced by the presence of vegetation on the soil. Indeed, enhancement of TNT biodegradation has been reported by Sung et al. (2004) in planted soil by comparison to non-planted soil

Our results are consistent with prior reports on the TNT uptake by plants [135, 136]. However, previous studies have shown that TNT exert phytotoxicity at rather low doses. Thompson et al. (1998) showed that exposure of poplar cuttings (*Populus deltoides* x *nigra* DN34) to TNT resulted in a dose-dependent reduction of both the transpiration rate and plant biomass at concentrations equal or above 5 mg / L. Peterson et al. (1998) reported that the growth rate of hydroponic switchgrass was significantly reduced by exposure to 15 mg / L in roots and 30 mg / L in shoots [178]. This discrepancy may be explained by the fact that the previously reported experiments were conducted with hydroponic plants, in which TNT is likely to be more bioavailable than TNT applied in soil. Indeed, in another study conducted with various plant species growing in soil, Gong et al. (1999) reported that two dicotyledons, Lepidium sativum (cress) and *Brassica rapa* (turnip) and two monocotyledons (*Acena sativa* (oat) and *Triticum aestivum* (wheat) showed higher sensitivities, with LOAELs ranging from 5-25 to 1,600 mg / kg soil [178].

Results from soybean exposure of 2,4'-DCBs showed variable toxicity levels. In one experiment, no observable effect was recorded at concentration up to 50 mg / kg soil,

while another experiment showed significant reduction of the plant biomass in soybean plants exposed to both 2,4'-DCB and 4'-OH-2,4'-DCB at concentration of 25 mg / L.

Analysis of 2,4'-DCB in plant tissues showed average concentrations of 9,000 to 17,000 ng/g of 2,4'-DCB (exposure 25 mg / kg). Uptake of PCBs by soybean was up to 12 times higher in the roots than in the aerial parts (exposure to 25 mg / kg). By comparison to the TNT content in plant tissue, the amount of PCB that has been up taken by soybean plants is 800 and 1500 times higher in roots and shoots, respectively, which again is explained by the higher stability of PCBs as compared with TNT.

In order to predict uptake of organic pollutants by plants, Briggs et al. (1982) and Burken and Schnoor (1998b) developed experimental relationships based on log K_{ow}. Based on their models, only 'moderately hydrophobic' compounds ($0.5 < \log K_{ow} < 4.5$) would be significantly taken up and translocated inside plant tissues [179, 120]. The plant uptake of TNT, with predicted $\log K_{ow} = -0.21$, is then expected to be much higher than the uptake of PCBs. Indeed, the plant uptake of PCBs – with log K_{ow} ranging from 4.5 (chlorobiphenyl) to 8.2 (decachlorobiphenyl) – is expected to be low, even for lower chlorinated congeners such as 2,4'-DCB. The relative higher accumulation of PCBs in plant tissues as compared with TNT that we observed is then likely explained by the transformation of TNT inside plant tissues.

CHAPTER 6 CONCLUSION

6.1 Effect of Silver Nanoparticles on *Arabidopsis thaliana*

Silver nanoparticles (AgNPs) are known to exert toxic effects on most living organisms including plants. Because plants are the basis of terrestrial food chain, their exposure to AgNPs may have significant consequences on human health and the environment. In the second chapter of this thesis, we presented the first genome-wide microarray experiment conducted to understand the transcriptional response of model plant, *A. thaliana,* exposed to AgNPs and soluble Ag^{+}. Our results have shown that exposure of plants to low concentrations of AgNPs (1.0 and 2.5 mg / L) resulted in significant increase of the biomass, although exposure to concentrations of 5.0 mg / L and higher resulted in reduction of the biomass. Similar results have been also reported by Mazumdar (2014).

Using genome-wide expression microarrays, we have shown that exposure to AgNPs and Ag^{+} resulted in differential expression of many genes involved in the plant response to stress and to biotic and abiotic stimuli. Simultaneous induction or repression of a significant proportion of genes by exposure to both AgNPs and Ag^{+} strongly suggest that the toxicity of AgNP was due partly to the release of silver from nanoparticles and partly to specific effects due to the nature of nanoparticles. Indeed, nanoparticles are known to be able to act mechanically by direct association with cellular structures and clogging pores in walls and membranes. Even though this is still a controversial question, our study has made an important contribution suggesting that nanoparticles act on cellular structure although mechanisms are distinct from the simple release of soluble materials.

6.2 Effect of Antiviral Drugs on *Arabidopsis thaliana*

As ubiquitous xenobiotic pollutants in the environment, pharmaceuticals have recently raised concerns about their potential effect on the environment and human health. Even though these chemicals are typically present at very low levels in the environment, the almost inexistence of chronic ecotoxicology data raises questions about long term effect of pharmaceuticals on living organisms. Certainly, pharmaceuticals have typically been designed to act on specific biological targets and to resist fast biodegradation upon introduction in the body. These characteristics makes them persistent and active in the environment for longer periods of time. Along with many other organic and inorganic compounds, pharmaceuticals are susceptible to be taken up and to some extent, get metabolized inside plant tissues. This observation, has a major practical consequence for phytotechnology because agricultural crops may be contaminated by pharmaceuticals through irrigation water, agricultural runoff, and land application of municipal sewage sludge on agricultural fields.

In the second phase of this research, we investigated the effects of the antiviral drugs, oseltamivir phosphate (OSP) and zanamivir (ZAN), on the model plant, *A. thaliana*, at the physiological and transcriptomic levels. OSP and ZAN have been widely detected in treated wastewater effluents during the influenza season, and we believe that they have the potential to contaminate agricultural plants by irrigation and land application of sludge. Our results showed a mild effect from OSP exposure on *A. thaliana*, although no significant effect was observed upon exposure to ZAN. Whole-genome expression analysis revealed significant transcriptional changes, including up- and down-regulation of many genes involved in the plant response to oxidative stresses

and response to stimuli. In order to further interpret our gene expression results, we compared genes up- and down-regulated in our study with data from an *Arabidopsis* gene expression database (Genevestigator), which revealed that many genes whose expression levels were affected by OSP and/or ZAN were similarly affected by exposure to a range of biotic and abiotic stresses, toxic chemicals, and hormonal stimuli, suggesting that OSP and ZAN have negative chronic effects on plants health.

6.3 Effect of TNT and PCBs on Soybean

Although a significant number of studies have shown the potential of aquatic plants for the removal of pharmaceuticals from wastewater, today there are questions that need to be addressed, including the potential accumulation of parent compounds and their toxic metabolites inside plant tissues, which eventually can release into the environment or transfer to the food chain. Further research, including transcriptomic, proteomic, and metabolomic approaches, is then desirable in order to assess the actual detoxification process that occurs inside plant tissues.

The last phase of this thesis focuses on the effects of two important toxic and persistent pollutants, 2,4,6-trinitrotoluene (TNT) and polychlorinated biphenyls (PCBs), on the growth of soybean plants, in order to assess the potential of using energy crops for the combined benefit of land remediation and biodiesel production. Our results have shown that short-term exposure of soybean plants to TNT and PCB (2,4'-dichlorobiphenyl - 2,4'-DCB) exerted no or mild observable effects on plant growth even when applied at very high concentrations (e.g., 100 mg / kg soil). The low toxicity of TNT that we observed is in disagreement with several prior publications showing phytotoxic effects at doses as low as 5 mg / L, which may be explained by the fact that

our experiments were conducted in soil, while most prior studies utilized hydroponic systems (where the bioavailability of TNT was likely to be higher). Exposure to TNT also resulted in a significant decrease of the average biomass of beans per plant after 120 days, which may have important consequences on the yield of biodiesel obtained from plants grown on contaminated lands. We also observed that exposure of soybean plants to both a parent PCB (2,4'-DCB) and a major metabolite (4'-OH-2,4'-DCB) resulted in similar phytotoxic effect. Analysis of TNT and PCBs (2,4'-DCB) in plant tissues revealed a higher accumulation of PCB as compared with TNT, which is unexpected based on the predicted uptake of the two compounds based on their respective log K_{ow}. This discrepancy was explained by a faster metabolism of TNT in plant tissues, which also accounted for the rapid disappearance of TNT from the soil.

This research has been supported by a grant from USDA: "Growing Energy Crops on Contaminated Land for the Combined Benefits of Phytoremediation and Sustainable Energy Production". This project is still active and will include further analyses in order to the determination of the molecular bases of the effects – both positive and negative – of TNT, PCBs, and OH-PCBs on soybean plants and beans.

6.4 Review of Gene Expression Studies Conducted with *A. thaliana* Exposed to AgNPs, ZAN and OSP, TNT, and PCBs

The paragraph below summarizes and compares the major gene expression patterns observed in *A. thaliana* in response to exposure to the contaminants used in this study, including AgNPs, the antiviral drugs, ZAN and OSP, and the conventional contaminants, TNT and PCBs. Results being discussed here include gene expression data

obtained during the present investigation (i.e., AgNPs, ZAN, and OSP), as well as data obtained from prior studied found in the literature (i.e., TNT and PCBs).

Based on our study and prior published reports, exposure of *A. thaliana* to AgNPs results in the increase of plant growth at low concentrations and increase of plant growth at higher levels. Our gene expression results (conducted on plants exposed to toxic levels of AgNPs and Ag^{+}) revealed up-regulation of genes involved in plant response to abiotic stimuli and oxidative stresses (e.g., vacuolar cation/proton exchangers, miraculin-like proteins, superoxide dismutases, cytochrome P-450 monooxygenases, and peroxidases). Stimulation of these genes is characteristic of metal-induced plant stress known to involve metal toxic effects and oxidative damage. On the other hand, we also observed down-regulation of genes involved in plant growth and development (e.g., ARGOS genes), which is consistent with the reduced biomass of exposed plants and general response to toxic stress. Observation of partial overlapping between genes differentially-expressed by exposure to AgNPs and Ag^{+} suggests the occurrence of both Ag- and nanoparticle-specific effects.

Unlike toxic metals that cannot be biodegraded by living organisms, organic pollutants, such as pesticides, nitroaromatic explosives, and chloroaromatic compounds, have been shown to undergo plant-mediated biodegradation inside plant tissues. Based on the observation that plants can metabolize pesticides, Sandermann (1994) introduced the green liver model, which suggests a three-step metabolic sequence similar to the one that occurs in the liver of mammals involving initial activation by oxidation or reduction (phase I), transferase-catalyzed conjugation of the activated compound (phase II), and sequestration of the conjugate in plant tissues (phase III) [112].

A few studies have been published on the transcriptional response of *A. thaliana* plants exposed to TNT [150, 141, 180]. Although conducted under different conditions and with different gene expression platforms, these investigations reported up-regulation of a series of genes involved in metabolism of TNT in plant tissues, which is consistent with the pathways of transformation of TNT by higher organisms. Several genes involved in the initial activation of TNT (phase I of the green liver model) were shown to be up-regulated, including nitrate reductase, cytochrome P-450 monooxygenases, and oxidoreductases. Several up-regulated genes were also found to be potentially involved in further conjugation of the TNT activated molecule (phase II), including UDP-glucosyltransferases, galacturonosyltransferases, and glutathione S-transferase. Finally, genes potentially involved in sequestration of the conjugate (phase III of the green liver model) have also been reported to be up-regulated, including sucrose-proton symporters, β-xylosidases, ABC transporter family proteins, and mannitol transporters.

Similarly, transformation of PCBs inside plant tissue is known to occur following a sequence that is consistent with the green liver model involving initial hydroxylation, conjugation with sulfate, and sequestration. Several genes potentially involved in this process have been shown to be up-regulated by exposure of *A. thaliana* plants to the model PCB (2,2',4,4'-tetrachlorobiphenyl) (Jin et al. 2011) [182]: genes involved in phase I of the green liver model include 12 oxidoreductases (including cytochrome P-450 monooxygenases) potentially involved in PCB hydroxylation. Genes involved in phase II of the green liver model include 12 transferases potentially catalyzing conjugation of hydroxylated PCBs to a molecule of plant origin (including UDP-glucuronosyltransferases). And finally genes potentially involved in phase III include 16

proteins involved in transport mechanisms (including proteins known to be involved in homeostasis and detoxification processes). In addition, overexpression of genes involved in lignin metabolism (reduction of cinnamaldehyde to cinnamyl alcohol) suggests that exposure to PCBs induces lignin synthesis, which known to be a mechanism of plant response to stress.

Exposure to antiviral drugs, ZAN and OSP, has shown a mild toxicity in exposed plants, which was expected based on toxicity data reported in other organisms. Transcriptional studies revealed a gene expression, which is consistent with a mild toxic effect of the compounds and the absence of known biological activities of neuraminidase inhibitors for plants. Accordingly, *A. thaliana* exposure to ZAN and OSP was shown to induce genes involved in plant defense and response to stress. As in prior transcriptional studies on *A. thaliana* exposure to organic compounds, we observed the induction of several genes potentially involved in biodegradation pathways of the compounds. Although there is currently no information about the biodegradability of ZAN and OSP by plants, knowledge about phytotransformation of other xenobiotic compounds suggest that antiviral drugs would be transformed according to the green liver model. Potential phase I genes that were up-regulated in our investigations include various oxidoreductases (e.g., fatty acyl-CoA reductase, glucose-methanol-choline oxidoreductase, 2-alkenal reductase), and cytochrome p-450 monooxygenases. Potential phase II genes include transferases (e.g., S-adenosyl-L-methionine-dependent methyltransferase). Several genes potentially involved in phase III of the green liver model include genes involve in carbohydrate metabolism and transport (e.g., nodulin MtN21/EamA-like transporter, xanthine dehydrogenase.

In summary, our microarray studies on *A. thaliana* exposed to AgNPs and Ag^+ are consistent with response to toxic metal and oxidative stress. On the other hand, the transcriptional analysis of plants exposed to ZAN and OSP also suggests plant response to stress. In addition, as prior microarray experiments conducted to investigate the response of *A. thaliana* exposed to TNT and PCBs, gene expression changes in response to ZAN and OSP are consistent with potential biotransformation of the compounds inside plant tissues and involved several genes potentially implicated in the three phases of the green liver model.

6.5 Further Perspectives

Observable toxic effects in plants exposed to environmental contaminants mostly include basic morphological changes and metric parameters that do not provide information on the nature of the mechanisms of cellular damages. Gene expression studies, such as the ones presented in this thesis, are expected to allow further understanding of the cellular mechanisms and, therefore, the molecular bases of toxicity of contaminants. It is noteworthy to recognize that whole-genome gene expression analyses frequently depict complex chain-reactions and suites of coregulated genes that do not prove the existence of causative interactions between toxic exposure and transcriptional responses. As an example, toxic environmental contaminants frequently result in the production ROS that induce genes involved in the response to oxidative stress. However, ROS are also produced by various cellular pathways and they are known to be involved in cellular stress signaling. Therefore the stimulation of genes involved in the response to oxidative stress may be triggered either directly by exposure to toxic contaminants or by the generation of ROS as secondary messengers of general cellular

stress [183, 184]. In order to provide meaningful results, gene expression analyses must be conducted in parallel with other morphological and physiological analyses. Whole-genome transcriptional analyses have brought and will continue to bring valuable information regarding the mechanisms of toxicity and the biodegradation pathways of environmental contaminants in plants. This situation will likely make more critical the need for more accessible microarray databases in order to compare in a meaningful way the growing number of data published. More adequate strategies in system biology will need to be designed for the development of molecular maps and gene expression networks [185].

6.6 Practical Considerations for Phytoremediation

Mass balance constitute important tools to predict the efficiency of phytoremediation. Detecting the amounts of contaminants and their metabolites in the plant tissues and soil, as well as evaluating toxicity data, is therefore of paramount importance to assess phytoremediation workability. Besides laboratory testing, running pilot studies in the field is recommended to test the selected plant species and estimate contaminant removal over longer periods of time. Recording environmental conditions (i.e., precipitation, soil composition, temperature, etc.) is also important as environmental factors can affect the phytoremediation process in ways that are not accounted for in small-scale laboratory experiments.

The toxicity of contaminant metabolites has also to be considered. For instance, the TNT reduction metabolites, ADNTs and DANTs, are much less toxic than the parent compound, making TNT biotransformation an effective detoxificationprocess. On the

contrary, OH-PCB metabolites generated in pant tissues are often more toxic and more bioavailable in the environment as compared to the parent PCBs [186].

Utilization of bioenergy plants for phytoremediation is an emerging strategy that has cost-benefit advantages, but can also raise practical obstacles. Energy crops are typically annual plants that need to be harvested every year. After collecting the beans, the rest of the plant, which is contaminated, has to be disposed in a way that will prevent the contaminants from returning to the soil. Also, the beans that are used for triglyceride extraction are likely to carry some of the contaminants, which can be present in the produced biodiesel. TNT and its metabolites may generate a few NO_x (in addition to CO_2) during combustion, which would be likely in small proportion in comparison to the amount of gases generated by the biofuel combustion itself. On the other side, PCB combustion may generate chlorinated dioxins, which are much more toxic than the PCBs themselves. This new aspect of phytoremediation needs to be evaluated according to the amount of contaminant and their metabolites that could be carried over into the generated biofuel.

6.7 Future Research

Using different contaminants and different plant species in this phytoremediation investigation allowed us to observe similarities and differences in the response of plants exposed to contaminants at both physiological and genetic levels. The first part of this thesis (Chapter 3 and 4) focused on the effects of emerging contaminants on the model plant, *A. thaliana*. This research was more fundamental and used hydroponic plants under sterile conditions. Results from this research are expected to open the road to future studies for understanding deeper the biodegradation pathways and molecular responses of

plants to new contaminants for which limited information is currently available. This approach is expected to lead to more efficient remediation and detoxification technologies and to more accurate methods for the assessment of the environmental risk associated with the contaminants.

The second part of this research focused on the removal of TNT and PCBs by soybean plants (Chapter 5). This study was part of a USDA-funded project. This project was more applied than the previous experiments and focused on the practical issues associated with growing plants for phytoremediation and biofuel production. Experiments were conducted under more applied conditions using real soil and non-sterile conditions. The selected plant species, soybean, was also an actual agricultural crop currently used for bioenergy production in the US.

Future experimental work suggested for the continuation and completion of this study includes the following:

a) Transcriptomic analysis of soybean exposed to TNT and PCBs will provide additional information on plant response at the molecular level.

b) Long-term exposure of soybean plants to PCB congeners and their OH-metabolites will allow observing the chronic toxicity and examining the quality and quantity of the beans produced from (OH-)PCB-exposed plants.

c) Analyzing the lipid content and lipid composition in the produced soy beans will allow estimating the effects of TNT and PCB on biofuel yield. This investigation could be coupled with transcriptional analyses regarding the effects of environmental stressors on triglyceride biosynthetic pathways in energy plants.

d) Completed mass balances of PCBs and TNT (and their metabolites) in soil and plant tissues will allow estimating the phytoremediation capability of soybean plants. [186] [154]

REFERENCES

[1] N. A. Anjum, S. S. Gill, A. C. Duarte, E. Pereira and I. Ahmad, "Silver nanoparticles in soil–plant systems," *Journal of Nanoparticle Research,* vol. 15, p. 1896, 2013.

[2] E. Navarro, A. Baun, R. Behra, N. Hartmann, J. Filser, A. Quigg, P. Santschi and L. Sigg, "Environmental behavior and ecotoxicity of engineered nanoparticles to algae, plants, and fungi," *ecotoxicology,* vol. 13, pp. 372-386, 2008.

[3] S. Klaine, P. Alvarez, G. Batley, T. Fernandes, R. Handy, D. Lyon, S. Mahendra, M. McLaughlin and J. Lead, "Nanomaterials in the environment: Behavior, fate, bioavailability, and effects," *Environmental Toxicology and Chemistry,* vol. 27, no. 9, pp. 1825-1851, 2008.

[4] R. Handy, G. Cornelis, T. Fernandes, O. Tsyusko, A. Decho, T. Sabo-Attwood, C. Metcalfe, J. Steevens, S. Klaine, A. Koelmans and N. Horne, "Ecotoxicity test methods for engineered nanomaterials: Practical experiences and recommendations from the bench," *Environmental Toxicology and Chemistry,* vol. 31, no. 1, pp. 15-31, 2012.

[5] A. Seaton, L. Tran, R. Aitken and K. Donaldson, "Nanoparticles, human health hazard and regulation," *Journal of the Royal Society Interface,* vol. 7, pp. S119-S129, 2010.

[6] M. Auffan, J. Rose, J. Bottero, G. Lowry, J. Jolivet and M. Wiesner, "Towards a definition of inorganic nanoparticles from an environmental, health and safety perspective," *Nature Nanotechnology,* vol. 4, pp. 634-641, 2009.

[7] EPA, "Pollution Prevention and Toxics," 2014. [Online]. Available: http://www.epa.gov/oppt/nano/. [Accessed Januery 2014].

[8] A. Poma and M. Di Giorgio, "Toxicogenomics to improve comprehension of the mechanisms underlying responses of in vitro and in vivo systems to nanomaterials: A review," *Current Genomics,* vol. 9, pp. 571-585, 2008.

[9] W. Stark, "Nanoparticles in biological systems," *Angewandte Chemie-International Edition,* vol. 50, pp. 1242-1258, 2011.

[10] O. Bondarenko, K. Juganson, A. Ivask, K. Kasemets, M. Mortimer and A. Kahru, "Toxicity of Ag, CuO and ZnO nanoparticles to selected environmentally relevant test organisms and mammalian cells in vitro: A critical review," *Archives of Toxicology,* vol. 87, pp. 1181-1200, 2013.

[11] K. Dietz and S. Herth, "Plant nanotoxicology," *Trends in Plant Science,* vol. 16, pp. 582-589, 2011.

[12] C. Rico, S. Majumdar, M. Duarte-Gardea, J. Peralta-Videa and J. Gardea-Torresdey, "Interaction of nanoparticles with edible plants and their possible implications in the food chain," *Journal of Agricultural and Food Chemistry,* vol. 59, pp. 3485-3498, 2011.

[13] P. Miralles, T. Church and A. Harris, "Toxicity, uptake, and translocation of engineered nanomaterials in vascular plants," *Environmental Science & Technology* , vol. 46, pp. 9224-9239, 2012.

[14] R. Kaveh, Y.-S. Li, S. Ranjbar, R. Tehrani, B. Van Aken and C. L. Brueck, "Changes in Arabidopsis thaliana Gene Expression in Response to Silver Nanoparticles and Silver Ions," *Environmental Science and Technology,* pp. 10637-10644, 2013.

[15] J. Wang, Y. Koo, A. Alexander, Y. Yang, S. Westerhof, Q. Zhang, J. Schnoor, V. Colvin, J. Braam and P. Alvarez, "Phytostimulation of poplars and Arabidopsis exposed to silver nanoparticles and Ag+ at sublethal concentrations," *Environmental Science & Technology,* vol. 47, no. 10, p. 5442–5449, 2013.

[16] W. Jiang, B. Y. Kim, J. T. Rutka and W. C. Chan, "Nanoparticle-mediated cellular response is size-dependent," *Nature Nanotechnology,* vol. 3, pp. 145-150, 2008.

[17] Y. S. El-Temsah and E. J. Joner, "Impact of Fe and Ag nanoparticles on seed germination and differences in bioavailability during exposure in aqueous suspension and soil," *Environmental Toxicology,* vol. 27, pp. 42-49, 2012.

[18] M. Kumari, A. Mukherjee and N. Chandrasekaran, "Genotoxicity of silver nanoparticles in Allium cepa," *Scince of the Total Environment,* vol. 407, pp. 5243-5246, 2009.

[19] T. M. Benn and P. Westerhoff, "Nanoparticle Silver Released into Water from Commercially Available Sock Fabrics," *Environtal Science & Technology,* vol. 42, p. 4133–4139, 2008.

[20] K. Schlich, T. Klawonn, K. Terytze and K. Hund-Rinke, "Hazard assessment of a silver nanoparticle in soil applied via sewage sludge," *Environmental Sciences Europe,* vol. 25, no. 17, pp. 1-14, 2013.

[21] D. Stampoulis, S. Sinha and J. White, "Assay-dependent phytotoxicity of nanoparticles to plants," *Environmental Science & Technology,* vol. 43, pp. 9473-9479, 2009.

[22] X. Ma, J. Geiser-Lee, Y. Deng and A. Kolmakov, "Interactions between engineered nanoparticles (ENPs) and plants: Phytotoxicity, uptake and accumulation," *Science of The Total Environment,* vol. 408, pp. 3053-3061, 2010.

[23] J. Fabrega, S. Luoma, C. Tyler, T. Galloway and J. Lead, "Silver nanoparticles: Behaviour and effects in the aquatic environment," *Environment International,* vol. 37, no. 2, pp. 517-531, 2011.

[24] L. Xu, T. Takemura, M. Xu and N. Hanagata, "Toxicity of silver nanoparticles as assessed by global gene expression analysis," *Materials Express,* vol. 1, no. 1, pp. 74-79, 2011.

[25] S. Blaser, M. Scheringer, M. MacLeod and K. Hungerbühler, "Estimation of cumulative aquatic exposure and risk due to silver: Contribution of nano-functionalized plastics and textiles," *Science of The Total Environment,* vol. 390, p. 396–409, 2008.

[26] R. Kaegi, A. Voegelin, B. Sinnet, S. Zuleeg, H. Hagendorfer, M. Burkhardt and H. Siegrist, "Behavior of metallic silver nanoparticles in a pilot wastewater treatment plant," *Environmental Science & Technology ,* vol. 45, pp. 3902-3908, 2011.

[27] B. Schwab, E. Hayes and J. Fiori, "Human pharmaceuticals in US surface waters: A human health risk assessment," *Regulatory Toxicology and Pharmacology,* vol. 42, pp. 3296-312, 2005.

[28] D. Kolpin, E. Furlong and M. Meyer, "Pharmaceuticals, hormones, and other organic wastewater contaminants in US streams, 1999-2000: A national reconnaissance," *Environmental science & technology,* vol. 36, pp. 61202-1211, 2002.

[29] C. Daughton and T. Ternes, "Pharmaceuticals and personal care products in the environment: Agents of subtle change?," *Environmental health perspectives,* vol. 107, pp. 907-938, 1999.

[30] G. Loraine and M. Pettigrove, "Seasonal Variations in Concentrations of Pharmaceuticals and Personal Care Products in Drinking Water and Reclaimed Wastewater in Southern California," *Environmental Science & Technology,* vol. 40, no. 3, pp. 687-695, 2006.

[31] P. Gao, Y. Ding, H. Li and L. Xagoraraki, "Occurrence of pharmaceuticals in a municipal wastewater treatment plant: Mass balance and removal processes," *Chemosphere,* vol. 88, no. 1, pp. 17-24, 2012.

[32] M. Gros, M. Petrovic, A. Ginebreda and D. Barceló, "Removal of pharmaceuticals during wastewater treatment and environmental risk assessment using hazard indexes," *Environment International,* vol. 36, pp. 15-26, 2010.

[33] K. Fent, A. Weston and D. Caminada, "Ecotoxicology of human pharmaceuticals," *Aquatic Toxicology,* vol. 76, pp. 2122-159, 2006.

[34] M. Celiz, T. Jerry and S. Daina, "Pharmaceutical metabolites in the environment: analytical challenges and ecological risks," *Environmental Toxicology and Chemistry*, vol. 28, p. 122473–2484, 2009.

[35] J. Burch, M. Corbett, C. Stock, K. Nicholson, A. J. Elliot, S. D. y, M. Westwood, S. Palmer and L. Stewart, "Prescription of anti-influenza drugs for healthy adults: a systematic review and meta-analysis," *Lancet Infectious Diseases*, vol. 9, p. 537–45, 2009.

[36] NCBI, "PubChem Compound," 2013. [Online]. Available: http://pubchem.ncbi.nlm.nih.gov/summary/summary.cgi?cid=60855. [Accessed 15 November 2013].

[37] RxList, "The Internet Drug Index," 2013. [Online]. Available: http://www.rxlist.com/relenza-drug.htm. [Accessed 15 November 2013].

[38] B. Freund, S. Gravenstein, M. Elliott and I. Miller, "Zanamivir A review of clinical safety," *Drug Safety*, vol. 21, no. 4, pp. 267-281, 1999.

[39] "Medicines Complete," 2013. [Online]. Available: http://www.medicinescomplete.com/mc/ahfs/current/a399040.htm. [Accessed Nov 2013].

[40] AHFS, "AHFS Drug Information," 2014. [Online]. Available: http://www.ahfsdruginformation.com/. [Accessed Feb 2014].

[41] T. Azuma, N. Nakada, N. Yamashita and H. Tanaka, "Mass balance of anti-influenza drugs discharged into the Yodo River system, Japan, under an influenza outbreak," *Chemosphere*, vol. 93, p. 1672–1677, 2013.

[42] H. Mestankovaa, K. Schirmer, B. Escher, U. Gunten and S. Canonica, "Removal of the antiviral agent oseltamivir and its biological activity by oxidative processes," *Environmental Pollution*, vol. 161, pp. 30-35, 2012.

[43] H. Soderstrom, J. D. Jarhult, B. Olsen, R. H. Lindberg, F. Tanaka and Jerker, "Detection of the Antiviral Drug Oseltamivir in Aquatic Environments," *Plus One*, vol. 4, no. 6, p. e6064, 2009.

[44] A. C. Singer, M. A. Nunn, E. A. Gould and A. C. Johnson, "Potential Risks Associated with the Proposed Widespread Use of Tamiflu," *Environmental Health Perspectives*, vol. 115, no. 1, p. 102–106, 2007.

[45] J. Fick, R. H. Lindberg, M. Tysklind, P. D. Haemig, J. Waldenström, A. Wallensten and B. Olsen, "Antiviral Oseltamivir Is not Removed or Degraded in Normal Sewage Water Treatment: Implications for Development of Resistance by Influenza A Virus," *PLoS ONE*, vol. 2, no. 10, p. e986, 2007.

[46] T. H. Hutchinson, A. Beesley, P. E. Frickers, J. W. Readman, J. P. Shaw and J. O. Straub, "Extending the environmental risk assessment for oseltamivir (Tamiflu®) under pandemic use conditions to the coastal marine compartment," *Environment International,* vol. 35, p. 931–936, 2009.

[47] J. O. Straub, "An environmental risk assessment for oseltamivir (Tamiflus) for sewageworks and surface waters under seasonal-influenza- and pandemic-use conditions," *Ecotoxicology and Environmental Safety,* vol. 72, no. 6, p. 1625–1634, 2009.

[48] B. I. Escher, N. Bramaz, J. Lienert, J. Neuwoehner and J. O. Straub, "Mixture toxicity of the antiviral drug Tamiflu® (oseltamivir ethylester) and its active metabolite oseltamivir acid," *Aquatic Toxicology,* vol. 96, pp. 194-202, 2010.

[49] A. Y. C. Tong, R. Braund, E. W. Tan, L. A. Tremblay, T. Stringer, K. Trought and B. M. Peake, "UV-induced photodegradation of oseltamivir (Tamiflu) in water," *Environmental Chemistry* , vol. 8, pp. 182-189, 2011.

[50] G. C. Ghosh, N. Nakada, N. Yamashita and H. Tanaka, "Oseltamivir Carboxylate, the Active Metabolite of Oseltamivir Phosphate (Tamiflu), Detected in Sewage Discharge and River Water in Japan," *Environmental Health Perspectives,* vol. 118, no. 1, p. 103–107, 2010.

[51] C. Accinelli, M. L. Saccà, J. Fick, M. Mencarelli, R. Lindberg and B. Olsen, "Dissipation and removal of oseltamivir (Tamiflu) in different aquatic environments," *Chemosphere,* vol. 79, p. 891–897, 2010.

[52] A. B. Caracciolo, P. Grenni and M. L. Sacca, "Effect of the Antiviral Drug Oseltamivir (Tamiflu) on the Bacterial Community Structure of a Surface Water Ecosystem Analyzed Using Fluorescence In Situ Hybridization," *Bulletin of Environmental Contamination and Toxicology,* vol. 85, pp. 443-446, 2010.

[53] P. Richter-Torres, A. Dorsey and C. S. Hodes, "Toxicological profile for 2,4,6-trinitrotoluene," Atlanta, GA, 1995.

[54] G. Adamin, M. Ghoghoberidze, D. Graves, G. Khatisashvili, G. Kvesitadze, E. Lomidze, D. Ugrekhelidze and G. Zaalishvili, "Absorption, distribution, and transformation of TNT in higher plants," *Ecotoxicology and Environmental Safety,* vol. 46, pp. 136-145, 2006.

[55] B. Clark and R. Boopathy, "Evaluation of bioremediation methods for the treatment of soil contaminated with explosives in Louisiana Army Ammunition plant, Minden, Louisiana," *Journal of Hazardous Materials,* vol. 143, pp. 643-648, 2007.

[56] M. Vila, S. Lorber-Pascal and F. Laurent, "Phytotoxicity to and uptake of TNT by rice," *Environmental Geochemistry and Health,* vol. 30, pp. 199-203, 2008.

[57] B. Hooker and R. Skeen, "Transgenic phytoremediation blasts onto the scene," *Nature Biotechnology,* vol. 17, p. 428, 1999.

[58] N. K. Hannink, S. J. Rosser and N. C. Bruce, "Phytoremediation of Explosives," *Critical Reviews in Plant Sciences,* vol. 21, no. 5, p. 511–538, 2002.

[59] T. Jenkins, D. Leggett, C. Grant and C. Bauer, "Reversed-phase high performance chromatographic determination of nitroorganics in munitions wastewater," *Analytical Chemistry,* vol. 58, p. 70–175, 1986.

[60] Z. Snellinx, A. Nepovim, S. Taghavi, J. Vangronsveld, T. Vanek and D. v. d. Lelie, "Biological remediation of explosives and related nitroaromatic compounds," *Environmental Science and Pollution Research,* vol. 9, no. 1, pp. 48-61, 2002.

[61] T. A. Lewis, D. A. Newcombeb and R. L. Crawford, "Bioremediation of soils contaminated with explosives," *Journal of Environmental Management,* vol. 70, no. 4, p. 291–307, 2004.

[62] K. Panz and K. Miksch, "Phytoremediation of explosives (TNT, RDX, HMX) by wild-type and transgenic plants," *Journal of Environmental Management,* vol. 113, pp. 85-92, 2012.

[63] J. Rodgers and N. Bunce, "Treatment methods for the remediation of nitroaromatic explosives," *Water Research,* vol. 35, no. 9, pp. 2101-2111, 2001.

[64] B. Van Aken and S. Agathos, "Biodegradation of nitro-substituted explosives by white-rot fungi: a mechanistic approach," *Advances in Applied Microbiology,* vol. 48, pp. 1-77, 2001.

[65] N. Fahrenfeld, J. Zoeckler, M. A. Widdowson and A. Pruden, "Effect of biostimulants on 2,4,6-trinitrotoluene (TNT) degradation and bacterial community composition in contaminated aquifer sediment enrichments," *Biodegradation,* vol. 24, p. 179–190, 2013.

[66] P. Thompson, L. Ramer and J. Schnoor, "Uptake and transformation of TNT by hybrid poplar trees," *Environment Science & Technology* , vol. 32, pp. 975-980, 1998.

[67] EPA, "Polychlorinated Biphenyls," 2013. [Online]. Available: http://www.epa.gov/epawaste/hazard/tsd/pcbs/index.htm. [Accessed November 2013].

[68] W. Y. Shiu and D. Mackay, "A Critical Review of Aqueous Solubilities, Vapor Pressures, Henry's Law Constants, and Octanol–Water Partition Coefficients of the Polychlorinated Biphenyls," *Journal of Physical and Chemical Reference Data,* vol. 15, no. 2, p. 911, 1986.

[69] K. Breivik, A. Sweetman, J. M. Pacyna and K. C. Jonesb, "Towards a global historical emission inventory for selected PCB congeners — a mass balance approach 2. Emissions," *Science of the Total Environment,* vol. 290, no. 1-3, pp. 199-224, 2002.

[70] D. Pieper and M. Seeger, "Bacterial metabolism of polychlorinated biphenyls," *Journal of Molecular Microbiology and Biotechnology,* vol. 15, p. 121–138, 2008.

[71] O. Faroon and J. Olson, Toxicological profile for polychlorinated biphenyls (PCBs), US Department of Health and Human Services, Public Health Service, Agency for Toxic Substances and Disease Registry, 2000.

[72] B. Mayes, E. McConnell, B. Neal, M. Brunner, S. Hamilton, T. Sullivan, A. Peters, M. Ryan, J. Toft, A. Singer, J. Brown, R. Menton and J. Moore, "Comparative carcinogenicity in Sprague-Dawley rats of the polychlorinated biphenyl mixtures Aroclors 1016, 1242, 1254, and 1260," *Toxicological Sciences,* vol. 41, pp. 62-76, 1998.

[73] B. Ulbrich and R. Stahlmann, "Developmental toxicity of polychlorinated biphenyls (PCBs): a systematic review of experimental data," *Archives of Toxicology,* vol. 78, p. 252–268, 2004.

[74] K. W. Hung, M. F. Suen, Y. Chen, H. Cai, Z. Mo and K. K. Yung, "Detection of water toxicity using cytochrome P450 transgenic zebrafish as live biosensor: For polychlorinated biphenyls toxicity," *Biosensors and Bioelectronics,* vol. 31, no. 1, p. 548–553, 2012.

[75] J. Borja, D. Taleon, J. Auresenia and S. Gallardo, "Polychlorinated biphenyls and their biodegradation," *Process Biochemistry,* vol. 40, p. 1999–2013, 2005.

[76] D. Pieper, "Aerobic degradation of polychlorinated biphenyls," *Applied Microbiology and Biotechnology,* vol. 67, p. 170–191, 2005.

[77] H. I. Gomes, C. Dias-Ferreira and A. B. Ribeiro, "Overview of in situ and ex situ remediation technologies for PCB-contaminated soils and sediments and obstacles for full-scale application," *Science of the Total Environment,* Vols. 445-446, pp. 237-260, 2013.

[78] P. Olson, K. Reardon and E. Pilon-Smits, "Ecology of rhizosphere bioremediation," in *Phytoremediation. Transformation and Control of Contaminants,* S. McCutcheon and J. Schnoor, Eds., Hoboken, John Wiley, 2003, pp. 317-353.

[79] W. Abraham, B. Nogales, P. Golyshin, D. Pieper and K. Timmis, "Polychlorinated biphenyl-degrading microbial communities in soils and sediments," *Current Opinion in Microbiology,* vol. 5, p. 246–253, 2002.

[80] J. Tiedje and S. Boyd, "Anaerobic degradation of chlorinated aromatic hydrocarbons," *Developments in Industrial Microbiology,* vol. 27, p. 117–127, 1987.

[81] K. Furukawa and H. Fujihara, "Microbial degradation of polychlorinated biphenyls: Biochemical and molecular features," *Journal of Bioscience and Bioengineering,* vol. 105, p. 433–449, 2008.

[82] G. Vasilyeva and E. Strijakova, "Bioremediation of soils and sediments contaminated by polychlorinated biphenyls," *Microbiology,* vol. 76, p. 639–653, 2007.

[83] H. Kohler, D. Kohlerstaub and D. Focht, "Co-metabolism of polychlorinated-biphenyls - Enhanced transformation of Aroclor 1254 by growing bacterial cells," *Applied and Environmental Microbiology,* vol. 54, p. 1940–1945, 1988.

[84] K. Furukawa, H. Suenaga and M. Goto, "Biphenyl dioxygenases: Functional versatilities and directed evolution," *Journal of Bacteriology,* vol. 186, p. 5189–5196, 2004.

[85] J. M. Brannon, W. M. Davis, V. A. McFarland and C. Hayes, "Organic Matter Quality and Partitioning of PCB," *Bulletin of Environmental Contamination and Toxicology,* vol. 61, pp. 333-338, 1998.

[86] D. L. Swackhamer and D. E. Armstrong, "Distribution and characterization of PCBs in lake Michigan water," *Journal of Great Lakes Research,* vol. 13, no. 1, pp. 24-36, 1987.

[87] H. Khoudi, Y. Maatar, F. Brini, A. Fourati, N. Ammar and K. Masmoudi, "Phytoremediation potential of Arabidopsis thaliana, expressing ectopically a vacuolar proton pump, for the industrial waste phosphogypsum," *Environmental Science and Pollution Research,* vol. 20, pp. 270-280, 2013.

[88] P. Kucerova, C. i. d. Wiesche, M. Wolter, T. Macek, F. Zadrazil and M. Mackova, "The ability of different plant species to remove polycyclic aromatic hydrocarbons and polychlorinated biphenyls from incubation media," *Biotechnology letters,* vol. 23, pp. 1355-1359, 2001.

[89] T. Macek, M. Macková and J. Kás, "Exploitation of plants for the removal of organics in environmental remediation," *Biotechnology Advances,* vol. 18, pp. 23-34, 2000.

[90] M. H. Hoffmann, "Biogeography of Arabidopsis thaliana (L.) Heynh. (Brassicaceae)," *Journal of Biogeography,* vol. 29, pp. 125-134, 2002.

[91] TAIR, "The Arabidopsis Information Resource," 2013. [Online]. Available: www.arabidopsis.org. [Accessed November 2013].

[92] X.-Y. Fu, W. Zhao, A.-S. Xiong, Y.-S. Tian, B. Zhu, R.-H. Peng and Q.-H. Yao, "Phytoremediation of triphenylmethane dyes by overexpressing a Citrobacter sp. triphenylmethane reductase in transgenic Arabidopsis," *Applied Microbiology and Biotechnology,* vol. 97, p. 1799–1806, 2013.

[93] J. Z. Zhang, R. A. Creelman and J.-k. Zhu, "From Laboratory to Field. Using Information from Arabidopsis to Engineer Salt, Cold, and Drought Tolerance in Crops 1," *Plant physiolog,* vol. 135, pp. 615-21, 2004.

[94] M. Cho, A. N. Chardonnens and K. Dietz, "Differential heavy metal tolerance of Arabidopsis halleri and Arabidopsis thaliana: a leaf slice test," *New Phytologist,* vol. 158, no. 2, pp. 287-293, 2003.

[95] "abcam," November 2013. [Online]. Available: http://www.abcam.com/ps/CMS/Images/Arabidopsis 2.jpg. [Accessed 2013].

[96] "AraPerox," 2013. [Online]. Available: http://www3.uis.no/araperoxv1/pictures/entire_plant_2.jpg.

[97] M. N. Riaz, Soy application in food, Boca Raton, Florida: CRC Press, 2006.

[98] J. Schmutz, S. B. Cannon, J. Schlueter, J. Ma and T. Mitros, "Genome sequence of the palaeopolyploid soybean," *Nature,* vol. 463, pp. 178-183, 2010.

[99] F. Ma and M. A. Hanna, "Biodiesel production: a review," *Bioresource Technology,* vol. 70, no. 1, pp. 1-15, 1999.

[100] "corbisimages," 2013. [Online]. Available: www.corbisimages.com.

[101] "Grain farmers of Ontario," 2013. [Online]. Available: growingon.wordpress.com.

[102] T. Vamerali, M. Bandiera and G. Mosca, "Field crops for phytoremediation of metal-contaminated land," *Environmental Chemistry Letters,* vol. 8, pp. 1-17, 2010.

[103] E. Dominguez-Rosado and J. Pichtel, "Phytoremediation of Soil Contaminated with Used Motor Oil: II. Greenhouse Studies," *Environmental Engineering Science,* vol. 21, no. 2, 2004.

[104] M. Boonsaner and D. W. Hawker, "Accumulation of oxytetracycline and norfloxacin from saline soil by soybeans," *Science of the Total Environment,* vol. 408, no. 7, pp. 1731-1737, 2010.

[105] R. A. Cropp, D. W. Hawker and M. Boonsaner, "Predicting the Accumulation of Organic Contaminants from Soil by Plants," *Bulletin of Environmental Contamination and Toxicology,* vol. 85, no. 5, pp. 525-529, 2010.

[106] S. A. Aransiola, J. I. Udeme Joshua and O. P. Abioye, "Phytoremediation of Lead Polluted Soil by Glycine Max L," *Applied and Environmental Soil Science,* vol. 2013, p. 7, 2013.

[107] D. Salt, R. Smith and I. Raskin, "Phytoremediation," *Annual Review of Plant Biology and Plant Molecular Biology,* vol. 49, pp. 643-668, 1998.

[108] J. Schnoor, L. Licht, S. McCutcheton, N. Wolfe and L. Carreira, "Phytoremediation of organic and nutrient contaminants," *Environment Science & Technology ,* vol. 29, pp. 7318A-323A, 1995.

[109] C. Frick, R. Farrell and J. Germida, "Assessment of Phytoremediation as an In-Situ Technique for Cleaning Oil-Contaminated Sites," Department of Soil Science, University of Saskatchewan, Saskatoon, SK Canada, 1999.

[110] E. Limbert and W. Betts, "Influence of substrate chemistry and microbial metabolic diversity on the bioremediation of xenobiotic contamination," *The Genetic Engineer and Biotechnologist,* vol. 16, pp. 3159-180, 1996.

[111] H. Sandermann, "Higher plant metabolism of xenobiotics: The 'green liver' concept," *Pharmacogenetics,* vol. 4, pp. 225-241, 1994.

[112] A. Daar, H. Thorsteinsdottir, D. Martin, A. Smith, S. Nast and P. Singer, "Top ten biotechnologies for improving health in developing countries," *Nature Genetics,* vol. 32, pp. 2229-232, 2002.

[113] S. McCutcheon and J. Schnoor, "Overview of phytotransformation and control of wastes," in *Phytoremediation. Transformation and Control of Contaminants, eds.*, 2003, pp. 3-58.

[114] R. Brooks, J. Lee, R. Reeves and T. Jaffre, "Detection of nickeliferous rocks by analysis of herbarium specimens of indicators plants," *Journal of Geochemical Exploration,* vol. 7, pp. 49-57, 1977.

[115] D. Cole, "Oxidation of xenobiotics in plants," *Progress in Pesticide Biochemistry and Toxicology,* vol. 3, pp. 199-253, 1983.

[116] B. Van Aken, A. Correa and J. Schnoor, "Phytoremediation of polychlorinated biphenyls: new trends and promises," *Environmental Science & Technology,* vol. 44, no. 8, p. 2767–76, 2010.

[117] R. Meagher, "Phytoremediation of toxic elemental and organic pollutants," *Current Opinion in Plant Biology,* vol. 3, pp. 2153-162, 2000.

[118] D. S.L., C. James, A. Moore and A.Vajzovic, "Enhanced phytoremediation of volatile environmental pollutants with transgenic trees," *Proceedings of the National Academy of Sciences,* vol. 104, pp. 16816-16821, 2007.

[119] S. Eapen, S. Singh and S. D'Souza, "Advances in development of transgenic plants for remediation of xenobiotic pollutants," *Biotechnology Advances,* vol. 25, pp. 442-451, 2007.

[120] J. Yoon, B. V. Aken and J. Schnoor, "Leaching of contaminated leaves following uptake and phytoremediation of RDX, HMX, and TNT by poplar," *International Journal of Phytoremediation,* vol. 8, pp. 181-94, 2006.

[121] B. Van Aken, "Transgenic plants for phytoremediation: helping nature to clean up environmental pollution," *Trends in Biotechnology,* vol. 26, pp. 5225-227, 2008.

[122] J. Burken and J. Schnoor, "Predictive relationships for uptake of organic contaminants by hybrid poplar trees," *Environmental Science & Technology,* vol. 32, pp. 213379-3385, 1998b.

[123] L. Newman and C. Reynolds, "Phytodegradation of organic compounds," *Current Opinion in Biotechnology,* vol. 15, pp. 3225-230, 2004.

[124] R. Chaney, M. Malik, Y. Li, S. Brown, E. Brewer, J. Angel and A. Baker, "Phytoremediation of soil metals," *Current Opnion in Biotechnology,* vol. 8, pp. 279-284, 1997.

[125] L. Newman, S. Strand and N. Choe, "Uptake and biotransformation of trichloroethylene by hybrid poplars," *Environmental Science & Technology,* vol. 31, pp. 41062-1067, 1997.

[126] B. V. Aken, J. Yoon and J. Schnoor, "Biodegradation of nitro-substituted explosives TNT, RDX, and HMX by a phytosymbiotic Methylobacterium sp. associated with poplars (Populus deltoides × nigra DN34)," *Applied and Environmental Microbiology,* vol. 70, pp. 508-517, 2004b.

[127] T. Anderson, E. Guthrie and B. Walton, "Bioremediation in the Rhizosphere," *Environmental Science & Technology,* vol. 27, pp. 132630-2636, 1993.

[128] Q. Chaudhry, M. Blom-Zandstra, S. Gupta and E. Joner, "Utilising the synergy between plants and rhizosphere microorganisms to enhance breakdown of organic pollutants in the environment," *Environmental Science and Pollution Research,* vol. 12, pp. 134-48, 2005.

[129] A. Ferro, M. Gefell, R. Kjelgren, D. Lipson, N. Zollinger and S. Jackson, "Maintaining hydraulic control using deep-rooted tree systems," *Advances in Biochemical Engineering/Biotechnology,* vol. 78, pp. 125-156, 2003.

[130] M. Mackova, D. Dowling and T. Macek, The chemical ecology of pollutants biodegradation.Phytoremediation and Rhizoremediation: Theoretical Background, Springer, 2006.

[131] Y. S. El-Temsah and E. J. Joner, "Impact of Fe and Ag nanoparticles on seed germination and differences in bioavailability during exposure in aqueous suspension and soil," *Environmental Toxicology* , vol. 27, pp. 42-49, 2012.

[132] R. Barrena, E. Casals, J. Colon, X. Font, A. Sanchez and V. Puntes, "Evaluation of the ecotoxicity of model nanoparticles," *Chemosphere,* vol. 75, pp. 850-857, 2009.

[133] J. Geisler-Lee, Q. Wang, Y. Yao, W. Zhang, M. Geisler and K. Li, "Phytotoxicity, accumulation and transport of silver nanoparticles by Arabidopsis thaliana," *Nanotoxicology,* vol. 7, pp. 323-337, 2013.

[134] R. Kaveh, Y.-S. Li, S. Ranjbar, R. Tehrani, V. A. benoit and C. L. Brueck, "Changes in Arabidopsis thaliana Gene Expression in Response to Silver Nanoparticles and Silver Ions," *Environmental Science & Technology,* pp. 10637-10644, 2013.

[135] J. C. Spain and J. B. Hughes, Biodegradation of Nitroaromatic Compounds and Explosives, J. C. Spain and J. Knackmuss, Eds., Lewis publishers, 2000, p. 456.

[136] P. Thompson, L. Ramer and J. Schnoor, "Uptake and transformation of TNT by hybrid poplar trees," *Environmental Science & Technology,* vol. 32, no. 7, p. 975–980, 1998.

[137] J. G. Burken, J. Shanks and T. P.L., "Phytoremediation and plant metabolism of explosives and nitroaromatic compounds," in *Biodegradation of Nitroaromatic Compounds and Explosives*, Boca Raton, Florida, CRC Press, 2000, p. 239– 276.

[138] C. D. Schott and E. Worthley, "The toxicity of TNT and related wastes to an aquatic flowering plant: Lemna perpusilla," Edgewood Arsenal, Aberdeen Prov. Ground, MD, 1974.

[139] A. J. Palazzo and D. C. Leggett, "Effect and Disposi- tion of TNT in a Terrestrial Plant," *Journal of Environmental Quality,* vol. 15, pp. 49-52, 1986.

[140] S. G. Pavlostathis, K. K. Comstock, M. E. Jacobson and F. M. Saunders, "Transformaton of 2,4,6–trini- trotoluene by the aquatic plant Myriophyllum spicatum," *Environmental Toxicology and Chemistry,* vol. 17, p. 2266–2273, 1998.

[141] E. Best, S. Sprecher, S. Larson, H. Fridrickson and D. Bader, "Environmental behavior and fate of explosives from groundwater from the Milan army ammunition plant in aquatic and wetland plant treatments. Mass balances of TNT and RDX," *Chemosphere,* vol. 38, p. 338, 1999.

[142] M. Peterson, G. Horst, S. Shea and S. Comfort, "Germination and seedling development of switchgrass and smooth bromegrass exposed to 2, 4, 6-trinitrotoluene," *Environmental Pollution,* vol. 99, no. 1, pp. 53-59, 1998.

[143] D. Ekman, W. Lorenz, A. Przybyla, N. Wolfe and J. Dean, "SAGE analysis of transcriptome responses in Arabidopsis roots exposed to 2, 4, 6-trinitrotoluene," *Plant physiology,* vol. 133, pp. 1397-1406, 2003.

[144] M. Rao, M. Halfhill, L. Abercrombie, P. Ranjan and J. Abercrombie, "Phytoremediation and phytosensing of chemical contaminants, RDX and TNT: Identification of the required target genes," *Functional & integrative genomics,* vol. 9, pp. 537-547, 2009.

[145] B. A. Zeeb, J. S. Amphlett, A. Rutter and K. J. Reimer, "Potential for phytoremediation of polychlorinated biphenyl-(PCB)-contaminated soil," *International Journal of Phytoremediation,* vol. 8, pp. 199-221, 2006.

[146] P. Kucerova, M. Mackova, L. Chroma, J. Burkhard, J. Trıska, K. Demnerova and T. Macek, "Metabolism of polychlorinated biphenyls by Solanum nigrum hairy root clone SNC-9O and analysis of transformation products," *Plant and Soil,* vol. 225, pp. 109-115, 2000.

[147] T. Macek, P. Kotrba, A. Svatos, M. Novakova, K. Demnerova and M. Mackova, "Novel roles for genetically modified plants in environmental protection," *Trends in Biotechnology,* vol. 26, p. 146– 152, 2008.

[148] A. H. Buckman, C. S. Wong, E. A. Chow, S. B. Brown, K. R. Solomon and A. T. Fisk, "Biotransformation of Polychlorinated Biphenyls (PCBs) and Bioformation of Hydroxylated PCBs in Fish," *Aquatic toxicology,* vol. 78, no. 2, pp. 176-85, 2006.

[149] P. Moza, I. Scheunert, W. Klein and F. Korte, "Studies with 2,4′,5- trichlorobiphenyl-14C and 2,2′,4,4′,6-pentachlorobiphenyl-14C in carrots, sugar beets, and soil," *Journal of Agricultural and Food Chemistry,* vol. 27, no. 5, pp. 1120-1124, 1979.

[150] C. Bock, M. Kolb, M. Bokern, HarmsH., M. Mackova, L. Chroma, T. Macek, J. Hughes, C. Just and J. Schnoor, "Advances in phytoremediation:phytotransformation. In Inovative Aproaches to the On-Site Assessment and Remediation of Contaminated Soils," vol. 15, Boston, Kluwer Academic Publisher, 2002, pp. 115-140.

[151] S. D. Cunningham and D. W. Ow, "Promises and Prospects of Phytoremediation," *Plant physiology,* vol. 110, no. 3, pp. 715-719, 1996.

[152] U. Krämer, "Phytoremediation: novel approaches to cleaning up polluted soils," *Current Opinion in Biotechnology,* vol. 16, no. 2, pp. 133-41, 2005.

[153] A. Mentewab, V. Cardoza and C. Stewart, "Genomic analysis of the response of Arabidopsis thaliana to trinitrotoluene as revealed by cDNA microarrays," *Plant Science,* vol. 168, pp. 1409-1424, 2005.

[154] P. Landa, R. Vankova, J. Andrlova, J. Hodek, P. Marsik, H. Storchova, J. White and T. Vanek, "Nanoparticle-specific changes in Arabidopsis thaliana gene expression after exposure to ZnO, TiO2, and fullerene soot," *Journal of Hazardous Materials,* vol. 241, pp. 55-62, 2012.

[155] F. Gandia-Herrero, A. Lorenz, T. Larson, I. Graham, D. Bowles, E. Rylott and N. Bruce, "Detoxification of the explosive 2, 4, 6- trinitrotoluene in Arabidopsis: discovery of bifunctional O- and C- glucosyltransferases," *Plant Journal,* vol. 56, p. 963–974, 2008.

[156] S. Tanaka, L. Brentner, K. Merchie, J. Schnoor, M. Jong and B. V. Aken, "Analysis of gene expression in poplar trees (Populusdeltoides x nigra, DN34) exposed to the toxic explosive hexahydro-1, 3, 5-trinitro-1, 3, 5-triazine (RDX)," *International Journal of Phytoremediation,* vol. 9, pp. 15-30, 2007.

[157] M. Rao, M. Halfhill, L. Abercrombie, P. Ranjan, J. Abercrombie, J. Gouffon, A. Saxton and C. Stewart Jr, "Phytoremediation and phytosensing of chemical contaminants, RDX and TNT: identification of the required target genes," *Functional & Integrative Genomics,* vol. 9, pp. 537-547, 2009.

[158] Y. Ze, C. Liu, L. Wang, M. Hong and F. Hong, "The Regulation of TiO2 nanoparticles on the expression of light-harvesting complex ii and photosynthesis of chloroplasts of Arabidopsis thaliana," *Biological Trace Element Research,* vol. 143, pp. 1131-1141, 2011.

[159] C. Dimkpa, J. McLean, N. Martineau, D. Britt, R. Haverkamp and A. Anderson, "Silver nanoparticles disrupt wheat (Triticum aestivum L.) growth in a sand matrix," *Environmental Science & Technology,* vol. 47, pp. 1082-1090, 2013.

[160] T. Frazier, C. Burklew and B. Zhang, "Titanium dioxide nanoparticles affect the growth and microRNA expression of tobacco (Nicotiana tabacum)," *Functional & Integrative Genomics,* vol. 14, pp. 75-83, 2014.

[161] D. Kargbo, R. Wilhelm and D. Campbell, "Natural gas plays in the Marcellus shale: Challenges and potential opportunities," *Environmental Science & Technology,* vol. 44.15, pp. 5679-5684, 2010.

[162] B. Focus, "Biofuels: Promise and Risks," World Bank, 2008.

[163] N. Courchesne, A. Parisien, B. Wang and C. Q. Lan, "Enhancement of lipid production using biochemical, genetic and transcription factor engineering approaches," *Journal of Biotechnology,* vol. 141, no. 1, pp. 31-41, 2009.

[164] M. N. Siddiquee and S. Rohani, "Lipid extraction and biodiesel production from municipal sewage sludges: A review," *Renewable and Sustainable Energy Reviews,* vol. 15.2, pp. 1067-1072, 2011.

[165] M. J. Haas and T. A. Foglia, "Alternate feedstocks and technologies for biodiesel production," *The biodiesel handbook*, pp. 42-61, 2005.

[166] J. Csavina, B. Stuart, R. Riefler and M. Vis, "Growth optimization of algae for biodiesel production," *Journal of Applied Microbiology*, vol. 111, pp. 312-318, 2011.

[167] G. Shi and Q. Cai, "Cadmium tolerance and accumulation in eight potential energy crops," *Biotechnology Advances*, vol. 27, pp. 555-561, 2009.

[168] E. Faessler, B. Robinson, W. Stauffer, S. Gupta, A. Papritz and R. Schulin, "Phytomanagement of metal-contaminated agricultural land using sunflower, maize and tobacco RID F-1208-2010," *Agriculture, Ecosystems & Environment*, vol. 136, pp. 49-58, 2010.

[169] E. Meers, S. V. Slycken, K. Adriaensen and A. Ruttens, "The use of bio-energy crops (Zea mays) for 'phytoattenuation' of heavy metals on moderately contaminated soils: A field experiment," *Chemosphere*, vol. 78, pp. 35-41, 2010.

[170] L. Brentner, S. Mukherji, K. Merchie, J. Yoon, J. Schnoor and B. V. Aken, "Expression of glutathione S-transferases in poplar trees (Populus trichocarpa) exposed to 2,4,6-trinitrotoluene (TNT)," *Chemosphere*, vol. 73, pp. 5657-662, 2008.

[171] B. Fallen, V. Pantalone, C. Sams, D. Kopsell, S. Vaughn and B. Moser, "Effect of soybean oil fatty acid composition and selenium application on biodiesel properties," *Journal of the American Oil Chemists' Society*, vol. 88, pp. 1019-1028, 2011.

[172] G. Ankley, G. Daston, S. Degitz, N. Denslow, R. Hoke, S. Kennedy, A. Miracle, E. Perkins, J. Snape, D. Tillitt, C. Tyler and D. Versteeg, "Toxicogenomics in regulatory ecotoxicology," *Environmental Science & Technology*, vol. 13, pp. 4055-4065, 2006.

[173] R. Simon, A. Lam, M.-C. Li, M. Ngan, S. Menenzes and Y. Zhao, "Analysis of gene expression data using BRB-Array Tools," *Cancer Informatics*, vol. 3, pp. 11-17, 2007.

[174] M. Pfaffl, G. Horgan and L. Dempfle, "Relative expression software tool (REST) for group-wise comparison and statistical analysis of relative expression results in real-time PCR.," *Nucleic Acids Research*, vol. 30, no. 9, p. e36, 2002.

[175] H. Jiang, M. Li, F. Chang, W. Li and L. Yin, "Physiological analysis of silver nanoparticles and AgNO3 toxicity to Spirodela polyrhiza," *Environmental Toxicology and Chemistry*, vol. 31, pp. 1880-1886, 2012.

[176] J. Yasur and R. P.U., "Environmental effects of nanosilver: Impact on castor seed germination, seedling growth, and plant physiology," *Environmental Science and Pollution Research*, vol. 20, no. 12, pp. 8636-48, 2013.

[177] R. Bari and J. Jones, "Role of plant hormones in plant defence responses," *Plant Molecular Biology,* vol. 69, pp. 473-488, 2009.

[178] M. Prasad and K. Strzalka, "Physiology and Biochemistry of Metal Toxicity and Tolerance in Plants," *Biochemistry & Biophysics,* p. p 462, 2002.

[179] S. Tsukuda, K. Gomi, H. Yamamoto and K. Akimitsu, "Characterization of cDNAs encoding two distinct miraculin-like proteins and stress-related modulation of the corresponding mRNAs in Citrus jambhiri Lush," *Plant Molecular Biology,* vol. 60, pp. 125-136, 2006.

[180] Y. Narusaka, M. Narusaka, M. Seki, T. Umezawa, J. Ishida, M. Nakajima, A. Enju and K. Shinozaki, "Crosstalk in the responses to abiotic and biotic stresses in Arabidopsis: Analysis of gene expression in cytochrome P450 gene superfamily by cDNA microarr," *Plant Molecular Biology* , vol. 55, pp. 327-342, 2004.

[181] B. Field and A. Osbourn, "Metabolic diversification - Independent assembly of operon-like gene clusters in different plants," *Science,* vol. 320, pp. 543-547, 2008.

[182] A. Osbourn, "Gene Clusters for secondary metabolic pathways: An emerging theme in plant biology," *Plant Physiology,* vol. 154, pp. 531-535, 2010.

[183] P. Zimmermann, M. Hirsch-Hoffmann, L. Hennig and W. Gruissem, "GENEVESTIGATOR. arabidopsis microarray database and analysis toolbox," *Plant Physiology,* vol. 136, no. 1, pp. 2621-32, 2004.

[184] P. Landa, H. Storchova, J. Hodek, R. Vankova and T. Vanek, "Transferases and transporters mediate the detoxification and capacity to tolerate trinitrotoluene in Arabidopsis," *Functional & integrative genomics,* vol. 10.4, pp. 547-559, 2010.

[185] X. Jin, J. Shuai, R. Peng, B. Zhu, F. X, Y. Tian, W. Zhao, H. Han, C. Chen and J. Xu, "Identification of candidate genes involved in responses of arabidopsis to polychlorinated biphenyls based on microarray analysis," *Plant Growth Regulation,* vol. 65, no. 1, pp. 127-35, 2011.

[186] D. McWilliams, D. Berglund and G. Endres, "Soybean growth and management," NDSU Extension Service, North Dakota, 1999.

[187] R. Bhadra, R. J. Spanggord, D. G. Wayment, J. B. Hughes and J. V. Shanks, "Confirmation of conjugation processes during TNT metabolism by axenic plant roots," *Environmental Science & Technology,* vol. 33, no. 3, pp. 446-452, 1999.

[188] P. Gong, B.-M. Wilke and S. Fleischmann, "Soil-based phytotoxicity of 2, 4, 6-trinitrotoluene (TNT) to terrestrial higher plants," *Archives of Environmental Contamination and Toxicology,* vol. 32, no. 6, pp. 152-157, 1999.

[189] G. Briggs, R. Bromilow and A. Evans, "Relationship between lipophilicity and root uptake and translocation of non-ionised chemicals by barley," *Pesticide Science,* vol. 13, pp. 495-504, 1982.

[190] X. Jin, J. Shuai, R. Peng, B. Zhu, F. X, Y. Tian, W. Zhao, H. Han, C. Chen and J. Xu, "Identification of candidate genes involved in responses of arabidopsis to polychlorinated biphenyls based on microarray analysis," *Plant Growth Regulation,* vol. 65, no. 1, pp. 127-35.

[191] N. Suzuki, S. Koussevitzky, R. Mittler and G. Miller, "ROS and redox signalling in the response of plants to abiotic stress," *Plant Cell and Environment,* vol. 35, pp. 259-270, 2012.

[192] O. Sytar, A. Kumar, D. Latowski, P. Kuczynska, K. Strzalka and M. Prasad, "Heavy metal-induced oxidative damage, defense reactions, and detoxification mechanisms in plants," *Acta Physiologiae Plantarum,* vol. 35, pp. 985-999, 2013.

[193] M. Moreno-Risueno, W. Busch and P. Benfey, "Omics meet networks - Using systems approaches to infer regulatory networks in plants," *Current Opinion in Plant Biology,* vol. 13, pp. 126-131, 2010.

[194] R. Tehrani, M. M. Lyv, R. Kaveh, J. L. Schnoor and B. V. Aken, "Biodegradation of mono-hydroxylated PCBs by Burkholderia xenovorans," *Biotechnology Letters,* vol. 34, p. 2247–2252, 2012.

[195] T. Hruz, O. Laule, G. Szabo, F. Wessendorp, S. Bleuler, L. Oertle, P. Widmayer, W. Gruissem and P. Zimmermann, "Genevestigator V3: a reference expression database for the meta-analysis of transcriptomes," *Advances in Bioinformatics,* p. 5, 2008.

[196] L. V. Kochian, M. A. Pineros and O. A. Hoekenga, "The physiology, genetics and molecular biology of plant aluminum resistance and toxicity," *Plant and Soil,* vol. 274, pp. 175-195, 2005.

[197] E. Pichersky and D. Gang, "Genetics and biochemistry of secondary metabolites in plants: an evolutionary perspective," *Trends in Plant Science,* vol. 5, no. 10, pp. 439-45, 2000.

[198] B. Van Aken and S. Agathos, "Biodegradation of nitro-substituted explosives by white-rot fungi: a mechanistic approach," *Advances in applied microbiology,* vol. 48, pp. 1-77, 2001.

[199] F. Gandia-Herrero, A. Lorenz, T. Larson, I. Graham, D. Bowles, E. Rylott and N. Bruce, "Detoxification of the explosive 2, 4, 6-trinitrotoluene in arabidopsis: Discovery of bifunctional O-and C-glucosyltransferases," *The Plant Journal,* vol. 56, no. 6, pp. 963-74, 2008.

[200] H. Mazumdar, "The Impact of Silver Nanoparticles on Plant Biomass and Chlorophyll Content," *International Journal of Engineering And Science,* vol. 4, no. 7, pp. 12-20, 2014.

[201] M. Farkas, J. Berry and D. Aga, "Chlortetracycline detoxification in maize via induction of glutathione S-transferases after antibiotic exposure," *Environment Science & Technology ,* vol. 41, no. 4, pp. 1450-6, 2007.

APPENDIX A Regulated genes in exposure to AgNP and Ag^+

Table A-1. Genes significantly upregulated (fold change > 2.0) in A. thaliana plants exposed for 10 days to silver nanoparticles (AgNPs) or silver ions (Ag^+)

TAIR ID	Gene Description	Fold Change	
		AgNP	Ag^+
AT3G28220	TRAF-like family protein	28.57	
AT1G14250	GDA1/CD39 nucleoside phosphatase family protein	21.74	
AT1G52040	Myrosinase-binding protein 1 (MBP1)	11.49	
AT1G73325	Kunitz family trypsin and protease inhibitor protein	10.10	
AT5G47990	Cytochrome P450 705A5 (CYP705A5)	9.09	
AT5G48010	Thalianol synthase 1 (THAS1)	8.33	
AT5G42800	Dihydroflavonol-4-reductase (DFR)	7.69	3.49
AT4G10860	Uncharacterized protein	6.67	
AT5G48000	Cytochrome P450 708A2 (CYP708A2)	6.67	
AT1G52400	Beta glucosidase 18 (BGLU18)	6.25	2.08
AT4G22880	Leucoanthocyanidin dioxygenase (LDOX)	6.25	2.85
AT2G01520	MLP-like protein 328 (MLP328)	5.56	
AT2G30670	Tropine dehydrogenase	5.56	
AT4G22870	Leucoanthocyanidin dioxygenase	5.56	
AT5G41280	Cysteine-rich repeat secretory protein 57	5.56	
AT4G17470	Palmitoyl-protein thioesterase	5.26	
AT5G01900	Putative WRKY transcription factor 62 (WRKY62)	5.00	
AT5G38020	S-adenosyl-L-methionine-dependent methyltransferase-like protein	5.00	
AT1G73330	Drought-repressed 4 protein (DR4)	4.76	3.86
AT4G11320	Putative cysteine proteinase	4.76	
AT4G29930	Transcription factor bhlh27	4.76	
AT5G26260	TRAF-like family protein	4.76	
AT1G52000	Jacalin-like lectin domain-containing protein	4.55	
AT2G38390	Peroxidase 23	4.55	2.63
AT4G28940	Phosphorylase-like protein protein	4.55	
AT5G22570	Putative WRKY transcription factor 38 (WRKY38)	4.55	
AT3G20590	Late embryogenesis abundant hydroxyproline-rich glycoprotein	4.35	
AT5G01490	Vacuolar cation/proton exchanger 4 (CAX4)	4.35	2.33
AT5G41300	Cysteine-rich repeat secretory protein 59	4.35	2.05
AT5G17220	Glutathione S-transferase phi 12 (GSTF12)	4.17	
AT5G54060	UDP-glucose:flavonoid 3-o-glucosyltransferase (UF3GT)	4.17	
AT2G23000	Serine carboxypeptidase-like 10 (scpl10)	4.00	
AT2G35070	Uncharacterized protein	4.00	
AT5G37990	S-adenosyl-L-methionine-dependent methyltransferase-like protein	4.00	2.61
AT1G78340	Glutathione S-transferase TAU 22 (GSTU22)	3.85	
AT5G36180	Serine carboxypeptidase-like 1 (scpl1)	3.85	
AT5G42590	Cytochrome P450 71A16 (CYP71A16)	3.85	3.26
AT3G28740	Cytochrome P450 CYP81D11 (CYP81D1)	3.70	
AT5G59490	Haloacid dehalogenase-like hydrolase domain-containing protein	3.57	

AT5G60020	Laccase 17 (LAC17)	3.57	
AT4G37410	Cytochrome P450, family 81, subfamily F, polypeptide 4 (CYP81F4)	3.47	
AT2G05440	Glycine-rich protein 9 (GRP9)	3.45	
AT4G14090	Anthocyanin 5-O-glucosyltransferase	3.45	2.35
AT5G03545	Uncharacterized protein	3.45	2.46
AT5G41290	Cysteine-rich repeat secretory protein 58	3.45	
AT1G66280	Beta-glucosidase 22 (BGLU22)	3.33	
AT1G76790	O-methyltransferase-like protein	3.33	
AT2G28190	Superoxide dismutase [Cu-Zn] (CSD2)	3.33	
AT5G23830	MD-2-related lipid recognition domain-containing protein	3.33	
AT1G14550	Peroxidase 5	3.23	
AT1G17180	Glutathione S-transferase TAU 25 (GSTU25)	3.23	2.75
AT1G24320	Mannosyl-oligosaccharide glucosidase	3.23	
AT3G54260	Protein trichome birefringence-like 36 (TBL36)	3.23	
AT5G03260	Laccase 11 (LAC11)	3.23	
AT1G14120	2-oxoglutarate (2OG) and Fe(II)-dependent oxygenase-like protein	3.13	
AT1G64590	Putative short-chain dehydrogenase	3.13	
AT1G66100	Thionin	3.13	
AT2G30660	3-hydroxyisobutyryl-coa hydrolase	3.13	
AT2G38080	Laccase-4 (IRX12)	3.13	
AT3G28270	Uncharacterized protein	3.13	
AT4G20240	Cytochrome P450, family 71, subfamily A, polypeptide 27 (CYP71A27)	3.13	2.66
AT5G52390	PAR1 protein	3.13	
AT1G08830	Superoxide dismutase [Cu-Zn] (CSD1)	3.03	3.63
AT1G29020	EF-hand, calcium binding motif-containing protein	3.03	
AT1G70850	MLP-like protein 34 (MLP34)	3.03	
AT1G76952	Inflorescence deficient in abscission (IDA)-like 5 protein (IDL5)	3.03	
AT2G01880	Purple acid phosphatase 7 (PAP7)	3.03	
AT2G04170	TRAF-like family protein	3.03	
AT2G47950	Uncharacterized protein	3.03	2.60
AT3G29590	HXXXD-type acyl-transferase-like protein	3.03	
AT3G48340	Putative cysteine proteinase	3.03	
AT3G58550	Bifunctional inhibitor/lipid-transfer protein/seed storage 2S albumin-like protein	3.03	3.03
AT5G38030	Mate efflux domain-containing protein	3.03	
AT1G10140	Uncharacterized protein	2.94	2.12
AT1G24430	HXXXD-type acyl-transferase-like protein	2.94	
AT1G47395	Uncharacterized protein	2.94	
AT1G61750	Receptor-like protein kinase-related protein	2.94	
AT2G39310	Jacalin-related lectin 22 (JAL22)	2.94	
AT3G44550	Putative fatty acyl-coa reductase 5 (FAR5)	2.94	
AT4G29270	HAD superfamily, subfamily IIIB acid phosphatase	2.94	
AT5G22500	Fatty acyl-coa reductase 1 (FAR1)	2.94	
AT1G04180	YUCCA 9 protein (YUC9)	2.86	

AT2G40370	Laccase 5 (LAC5)	2.86	
AT3G16400	Nitrile-specifier protein 1 (NSP1)	2.86	
AT3G16920	Chitinase-like protein 2 (CTL2)	2.86	3.17
AT3G21770	Peroxidase 30	2.86	
AT4G11880	Agamous-like MADS-box protein AGL14 (AGL14)	2.86	7.67
AT2G18193	P-loop containing nucleoside triphosphate hydrolase-like protein	2.78	
AT2G28315	Nucleotide/sugar transporter-like protein	2.78	3.79
AT3G15990	Putative sulfate transporter 3.4 (SULTR3;4)	2.78	3.17
AT4G31020	Esterase/lipase domain-containing protein	2.78	
AT5G05390	Laccase 12 (LAC12)	2.78	5.54
AT1G06620	1-aminocyclopropane-1-carboxylate oxidase-1	2.70	
AT1G15630	Uncharacterized protein	2.70	
AT1G26820	Ribonuclease 3 (RNS3)	2.70	
AT1G61820	Beta glucosidase 46 (BGLU46)	2.70	6.88
AT1G80820	Cinnamoyl-coa reductase (CCR2)	2.70	
AT3G07970	Polygalacturonase QRT2 (QRT2)	2.70	
AT3G32030	Terpene cyclase, C1 domain-containing protein	2.70	2.48
AT4G15380	Cytochrome P450, family 705, subfamily A, polypeptide 4 (CYP705A4)	2.70	6.72
AT5G40000	AAA-type atpase family protein	2.70	
AT1G52140	Uncharacterized protein	2.63	
AT1G65500	Uncharacterized protein	2.63	3.84
AT2G16980	Major facilitator protein	2.63	
AT2G27550	Protein centroradialis	2.63	2.26
AT2G43610	Putative chitinase	2.63	
AT4G01080	Protein trichome birefringence-like 26 (TBL26)	2.63	
AT4G15230	ABC transporter G family member 30 (PDR2)	2.63	
AT4G29690	Alkaline-phosphatase-like protein	2.63	
AT5G10040	Uncharacterized protein	2.63	2.01
AT5G62130	Per1-like family protein	2.63	2.56
AT1G43790	Tracheary element differentiation-related 6 protein (TED6)	2.56	
AT2G21640	Uncharacterized protein	2.56	4.28
AT3G09270	Glutathione S-transferase TAU 8 (GSTU8)	2.56	2.78
AT3G18280	Protease inhibitor/seed storage/lipid transfer protein (LTP) family protein	2.56	
AT3G27400	Pectate lyase	2.56	
AT4G10370	Cysteine/histidine-rich C1 domain-containing protein	2.56	
AT5G19600	Putative sulfate transporter 3.5 (SULTR3;5)	2.56	
AT1G63295	Remorin family protein	2.50	6.51
AT1G74460	GDSL esterase/lipase	2.50	
AT2G18150	Peroxidase 15	2.50	
AT2G18370	Non-specific lipid-transfer protein 8	2.50	
AT2G22770	Transcription factor NAI1 (NAI1)	2.50	
AT2G32990	Endoglucanase 11 (GH9B8)	2.50	
AT3G23250	Myb domain protein 15 (MYB15)	2.50	

AT3G53980	Bifunctional inhibitor/lipid-transfer protein/seed storage 2S albumin-like protein	2.50	2.36
AT4G22610	Bifunctional inhibitor/lipid-transfer protein/seed storage 2S albumin-like protein	2.50	2.06
AT5G23820	MD-2-related lipid recognition domain-containing protein	2.50	
AT5G47635	Pollen Ole e 1 allergen and extensin family protein	2.50	
AT1G26450	Carbohydrate-binding X8 domain-containing protein	2.44	3.28
AT1G55990	Glycine-rich protein	2.44	
AT1G66270	Beta-glucosidase 21 (BGLU21)	2.44	
AT2G04680	Cysteine/histidine-rich C1 domain-containing protein	2.44	2.54
AT2G25160	Cytochrome P450, family 82, subfamily F, polypeptide 1 (CYP82F1)	2.44	
AT2G33205	Serinc-domain containing serine and sphingolipid biosynthesis protein	2.44	
AT2G39700	Expansin A4 (EXPA4)	2.44	
AT3G01190	Peroxidase 27	2.44	
AT3G49780	Phytosulfokine-beta (PSK4)	2.44	
AT4G22070	WRKY DNA-binding protein 31 (WRKY31)	2.44	3.75
AT4G25400	Transcription factor bhlh118	2.44	
AT5G07990	Flavonoid 3'-monooxygenase (TT7)	2.44	
AT5G09220	Amino acid permease 2 (AAP2)	2.44	
AT5G12870	Transcription factor MYB46 (MYB46)	2.44	
AT5G14340	Myb domain protein 40 (MYB40)	2.44	
AT5G23220	Nicotinamidase 3 (NIC3)	2.44	
AT5G35110	Uncharacterized protein	2.44	
AT5G37690	GDSL esterase/lipase	2.44	2.11
AT5G44400	FAD-binding and BBE domain-containing protein	2.44	
AT5G51890	Peroxidase 66	2.44	2.69
AT5G58860	Cytochrome P450 86A1 (CYP86A1)	2.44	2.17
AT5G63560	HXXXD-type acyl-transferase-like protein	2.44	2.17
AT1G12520	Copper chaperone for SOD1 (CCS)	2.38	3.51
AT1G14780	MAC/Perforin domain-containing protein	2.38	
AT1G19540	Nmra-like negative transcriptional regulator-like protein	2.38	
AT1G77640	Ethylene-responsive transcription factor ERF013	2.38	
AT2G24430	NAC domain containing protein 38 (NAC038)	2.38	2.96
AT2G29440	Glutathione S-transferase (GSTU6)	2.38	2.50
AT2G38060	Putative anion transporter 3 (PHT4;2)	2.38	
AT3G20370	TRAF-like family protein	2.38	3.17
AT3G21680	Uncharacterized protein	2.38	
AT4G01440	Nodulin mtn21 /eama-like transporter family protein	2.38	
AT4G13860	RNA recognition motif-containing protein	2.38	
AT4G20390	Uncharacterized protein	2.38	3.20
AT5G18860	Inosine-uridine preferring nucleoside hydrolase family protein	2.38	
AT1G05340	Uncharacterized protein	2.33	
AT1G58270	TRAF-like protein (ZW9)	2.33	
AT2G15220	Basic secretory protein family protein	2.33	
AT2G15490	UDP-glycosyltransferase 73B4 (UGT73B4)	2.33	

AT3G06778	DNAj-domain-containing protein	2.33	
AT3G13432	Uncharacterized protein	2.33	
AT4G09820	Transcription factor TT8 (TT8)	2.33	2.76
AT4G29700	Alkaline-phosphatase-like protein	2.33	
AT5G09520	Hydroxyproline-rich glycoprotein family protein	2.33	
AT5G19410	ABC transporter G family member 23	2.33	14.30
AT5G26290	TRAF-like family protein	2.33	
AT5G47950	HXXXD-type acyl-transferase-like protein	2.33	
AT5G64700	Nodulin mtn21 /eama-like transporter family protein	2.33	4.02
AT1G07880	Mitogen-activated protein kinase 13	2.27	
AT1G23720	Proline-rich extensin-like family protein	2.27	
AT1G28400	Uncharacterized protein	2.27	2.04
AT1G35250	Thioesterase family protein	2.27	
AT1G45191	Beta-glucosidase 1	2.27	
AT2G16580	SAUR-like auxin-responsive protein	2.27	
AT2G36120	Glycine-rich protein (DOT1)	2.27	
AT3G47780	ABC transporter A family member 7	2.27	8.95
AT4G03610	Metallo-beta-lactamase domain-containing protein	2.27	
AT4G22950	Agamous-like MADS-box protein AGL19 (AGL19)	2.27	
AT5G09530	Hydroxyproline-rich glycoprotein family protein	2.27	
AT5G15630	COBRA-like protein 4 (IRX6)	2.27	
AT5G44050	Mate efflux domain-containing protein	2.27	2.29
AT3G25820	1,8-cineole synthase (TPS-CIN)	2.22	
AT1G14730	Cytochrome b561/ferric reductase transmembrane-like protein	2.22	
AT1G65860	Flavin-containing monooxygenase FMO GS-OX1 (FMO GS-OX1)	2.22	
AT1G70470	Uncharacterized protein	2.22	
AT1G78370	Glutathione S-transferase TAU 20 (GSTU20)	2.22	
AT2G01275	RING/FYVE/PHD zinc finger-containing protein	2.22	
AT2G23960	Class I glutamine amidotransferase-like domain-containing protein	2.22	
AT2G37090	Nucleotide-diphospho-sugar transferases-like protein (IRX9)	2.22	2.77
AT3G03530	Phospholipase C (NPC4)	2.22	
AT3G29250	Rossmann-fold NAD(P)-binding domain-containing protein	2.22	
AT3G48346	Uncharacterized protein	2.22	
AT3G49580	Response to low sulfur 1 protein (LSU1)	2.22	
AT4G04830	Peptide methionine sulfoxide reductase B5 (MSRB5)	2.22	
AT4G34600	Uncharacterized protein	2.22	
AT5G19100	Eukaryotic aspartyl protease family protein	2.22	
AT1G05280	Uncharacterized protein	2.17	
AT1G26730	Phosphate transporter PHO1-7	2.17	
AT1G65481	Uncharacterized protein	2.17	6.39
AT2G22920	Serine carboxypeptidase-like 12 (SCPL12)	2.17	
AT2G37280	ABC transporter G family member 33 (PDR5)	2.17	
AT3G16430	Jacalin-related lectin 31 (JAL31)	2.17	

AT3G16460	Jacalin-like lectin domain-containing protein	2.17	
AT3G23190	HR-like lesion-inducing protein-like protein	2.17	
AT3G44540	Putative fatty acyl-coa reductase 4 (FAR4)	2.17	
AT4G13235	Defensin-like protein 37 (EDA21)	2.17	2.18
AT4G18340	Glycosyl hydrolase family 17 protein	2.17	
AT4G39720	VQ motif-containing protein	2.17	
AT5G01870	Non-specific lipid-transfer protein 10	2.17	
AT5G16490	ROP-interactive CRIB motif-containing protein 4 (RIC4)	2.17	
AT5G18270	NAC domain containing protein 87 (ANAC087)	2.17	
AT5G63970	Copine (Calcium-dependent phospholipid-binding protein) family	2.17	
AT5G65870	Phytosulfokine-beta (PSK5)	2.17	
AT1G11580	Bifunctional pectinesterase 18/rRNA N-glycosylase (PMEPCRA)	2.13	
AT1G31950	Terpene cyclase, C1 domain-containing protein	2.13	
AT1G48510	Surfeit locus 1 cytochrome c oxidase biogenesis protein	2.13	
AT1G54010	GDSL esterase/lipase	2.13	
AT2G29750	UDP-glucosyl transferase 71C1 (UGT71C1)	2.13	
AT2G44130	F-box/kelch-repeat protein	2.13	
AT3G44730	Kinesin-like protein 1 (KP1)	2.13	
AT3G50400	GDSL esterase/lipase	2.13	
AT3G54770	RNA recognition motif-containing protein	2.13	
AT3G54990	AP2-like ethylene-responsive transcription factor SMZ (SMZ)	2.13	3.70
AT3G55515	Protein rotundifolia like 7 (RTFL7)	2.13	
AT4G04840	Peptide methionine sulfoxide reductase B6 (MSRB6)	2.13	
AT4G19230	Abscisic acid 8'-hydroxylase 1 (CYP707A1)	2.13	
AT4G26790	GDSL esterase/lipase	2.13	
AT4G35350	Xylem cysteine proteinase 1 (XCP1)	2.13	
AT5G40980	Uncharacterized protein	2.13	
AT5G42200	E3 ubiquitin-protein ligase ATL23	2.13	2.42
AT5G58310	Methyl esterase 18 (MES18)	2.13	
AT5G60890	Myb domain protein 34 (MYB34)	2.13	
AT5G67210	Uncharacterized protein	2.13	9.29
AT1G18140	Laccase 1 (LAC1)	2.08	
AT1G22490	Transcription factor bhlh94	2.08	
AT1G23200	Pectinesterase 6	2.08	
AT1G47600	Myrosinase 4 (BGLU34)	2.08	3.51
AT1G74500	Transcription factor bhlh135 (BS1)	2.08	
AT2G29220	Concanavalin A-like lectin protein kinase-like protein	2.08	
AT2G34600	Protein TIFY 5B (JAZ7)	2.08	2.30
AT3G04570	AT-hook motif nuclear-localized protein 19 (AHL19)	2.08	2.26
AT3G22620	Bifunctional inhibitor/lipid-transfer protein/seed storage 2S albumin-like protein	2.08	
AT3G23175	HR-like lesion-inducing protein-like protein	2.08	
AT3G24240	Receptor-like protein kinase 2	2.08	
AT4G17480	Palmitoyl protein thioesterase family protein	2.08	

AT4G25560	Transcription factor LAF1 (MYB18)	2.08	
AT4G30850	Heptahelical transmembrane protein2 (HHP2)	2.08	2.21
AT5G09480	Hydroxyproline-rich glycoprotein family protein	2.08	
AT5G14130	Peroxidase 55	2.08	2.73
AT5G15130	Putative WRKY transcription factor 72 (WRKY72)	2.08	
AT5G26330	Plastocyanin-like domain-containing protein / putative mavicyanin	2.08	
AT5G60200	Dof zinc finger protein DOF5.3 (TMO6)	2.08	
AT1G03495	HXXXD-type acyl-transferase-like protein	2.04	2.45
AT1G15210	ABC transporter G family member 35 (PDR7)	2.04	
AT1G58070	Uncharacterized protein	2.04	
AT1G72140	Putative peptide/nitrate transporter	2.04	
AT2G14520	CBS and transporter associated domain-containing protein	2.04	2.80
AT2G28510	Dof zinc finger protein DOF2.1	2.04	3.72
AT2G43535	Defensin-like protein 196	2.04	
AT3G20860	NIMA-related kinase 5 (NEK5)	2.04	
AT3G23470	Cyclopropane-fatty-acyl-phospholipid synthase	2.04	
AT4G08780	Peroxidase 38	2.04	2.52
AT1G12805	Nucleotide binding protein	2.00	
AT1G16070	Tubby-like protein 8 (TLP8)	2.00	
AT1G30730	FAD-binding and BBE domain-containing protein	2.00	
AT1G32100	Pinoresinol reductase 1 (PRR1)	2.00	
AT1G33700	Beta-glucosidase, GBA2 type protein	2.00	2.79
AT1G56550	Rhamnogalacturonan II specific xylosyltransferase (RXGT1)	2.00	4.44
AT1G59780	NB-ARC domain-containing disease resistance protein	2.00	7.25
AT1G72230	Plastocyanin-like domain-containing protein	2.00	
AT1G78000	Sulfate transporter 1.2 (SULTR1;2)	2.00	2.13
AT2G21045	Rhodanese-like domain-containing protein	2.00	
AT2G42060	Cysteine/histidine-rich C1 domain-containing protein	2.00	3.87
AT3G22415	Uncharacterized protein	2.00	
AT4G29080	Auxin-responsive protein IAA27 (PAP2)	2.00	
AT5G02350	Cysteine/histidine-rich C1 domain-containing protein	2.00	
AT5G17420	Cellulose synthase A catalytic subunit 7 [UDP-forming] (IRX3)	2.00	
AT1G22065	Uncharacterized protein		2.21
AT1G24030	Protein kinase-like protein		5.17
AT1G24095	Putative thiol-disulfide oxidoreductase DCC		2.56
AT1G35910	Haloacid dehalogenase-like hydrolase domain-containing protein		4.33
AT2G04050	MATE efflux family protein		4.03
AT2G36750	Cytokinin-O-glucosyltransferase 1 (UGT73C1)		2.66
AT3G18260	Reticulon-like protein B9		2.56
AT3G61850	Dof zinc finger protein DOF3.7 (DAG1)		3.82
AT4G15610	Uncharacterized protein		2.31
AT5G06720	Peroxidase 53 (PA2)		3.83
AT5G19520	Mechanosensitive channel of small conductance-like 9 (MSL9)		2.72
AT5G38280	PR5-like receptor kinase (PR5K)		3.01

Table A-2. Gene significantly downregulated (fold change < 0.5) in A. thaliana plants exposed for 10 days to silver nanoparticles (AgNPs) or silver ions (Ag^+)

TAIR ID	Gene Description	Fold Change	
		AgNP	Ag^+
AT2G15020	Uncharacterized protein	0.50	
AT3G52340	Putative sucrose-phosphatase 3b (SPP2)	0.50	
AT5G24570	Uncharacterized protein	0.49	
AT4G36410	Putative ubiquitin-conjugating enzyme E2 17 (UBC17)	0.49	
AT1G19350	Protein brassinazole-resistant 2 (BES1)	0.48	0.47
AT2G02930	Glutathione S-transferase 16 (GSTF3)	0.48	
AT2G11522	Uncharacterized protein	0.48	
AT4G16880	Leucine-rich repeat (LRR) family protein	0.47	
AT3G13960	Growth-regulating factor 5 (GRF5)	0.47	
AT1G75470	Purine permease 15 (PUP15)	0.47	
AT3G28070	Nodulin mtn21 /eama-like transporter family protein	0.47	
AT4G13575	Uncharacterized protein	0.47	
AT2G29310	Tropine dehydrogenase	0.46	
AT1G62380	Aminocyclopropanecarboxylate oxidase (ACO2)	0.46	0.43
AT2G40940	Ethylene response sensor 1 (ERS1)	0.46	0.46
AT1G43160	Ethylene-responsive transcription factor RAP2-6 (RAP2.6)	0.45	
AT5G44582	Uncharacterized protein	0.45	
AT4G27310	B-box type zinc finger-containing protein	0.45	
AT5G14780	Formate dehydrogenase (FDH)	0.45	
AT4G13570	Histone H2A (HTA4)	0.44	0.36
AT5G17780	Hydrolase, alpha/beta fold family protein	0.44	
AT1G71030	Myb proto-oncogene protein (MYBL2)	0.44	0.36
AT4G25100	Superoxide dismutase [Fe] (FSD1)	0.44	0.40
AT1G73830	Transcription factor BEE 3 (BEE3)	0.44	0.29
AT1G68840	AP2/ERF and B3 domain-containing transcription factor RAV2 (RAV2)	0.43	
AT3G14630	Cytochrome P450, family 72, subfamily A, polypeptide 9 (CYP72A9)	0.43	
AT1G02470	SRPBCC ligand-binding domain-containing protein	0.43	
AT4G13572	Uncharacterized protein	0.43	
AT2G42870	Phy rapidly regulated 1 (PAR1)	0.43	
AT5G35480	Uncharacterized protein	0.41	
AT4G16940	TIR-NBS-LRR class disease resistance protein	0.41	
AT1G69500	Cytochrome P450, family 704, subfamily B, polypeptide 1 (CYP704B1)	0.40	
AT5G14920	Gibberellin-regulated protein	0.40	
AT3G09450	Uncharacterized protein	0.39	
AT1G28660	GDSL esterase/lipase	0.39	
AT1G23060	Uncharacterized protein	0.38	
AT2G30230	Uncharacterized protein	0.38	0.39
AT5G16570	Glutamine synthetase cytosolic isozyme 1-4 (GLN1;4)	0.38	

AT5G22580	Stress responsive A/B Barrel domain-containing protein	0.37	
AT2G25625	Uncharacterized protein	0.37	
AT2G43140	Transcription factor bhlh129	0.37	
AT1G23730	Beta carbonic anhydrase 3 (BCA3)	0.37	
AT1G72910	Toll-Interleukin-Resistance domain-containing protein	0.37	
AT4G11460	Putative cysteine-rich receptor-like protein kinase 30 (CRK30)	0.37	0.35
AT4G28790	Transcription factor bhlh23	0.36	
AT1G21320	Nucleic acid/nucleotide binding protein	0.36	
AT4G11521	Putative cysteine-rich receptor-like protein kinase 34	0.34	0.37
AT5G54190	Protochlorophyllide reductase A (PORA)	0.34	0.25
AT3G46900	Copper transporter 2 (COPT2)	0.34	0.32
AT3G60290	Oxidoreductase	0.34	
AT5G14570	High affinity nitrate transporter 2.7 (NRT2.7)	0.33	0.22
AT5G44580	Uncharacterized protein	0.32	0.26
AT4G16146	Camp-regulated phosphoprotein 19-related protein	0.32	
AT5G57181	Uncharacterized protein	0.31	
AT1G53870	LURP-one-related 3 protein	0.31	
AT3G57240	Beta-1,3-glucanase 3 (BG3)	0.31	
AT1G80130	Tetratricopeptide repeat domain-containing protein	0.30	
AT5G38940	Germin-like protein subfamily 1 member 11	0.30	
AT1G68845	Uncharacterized protein	0.29	0.38
AT3G19850	Phototropic-responsive NPH3 family protein	0.29	0.25
AT5G23980	Ferric reduction oxidase 4 (FRO4)	0.29	
AT5G62280	Uncharacterized protein	0.28	
AT3G16670	Pollen Ole e 1 allergen and extensin family protein	0.28	
AT4G12470	Azelaic acid induced 1 (AZI1)	0.27	0.19
AT2G36690	2-oxoglutarate (2OG) and Fe(II)-dependent oxygenase-like protein	0.27	
AT5G61160	Anthocyanin 5-aromatic acyltransferase 1 (AACT1)	0.26	
AT1G12940	Nitrate transporter2.5 (NRT2.5)	0.24	0.16
AT5G25350	EIN3-binding F-box protein 2 (EBF2)	0.23	0.23
AT2G44080	ARGOS-like protein (ARL)	0.23	
AT5G46330	LRR receptor-like serine/threonine-protein kinase FLS2 (FLS2)	0.23	0.20
AT5G39610	NAC domain containing protein 6 (NAC6)	0.23	0.30
AT5G19890	Peroxidase 59	0.22	
AT1G69490	NAC domain-containing protein 29 (NAP)	0.20	0.19
AT5G44260	Zinc finger CCCH domain-containing protein 61	0.17	0.15
AT3G16770	Ethylene-responsive transcription factor RAP2-3 (EBP)	0.15	0.19
AT2G41230	Uncharacterized protein	0.14	0.17
AT4G25750	ABC transporter G family member 4	0.11	0.11
AT5G57760	Uncharacterized protein	0.11	0.10
AT2G40670	Two-component response regulator ARR16 (RR16)	0.11	0.13
AT5G02760	Putative protein phosphatase 2C 67	0.09	
AT3G59900	ARGOS protein (ARGOS)	0.08	0.09

AT1G21460	Nodulin mtn3-like protein	0.49
AT2G22240	Inositol-3-phosphate synthase isozyme 2 (MIPS2)	0.49
AT5G38410	Ribulose bisphosphate carboxylase small chain 3B	0.49
AT1G04110	Subtilase-like protein (SDD1)	0.48
AT1G30520	Acyl-activating enzyme 14 (AAE14)	0.48
AT5G04390	C2H2-type zinc finger protein	0.47
AT5G46490	TIR-NBS-LRR class disease resistance protein	0.47
AT1G10760	Alpha-glucan water dikinase 1 (SEX1)	0.45
AT1G23080	Auxin efflux carrier component 7 (PIN7)	0.45
AT1G51940	Lysm type receptor kinase-like protein	0.45
AT4G02420	Concanavalin A-like lectin kinase-like protein	0.45
AT5G02160	Uncharacterized protein	0.45
AT5G02540	Rossmann-fold NAD(P)-binding domain-containing protein	0.45
AT5G24380	Metal-nicotianamine transporter YSL2 (YSL2)	0.44
AT1G52870	Peroxisomal membrane 22 kda (Mpv17/PMP22) family protein	0.42
AT3G21950	Methyltransferase	0.42
AT4G17680	SBP (S-ribonuclease binding protein) family protein	0.41
AT3G23010	Receptor like protein 36 (RLP36)	0.40
AT5G44130	Fasciclin-like arabinogalactan protein 13 (FLA13)	0.39
AT5G45650	Subtilase family protein	0.39
AT1G12090	Extensin-like protein (ELP)	0.38
AT4G27440	Protochlorophyllide reductase B (PORB)	0.38
AT3G53800	Hsp70-interacting protein (Fes1B)	0.37
AT4G29190	Zinc finger CCCH domain-containing protein 49	0.31

APPENDIX B Regulated genes in exposure to zanamivir and oseltamivir

Table B-1. Genes significantly up-regulated (fold change ≥ 2.0) in A. thaliana plants exposed to oseltamivir phosphate and zanamivir for 21 days

TAIR ID	Gene Description	Fold Change	
		OSP	ZAN
AT5G37970	S-adenosyl-L-methionine-dependent methyltransferase-like protein	10.35	
AT2G20870	Putative cell wall protein	10.04	
AT1G57750	Cytochrome P450, family 96, subfamily A, polypeptide 15 (CYP96A15)	5.93	
AT5G22430	Pollen Ole e 1 allergen and extensin family protein	5.45	
AT5G59310	Non-specific lipid-transfer protein 4 (LTP4)	5.32	
AT4G33790	Fatty acyl-CoA reductase 3 (CER4)	2.86	
AT3G04721	Uncharacterized protein	2.82	3.04
AT3G62907	Uncharacterized protein	2.74	
AT1G12570	Glucose-methanol-choline (GMC) oxidoreductase-like protein	2.4	
AT5G37940	2-alkenal reductase	2.33	
AT5G45820	CBL-interacting serine/threonine-protein kinase 20 (CIPK20)	2.24	2.06
AT5G36658	ECA1 gametogenesis related family protein	2.23	
AT1G74890	Two-component response regulator ARR15 (ARR15)	2.19	2.25
AT3G24300	Ammonium transporter 1;3 (AMT1;3)	2.12	
AT4G25630	fibrillarin 2 (FIB2) identical to fibrillarin 2	2.07	
AT1G21890	Nodulin MtN21 /EamA-like transporter-like protein		4.01
AT5G07690	Myb domain protein 29 (MYB29)		3.23
AT2G33830	Dormancy/auxin associated protein		2.87
AT1G02640	Beta-glucosidase (BXL2)		2.85
AT3G46880	Uncharacterized protein		2.84
AT5G58360	Ovate family protein 3 (OFP3)		2.71
AT5G39860	Basic helix-loop-helix (bHLH) DNA-binding family protein (PRE1)		2.63
AT4G38825	SAUR-like auxin-responsive protein		2.51
AT4G21650	Subtilase family protein		2.5
AT2G37640	Expansin-A3 (EXP3)		2.5
AT5G24580	Heavy metal transport/detoxification domain-containing protein		2.44
AT2G40610	Expansin A8 (EXPA8)		2.43
AT1G52190	Putative peptide transporter		2.41
AT5G51950	Glucose-methanol-choline (GMC) oxidoreductase family protein		2.38
AT2G39850	Subtilisin-like serine protease		2.35
AT5G18600	Monothiol glutaredoxin-S2		2.34
AT4G34970	Actin depolymerizing factor 9 (ADF9)		2.32
AT1G74670	Putative gibberellin-regulated protein		2.31
AT5G48900	Putative pectate lyase 20		2.3

AT3G15450	Aluminum induced protein with YGL and LRDR motif	2.29
AT3G01670	Uncharacterized protein	2.29
AT1G26780	Myb domain protein 117 (MYB117)	2.28
AT4G04630	Uncharacterized protein	2.28
AT2G05720	WD40 domain-containing protein	2.24
AT1G16410	Dihomomethionine N-hydroxylase (CYP79F1)	2.23
AT1G78970	Lupeol synthase 1 (LUP1)	2.22
AT2G32860	Beta glucosidase 33 (BGLU33)	2.19
AT4G30180	Transcription factor/ transcription regulator	2.18
AT1G75240	Homeobox protein 33 (HB33)	2.15
AT5G27220	Frigida-like protein	2.1
AT4G34900	Xanthine dehydrogenase 2 (XDH2)	2.08
AT1G79700	AP2-like ethylene-responsive transcription factor	2.07
AT1G49490	Pollen-specific leucine-rich repeat extensin-like protein 2	2.07
AT5G06930	Uncharacterized protein	2
AT2G44740	Cyclin-U4-1 (CYCP4;1)	2
AT1G25230	Purple acid phosphatase 4	2
AT1G67865	Uncharacterized protein	2

Table B-2. Genes significantly down-regulated (fold change ≤ 0.5) in A. thaliana plants exposed to oseltamivir phosphate and zanamivir for 21 days

TAIR ID	Gene Description	Fold Change	
		OSP	ZAN
AT3G28740	Cytochrome P450 81D1 (CYP81D1)		0.5
AT1G74020	Strictosidine synthase 1 (SS2)		0.5
AT5G11210	Glutamate receptor 2.5 (GLR2.5)		0.5
AT5G44390	FAD-binding and BBE domain-containing protein		0.5
AT3G48580	Xyloglucan:xyloglucosyl transferase (XTH11)		0.5
AT2G46430	Cyclic nucleotide gated channel (CNGC3)		0.5
AT5G24160	Squalene monooxygenase 1,2 (SQE6)		0.5
AT4G38560	Phospholipase like protein (PEARLI 4)		0.5
AT5G54720	Ankyrin repeat-containing protein		0.5
AT3G50770	Putative calcium-binding protein CML41 (CML41)		0.5
AT1G56120	Leucine-rich repeat transmembrane protein kinase		0.5
AT5G24660	Response to low sulfur 2 (LSU2)		0.5
AT4G22460	Bifunctional inhibitor/lipid-transfer protein/seed storage 2S albumin-like protein		0.5
AT2G14247	Uncharacterized protein		0.5
AT5G13930	Chalcone synthase (TT4)		0.5
AT1G32960	Subtilase-like protein (SBT3.3)		0.5
AT4G04490	Cysteine-rich receptor-like protein kinase 36 (CRK36)		0.5
AT3G57710	Protein kinase family protein		0.49
AT5G39810	Protein agamous-like 98 (AGL98)		0.49

AT1G80130	Tetratricopeptide repeat domain-containing protein		0.49
	Peptide methionine sulfoxide reductase B5 (MSRB5)		0.49
AT3G48320	Cytochrome P450 71A21 (CYP71A21)		0.49
AT4G23260	Cysteine-rich receptor-like protein kinase 18 (CRK18)		0.49
AT4G14090	Anthocyanin 5-O-glucosyltransferase		0.49
AT4G28085	Uncharacterized protein		0.49
AT5G48540	Cysteine-rich repeat secretory protein 55		0.49
AT5G48880	3-ketoacyl-CoA thiolase 5 (PKT2)		0.49
AT3G43250	Uncharacterized protein		0.49
AT1G69480	Phosphate transporter PHO1-10		0.48
AT2G21185	Uncharacterized protein		0.48
AT1G55020	Lipoxygenase 1 (LOX1)		0.48
AT2G32680	Receptor like protein 23 (RLP23)		0.48
AT5G41610	Cation/H(+) antiporter 18 (CHX18)		0.48
AT5G59670	Receptor-like protein kinase		0.48
AT2G43530	Defensin-like protein 194		0.47
AT5G54710	Ankyrin repeat-containing protein		0.47
AT4G13920	Receptor like protein 50 (RLP50)		0.47
AT4G15233	ABC transporter G family member 42		0.47
AT1G43910	P-loop containing nucleoside triphosphate hydrolase-like protein		0.47
AT1G04770	Male sterility MS5 family protein		0.47
AT3G14620	Cytochrome P450, family 72, subfamily A, polypeptide 8 (CYP72A8)		0.47
AT3G52780	Putative purple acid phosphatase 20 (PAP20)		0.47
AT3G26840	Acyltransferase-like protein		0.47
AT5G05365	Metal ion binding protein		0.47
AT5G67340	U-box domain-containing protein 2		0.47
AT2G04495	Uncharacterized protein		0.47
AT3G44300	Nitrilase 2 (NIT2)		0.47
AT1G62910	Pentatricopeptide repeat-containing protein		0.47
AT1G26730	Phosphate transporter PHO1-7	0.49	0.46
AT2G42360	E3 ubiquitin-protein ligase ATL41		0.46
AT1G36370	Serine hydroxymethyltransferase 7 (SHM7)		0.46
AT2G25440	Receptor like protein 20 (RLP20)		0.46
AT1G56650	Transcription factor MYB75 (PAP1)		0.46
AT3G48300	Cytochrome P450 71A23 (CYP71A23)		0.46
AT1G07620	GTP-binding protein Obg/CgtA		0.46
AT3G22840	Chlorophyll A-B binding, early light-inducible protein (ELIP1)		0.46
AT1G65790	Receptor kinase 1 (RK1)		0.46
AT2G15220	Basic secretory protein family protein		0.46
AT5G13550	Sulfate transporter 4.1 (SULTR4;1)		0.46
AT1G54570	Acyltransferase-like protein		0.46

AT4G14370	TIR-NBS-LRR class disease resistance protein		0.45
AT1G65690	Late embryogenesis abundant (LEA) hydroxyproline-rich glycoprotein		0.45
AT5G48180	Nitrile specifier protein 5 (NSP5)		0.45
AT5G53420	CCT motif family protein		0.45
AT4G37530	Peroxidase 51		0.45
AT5G18290	Putative aquaporin SIP1-2 (SIP1;2)		0.45
	Protein kinase-like protein		0.45
AT2G45135	RING/U-box family protein		0.45
AT1G32940	Subtilase-like protein (SBT3.5)		0.45
AT2G32830	Putative inorganic phosphate transporter 1-5 (PHT1;5)		0.44
AT2G35070	Uncharacterized protein		0.44
AT3G44970	Cytochrome P450 family protein		0.44
AT5G46350	Putative WRKY transcription factor 8 (WRKY8)		0.43
AT4G21990	5'-adenylylsulfate reductase 3 (APR3)		0.43
AT3G51450	Strictosidine synthase family protein		0.43
AT5G05600	Oxidoreductase, 2OG-Fe(II) oxygenase family protein		0.43
AT3G14060	Uncharacterized protein		0.43
AT1G59865	Uncharacterized protein		0.43
AT3G54420	Chitinase (EP3)		0.42
AT1G47400	Uncharacterized protein		0.42
AT2G32660	Receptor like protein 22 (RLP22)		0.41
AT3G05400	Sugar transporter ERD6-like 12		0.41
AT4G23600	Cystine lyase (CORI3)		0.41
AT5G28237	Tryptophan synthase beta chain	0.44	0.4
AT4G35640	Serine acetyltransferase 4 (SERAT3;2)		0.4
AT5G24150	Squalene monooxygenase 1,1 (SQP1)		0.4
AT3G60120	Beta glucosidase 27 (BGLU27)		0.4
AT1G68620	Alpha/beta-hydrolase domain-containing protein		0.4
AT3G12520	Putative sulfate transporter 4.2 (SULTR4;2)		0.4
AT5G42800	Dihydroflavonol-4-reductase (DFR)	0.49	0.39
AT3G23550	Mate efflux domain-containing protein		0.39
AT3G44320	Nitrilase 3 (NIT3)		0.39
AT1G75290	Isoflavone reductase-like protein		0.39
	known chromosome, gene:AT1G55525, transcript:AT1G55525.1		0.39
AT1G11925	Stigma-specific stig1-like protein		0.39
AT3G51860	Vacuolar cation/proton exchanger 3 (CAX3)		0.38
AT2G29470	Glutathione S-transferase tau 3 (GSTU3)		0.38
AT3G56200	Transmembrane amino acid transporter-like protein		0.38
AT1G66370	Transcription factor MYB113 (MYB113)		0.38
AT1G26390	FAD-binding and BBE domain-containing protein		0.38
AT5G13170	Senescence-associated protein 29 (SAG29)		0.37
AT4G36700	Cupin family protein	0.38	0.36

AT5G17220	Glutathione S-transferase phi 12 (GSTF12)		0.36
AT4G23700	Cation/H(+) antiporter 17 (CHX17)		0.36
AT1G09500	Rossmann-fold NAD(P)-binding domain-containing protein		0.36
AT1G12030	Uncharacterized protein		0.36
AT5G07990	Flavonoid 3'-monooxygenase (TT7)		0.35
AT5G54060	UDP-glucose:flavonoid 3-o-glucosyltransferase (UF3GT)	0.47	0.34
AT5G67080	Mitogen-activated protein kinase kinase kinase 19 (MAPKKK19)		0.34
AT2G24850	Tyrosine aminotransferase 3 (TAT3)		0.34
AT2G43570	Chitinase class 4-like protein (CHI)		0.34
AT4G09420	TIR-NBS class of disease resistance protein		0.33
AT1G65490	Uncharacterized protein		0.33
AT5G13220	Protein TIFY 9 (JAZ10)		0.33
AT5G39720	Avirulence induced protein 2 like protein (AIG2L)		0.33
AT3G25760	Allene oxide cyclase 1 (AOC1)		0.33
	MI0005382 miR826 stem-loop		0.32
AT1G73260	Kunitz trypsin inhibitor 1 (KTI1)		0.32
AT4G19810	Glycosyl hydrolase family protein with chitinase insertion domain		0.32
AT3G08860	PYRIMIDINE 4 (PYD4)		0.32
AT2G02990	Ribonuclease 1 (RNS1)		0.32
AT1G47510	Type I inositol-1,4,5-trisphosphate 5-phosphatase 11 (5PTASE11)	0.5	0.31
AT3G24982	Receptor like protein 40 (RLP40)	0.4	0.31
AT3G25770	Allene oxide cyclase 2 (AOC2)		0.31
AT2G37770	NAD(P)-linked oxidoreductase-like protein		0.31
AT4G22870	Leucoanthocyanidin dioxygenase	0.44	0.3
AT3G46660	UDP-glucosyl transferase 76E12 (UGT76E12)	0.32	0.3
AT3G49580	Response to low sulfur 1 protein (LSU1)		0.3
AT4G31970	Cytochrome P450, family 82, subfamily C, polypeptide 2 (CYP82C2)		0.3
AT2G44460	Beta glucosidase 28 (BGLU28)		0.29
AT4G08870	Putative arginase		0.28
AT5G26220	ChaC-like family protein		0.28
AT1G32350	Alternative oxidase 3 (AOX1D)		0.28
	Nudix hydrolase 24 (NUDT24)		0.28
AT4G22880	Leucoanthocyanidin dioxygenase (LDOX)	0.43	0.27
AT4G24000	Cellulose synthase-like protein G2 (CSLG2)		0.27
AT1G45616	Receptor like protein 6 (RLP6)		0.27
AT1G09380	Nodulin MtN21 /EamA-like transporter protein		0.26
AT1G61800	Glucose-6-phosphate/phosphate translocator 2 (GPT2)		0.25
AT3G45130	Lanosterol synthase 1 (LAS1)		0.25
AT1G23730	Beta carbonic anhydrase 3 (BCA3)	0.49	0.24
AT4G25000	Alpha-amylase (AMY1)	0.47	0.24

AT4G37990	Cinnamyl alcohol dehydrogenase 8 (ELI3-2)		0.24
AT1G74010	Strictosidine synthase		0.24
AT5G27060	Receptor like protein 53 (RLP53)	0.33	0.23
AT2G38240	2-oxoglutarate (2OG) and Fe(II)-dependent oxygenase-like protein	0.21	0.23
AT3G21850	S-phase kinase-associated protein 1 (SK9)		0.23
AT2G29350	Senescence-associated protein 13 (SAG13)		0.23
AT3G44860	Farnesoic acid carboxyl-O-methyltransferase (FAMT)	0.33	0.22
	Palmitoyl-protein thioesterase		0.22
AT2G43510	Defensin-like protein 195 (TI1)		0.22
AT2G33380	Caleosin-related protein (RD20)		0.22
AT4G21830	Peptide methionine sulfoxide reductase B7 (MSRB7)		0.21
AT4G21840	Peptide methionine sulfoxide reductase B8 (MSRB8)		0.21
AT1G73325	Kunitz family trypsin and protease inhibitor protein		0.21
AT4G24340	Phosphorylase family protein		0.21
AT1G80160	Lactoylglutathione lyase / glyoxalase I-like protein		0.2
AT2G39030	Acyl-CoA N-acyltransferases-like protein		0.2
AT3G60140	Beta-glucosidase 30 (DIN2)		0.18
AT4G21680	Nitrate transporter 1.8 (NRT1.8)		0.18
AT5G48850	Tetratricopeptide repeat domain-containing protein	0.48	0.14
AT3G55970	Jasmonate-regulated protein (JRG21)		0.13
AT1G61120	Terpene synthase 04 (TPS04)	0.22	0.11
AT4G15210	Beta-amylase 5 (BAM5)	0.44	0.1
AT3G21500	1-deoxy-D-xylulose 5-phosphate synthase 1 (DXPS1)	0.29	0.1
AT4G13300	Terpenoid synthase 13 (TPS13)	0.5	
AT1G56540	TIR-NBS-LRR class disease resistance protein	0.48	
AT1G19250	Putative flavin-containing monooxygenase 1 (FMO1)	0.47	
AT1G61610	S-locus lectin protein kinase-like protein	0.46	
AT4G17660	Protein kinase family protein	0.46	
AT1G55525	known chromosome: gene:AT1G55525 transcript:AT1G55525.1	0.42	
AT1G52040	Myrosinase-binding protein 1 (MBP1)	0.38	
AT3G49110	Peroxidase 33 (PRXCA)	0.38	
	MI0005382 miR826 stem-loop	0.38	
AT1G76960	Uncharacterized protein	0.37	
	MI0001015 miR397a stem-loop	0.36	
AT1G76470	Rossmann-fold NAD(P)-binding domain-containing protein	0.3	
AT5G44430	Defensin-like protein 17 (PDF1.2c)	0.13	